# Some Studies On The Effects Of Crowding Agents On The Structure, Functionality And Activity Of Biomolecules

Thesis submitted for award of the degree of

**Doctor of Philosophy (Science)**

**in**

**Chemistry (Physical)**

**by**

**SAIKAT PAL**

**Department of Chemistry**

**University of Calcutta**

**2021**

*Dedicated to*

**My Mother (Papia Pal),**

**Father (Lt. Santosh Pal)**

**and Sister (Shilpa Pal)……**

# Declaration

I hereby declare that the works manifested in the thesis "Some Studies On The Effects Of Crowding Agents On The Structure, Functionality And Activity Of Biomolecules" are original. The experimental measurements and instrumentation set up have been carried out by me during my Ph.D. work with the assistance of my lab mates and my supervisor Prof. Rajib Kumar Mitra at Satyendra Nath Bose National Centre for Basic Sciences, Saltlake, Kolkata. I also declare that these results and experimental observation have not been used for the award of any degree diploma from any university or institute.

Saikat Pal (E-mail: ***saikatchem279@gmail.com***)
Senior Research Fellow (CSIR)
S.N.Bose National Centre for Basic Sciences
Block-JD, Sector-III, Salt Lake, Kolkata-700106

# *Table of contents*

*This page is intentionally left blank*

*……*

# Acknowledgements

*Writing my thesis would remain incomplete without acknowledging all of the nice people who have directly or indirectly assisted me in my Ph.D. journey. Without their generous help, I wouldn't have been able to study so far. I am very much grateful to them.*

*At first, I want to express my gratitude and respect to the first teacher in my life, my Mother and also to my Father (who recently got passed away). Their affection, enthusiasm, philosophy, ideology, principles, positive attitude, unconditional love always inspire me to be established in life as well as to become a good human being. What I have achieved till today is because of their constant support, guidance, motivation and inspiration. I have no words to show gratitude to them. I want to convey respect to my grandmothers (Dida and Thakuma) who sacrificed a lot in their life to achieve my success. I want to express my profound love and affection to my younger sister (Shilpa) to support me always in my every ups and downs. I will never ever forget the sweet memories and small moments in my childhood that I shared with her. I would like to thank my brother-in-law (Amit) to inspire me and to give company in my bad days.*

*I would like to express my sincere respect and gratitude to my Bengali teacher Tapan Mandal; Sir came in my life like a God-father and has been helping me unconditionally in every moment till now. His ideology, inspiration, principles always guide me how to balance in life through every ups and downs. He was the only person who inspired me to*

*study pure science in class XI and what I am today is because of his inspiration, thoughts and guidance. I am very much lucky to have such a great person in my life. Apart from that, kakima (Kabita Mandal, Tapan sir's wife) also supports and guides me in my every phase of life till today. I am very much indebted to them and I will never be able to pay them back.*

*It is a great opportunity to convey my earnest respect and gratitude to my Ph.D. mentor Prof. Rajib Kumar Mitra. His valuable suggestions, constant motivation, continuous support in every small research areas helped me to think differently in every problems and to find out proper scientific solutions. I have learnt many scientific basic techniques like preparation of scientific graphs in a proper format, presentation of experimental data in proper scientific method, writing research articles in scientific way etc. He always discussed every research problems starting from the core level to the advanced level to get its better solutions. He always tried to maintain a friendly environment in our 'Group-Meeting' discussions. His valuable advice, guidance and suggestions will always help me to make progress in the future days of my life.*

*Apart from my supervisor, I would like to acknowledge my collaborator Prof. Simon Ebbinghaus (Institute of Theoretical and Physical Chemistry, Branschweig, Germany) for his valuable suggestions, advice, corrections and reviewing many times of my manuscript. I learnt "Anova-Test" for my experimental results according to his suggestion; before that I had no idea about this test and its significance. I am really grateful to him.*

*Next, I want to thank my past and present lab-members from our "THz Lab" (currently known as "Biophotonics Lab") : Dr. Animesh Patra, Dr. Nirnay Samanta, Dr. Debasish Das Mahanta, Dr. Arindam Das, Dr. Dipak Kumar Das, Dr. Chaitrali Sengupta, Dr. Bibhab Bandhu Majumdar, Dr. Shubhadip Chakrabarti, Sk Imadul Islam, Partha Pyne, Sumana Pyne, Didhiti Bhattacharya, Ria Saha, Shubhajit Singha, Debkumar Rana, Amit Barh, Sayantan Adak, Anulekha De and Sudip Majumdar for working together maintaining a friendly and cooperative environment in our experimental Biophysical lab. I am greatly pleased to them for all the enjoyment we celebrated during the last five years like Birthday celebration, going for a walk heither and thither, Dinner parties in several restaurants and dhabas, cooking parties in our hostel rooms etc. I would like to give special thanks to my two great seniors Nirnay Da and Debasish Da; from them I have learnt many preliminary basic research related things like preparation of graphs in Origin and Sigma softwares, basic instrumentation handling technique, data reading and analysis, usage of Endnote, CDNN, Gauss-view, Gaussian softwares and different parts of MS-office like Ms-word, Powerpoint, Excel etc. Whenever I asked any research related questions, they tried to pay attention to me despite the business of their work. I am happy enough to have two such seniors. After them, my special thanks goes to Imadul (used to call him as 'Partner') for his continuous help, supports, healthy and friendly cooperation during my Ph.D. tenure. He has always been by my side especially in my bad days. Without his kind and generous help, it wouldn't be possible for me to spend five years research life. I am thankful enough to my junior, Didhiti (used to call her as 'Ma'), with whom I used to often*

*share and discuss different problems and topics whether it would be research related or not. I really enjoyed fruitful and long discussions, debate and fun with her. Besides this, she helped me a lot to understand various scientific problems through physics point of view. I am really fortunate to have such lab-members.*

*Sometimes, we, the THz lab-members spent some delightful evening party in the resident of our Sir and Madam (Dr. Sukanya chakrabarty). Sir and Madam prepared all the delicious dishes for us and we really enjoyed every dinner party. We spent some memorable evening time especially in kali-puja by burning different crackers and fireworks on the roof of Sir's flat and enjoyed the 'Bhog and Prasad' in the puja times. Apart from, we enjoyed delightful dinner parties in various restaurants and used to taste different dishes and foods together. Thanks to Sir and Madam once again for giving us those wonderful moments and special dinners. I also want to thank Imadul (our chief chef), Nazma bhabhi (wife of Imadul), Nirnay da, Animesh da, Sonali di, Sumana to prepare different delicious foods and dishes (Chop muri, Chicken kosha, Katla kalia, Rui kosha, Egg curry, Payes etc.) in their rooms.*

*Aside from my lab-members, I would like to acknowledge my friends at the S.N.Bose Centre who helped me differently in my Ph.D days and giving me the long-lasting memories. A special thanks to Akash (used to call him as 'Man'); I used to share my problems to him and he supported me a lot to overcome those problems. We often used to discuss different non-research related topics like political debate, sports related and many others in our hostel room. Thanks to Sudipta also for giving company in my bad time and also for the wonderful discussion at night. I am very*

*much grateful to Piya di, from whom I not only learnt different MD simulation technique, but also she supported and cared for me continuously like her brother. Thanks to Sayantan, Koustav, Sayan Routh, Sasthi, Kaushik, Dipanjan, Shubhrasish, Pabi, Rafiqul, Shubhadip, Riju, Samir, Subrata, Dipika, Prantik, Kajal, Jayita. A special thanks goes to the cooking staffs (Sanjay da, Kajol, Ramu, Rajib, Ganesh, Shyamal and Manoranjan da) of our SNB mess to provide daily foods in breakfast, lunch and dinner times.*

*Nevertheless, I would not be able to forget my B.Sc college friends from R.K.M Vidyamandira, Belur Math; Amartya, Sanjoy, Sajal, Tuhin, Animesh, Sayan, Mrinmoy, Sourav, Subhas, Palash, Banibrata, Kajal, Utsarga, Somnath, Swarup, Jadab, Arnab, Raunak, Himadri, Debarshi, Tomojit. Those three years' graduation life is my most precious days. I always remember those special moments and wonderful days spent together with my special friends. Besides, thanks to my M.Sc friends Tanoy, Souvik, Mahuya, Tonima, Gurupada, Aindrila, Atanu, Mangaldeep for spending those days together.*

*I want to express my deep respect and gratitude to my beloved teachers from school days, B.Sc and M.Sc: Sri Pada Sir, A.B.H Sir, S.R. Sir, A.B. Sir, S.S.R Sir, D.J Sir, K.R Sir, R.D. Sir, K.B. Sir, Swapan Sir, Pinaki Sir, N.G. Sir, Kamal Sir, D.M. Sir, Chaitali Ma'am, Tanushree Ma'am, Sanchita Ma'am, Chanda Ma'am. I would like to express my sincere gratitude to the Maharajas and Brahmacharis especially Binay Maharaj who gave me the valuable and inspiring life lessons in my graduation days.*

*I would like to acknowledge all the research scholars, faculty members, academic and non-academic staffs, security guards of S.N.B.N.C.B.S for their continuous support, kindness, help and hearty co-operation throughout my Ph.D journey. I want to express my gratitude to Prof. Jaydeb Chakrabarti for teaching me MD simulation using GROMACS software technique. I am also grateful to my external and internal thesis committee members for every yearly evaluation of my Ph.D work. Thanks to the Council for Scientific and Industrial Research (CSIR) for granting my Ph.D. fellowship and once again S.N.Bose National Centre for Basic Sciences (S.N.B.N.C.B.S) for offering me the podium for research.*

*Finally yet importantly, I want to convey a special warm gratitude to my girlfriend "Tonima"; her colossal support, wholehearted help, boundless caring personality, childish behavior encourage and motivate me all the time in ebb and flow of the tenacious journey of academic career of my life. Even though, just being thankful is not ample to address her immense efforts. Whenever, I was in trouble, she stretched out her arms and pulled me out of these difficult situations. Please continue to stand by my side in the future.*

*To conclude, I want to acknowledge a few regularly visited websites like Google Chrome, YouTube, Sci-Hub, SciFinder, ResearchGate, Cricbuzz and also several Social Media Sites like Facebook, Messenger, Whatsapp, Telegram etc. to provide me useful information and for entertainment purpose. I would like to give thanks to various newspapers like Anandabazar Patrika, Ei Samay, Bartaman, Aajkaal, Times of India, The Hindu, Telegram, The Economic Times which I used to read routinely at our S.N. Bose Library premises. It would be a very bad thing if I don't give*

*thanks to the admins of "Horek Rokom Family", my entertainment supplier. They used to provide me Movies and Webseries freely almost all the time which were released in Netflix, Hotstar, Hoichoi, Amazon Prime etc. paid sites. Apart from that, I thank various meme providing groups and their hilarious and playful contents always stay me fair-minded, logical and healthy. High Impact Ph.D. memes, Viral Thread, Sarcasm, 9GAG, College Humor, Classical Art Memes, Funny or Die, Cyanide & Happiness – thank you very much.*

***Signature:*** ***Date: 01.01.2022***

Saikat Pal
E-mail: **saikatchem279@gmail.com**
**saikatpal@bose.res.in**

S. N. Bose National Centre for Basic Sciences
Department of Chemical, Biological & Macro-Molecular Sciences
Block-JD, Sector-III, Salt Lake City, Kolkata-700106, India

# *List of Publications*

**The following publications and manuscripts are based on this thesis:**

1. **Pal, S.**, Pyne, P., Samanta, N., Ebbinghaus, S. and Mitra, R. K. (2020) "Thermal stability modulation of the native and chemically-unfolded state of bovine serum albumin by amino acids", *Phys. Chem. Chem. Phys. 22*, 179-188.

2. **Pal, S.** and Mitra, R. K. **"**Spectroscopic Investigation about the Effect of Hydrophobicity of Amino Acids as Macromolecular Crowders on the Stability of Protein" ***[Under Review]***

3. **Pal, S.** and Mitra, R. K. **"**Effect of Hydrophobic Amino Acids as Co-solutes on the Enzymatic Activity of Lysozyme" ***[Manuscript to be submitted]***

4. **Pal, S.** Samanta, N.and Mitra, R. K. " Role of Hydration Dynamics on the Contrasting Behavior of Guanidinium Chloride and Guanidinium Sulphate on the Stability of Human Serum Albumin" ***[Manuscript under preparation]***

# *Abbreviations*

| | |
|---|---|
| **AA** | Amino Acid |
| **BSA** | Bovine Serum Albumin |
| **CD** | Circular Dichroism |
| **DSC** | Differential Scanning Calorimetry |
| **FTIR** | Fourier Transform Infrared Spectroscopy |
| **GdmCl** | Guanidinium Chloride |
| **HEWL** | Hen Egg White Lysozyme |
| **HSA** | Human Serum Albumin |
| **SASA** | Solvent Accessible Surface Area |
| **THz** | Terahertz |
| **Trp** | Tryptophan |
| **TTDS** | Terahertz Time Domain Spectroscopy |
| **UV** | Ultra-Violet |

# *Abstract*

Several co-solutes like salts, osmolytes, nucleic acids, peptides, proteins etc. surrounding body cells create crowded environment around cells. The protein folding equilibrium is modulated by these co-solutes in different ways, however, an accurate concept stands intangible. To understand the co-solute size-effect, macromolecular crowders are generally compared to their monomeric building blocks though the molecular level studies for protein crowders are not well reported till now. Hence, how single amino acids modulate the protein folding equilibrium is still very obscure. We have addressed the effect of some amino acids (Glycine, L-Alanine, L-Arginine, L-Proline) on the stability of a model globular protein bovine serum albumin (BSA) upon thermal and urea-induced unfolding using spectroscopic and calorimetric techniques. This study manifests that hydration effects play a significant role to understand their effect. Apart from that, to investigate the hydrophobic effect of co-solutes, we have taken different non-polar hydrophobic amino acids (L-Valine, L-Leucine and L-Isoleucine) to study the structural and thermal stability of different proteins (Human serum albumin, Lysozyme and Ribonuclease-A) containing varying α-helical content using circular dichroism (CD) measurement procedure. Our study affirms that the conformational stability of proteins and the associated thermodynamics do not depend on the hydrophobicity of these amino acids, rather they are protein specific where α- helicity of the protein has significant contribution. We have also investigated the role of these non-polar amino acids on the enzymatic activity of lysozyme towards a dead cell (M. Lys.) acting as a substrate. It has been found that except Ile, all other amino acids show a bell shaped profile of catalytic efficiency ($k_{cat}/K_m$) of lysozyme with the increasing concentration of used amino acids. The trend of activation energy ($E_a$) is also well correlated with the catalytic efficiency of lysozyme. This activity study explores that at low concentration of amino acids, soft interaction predominates whereas, at higher concentration range excluded volume, viscosity, hydrophobicity combinedly decrease the activity of lysozyme. In another work,

## Abstract

I have tried to look into the contrasting behavior of two Guanidinium salts; Guanidinium chloride (GdmCl) is a well-known strong protein denaturant whereas, Guanidinium sulphate ($Gdm_2SO_4$) stabilizes the protein slightly by observing their opposite hydration dynamics using Mid-infrared (MIR) and Terahertz time-domain spectroscopic (TTDS) measurement techniques. It has been explored that neither individual cation nor anion controls the hydration dynamics rather their combined effect alters the water structure network which influences the stability of the protein.

# Chapter 1

## Introduction

Biomolecules, the organic polymers produced in living cells and organisms, are essential to control the cellular processes. The sizes and structures of biomolecules are very broad and they are responsible for different biological functions such as development of living body, morphogenesis, cell division and many others.[1] Several small and large substances fall under this category of biomolecules; among them protein is one of the major contributors which is the main building block of the living body. It plays pivotal role in several processes of living organisms such as transport, reception, storage, signal transmission, enzyme catalysis, pH maintenance, balances of body fluids etc.[2-13] Proteins are composed of polypeptide chains maintaining a particular sequence of twenty canonical amino acids occurring in nature and commonly familiar as *building components of proteins*; nine of them are called essential and can be consumed through diet, while five of them are non-essential and formed by our human body. Each amino acid contains a central alpha (α) carbon atom bonded with a common carboxyl (COOH) group and an amino ($NH_2$) group. Amino acids can take three different ionization forms based upon the pH of the medium; (a) cationic (COOH and $NH_3^+$), (b) zwitterionic ($COO^-$ and $NH_3^+$) and (c) anionic ($COO^-$ and $NH_2$). On the basis of sequential ordering and arrangement of amino acids, protein's structure can be classified into four types; (a) *primary*, (b) *secondary*, (c) *tertiary* and (d) *quaternary*. The linear pattern of canonical amino acids linked by the peptide chain to form the entire protein is called primary structure of that protein.[14] The repeated, regular spatial arrangement of adjacent amino acid residues in a chain of polypeptides forms the secondary structure which consists of four major parts: α-helix, β-sheet (parallel and anti-parallel), β-turn and random coil. The right handed coiled strand stabilized by hydrogen bonds formed amidst the hydrogen atoms of amide bond and oxygen atoms of the carbonyl bond in backbone of a peptide is known as α-helix. In β-sheet conformation, hydrogen bond develops among oxygens of the carbonyl bond of one strand and hydrogens of amide bond with adjacent strand. Several sheets are lying side by side either in parallel fashion or in anti-

parallel conformation. The peptide backbone's orientation of four consecutive amino acids changes in β-turn and folds the protein whereas, in random coil conformation the secondary structure of protein completely breaks and protein no longer retains its native structure.[15] The complete three-dimensional configuration of a chain of polypeptide is called the tertiary structure stabilized by various interactions like ionic, dipole-dipole, hydrogen bonding, hydrophobic, covalent disulphide linkages (S-S) etc. between hydrophilic and hydrophobic moiety of amino acids.[16] The quaternary structure of protein is formed by the tightly packing arrangement of several protein chains or subunits attached by the hydrogen bonds and van der Waals interactions among side chains of hydrophobic moiety.[17]

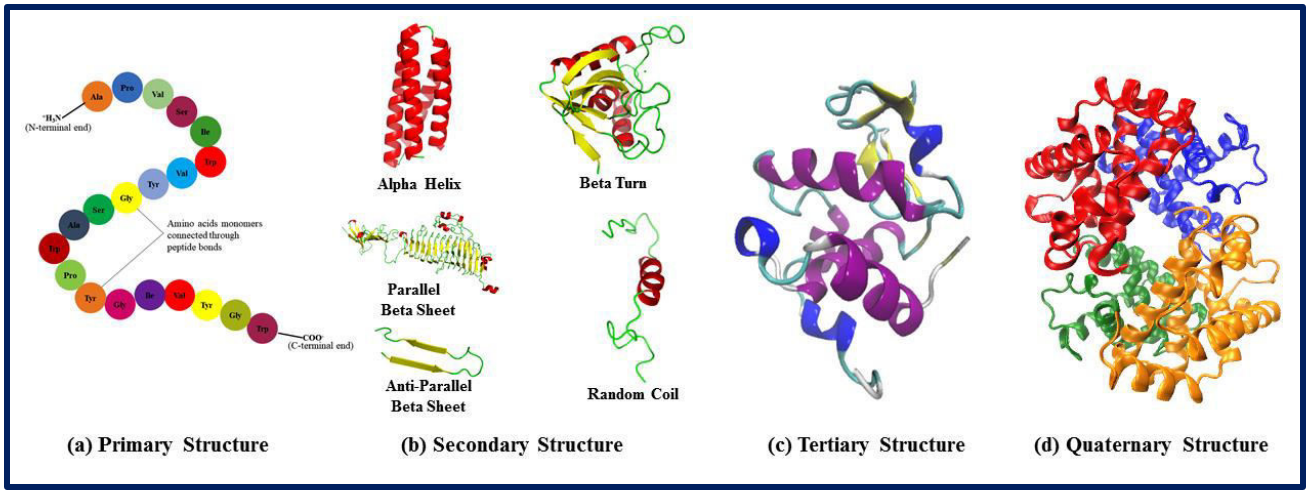


**Figure 1.1:** Representation of (a) Primary, (b) Secondary, (c) Tertiary and (d) Quaternary structures of protein.

Depending on the charges at neutral pH and water accessibility of their side chains, amino acids (AA) are of two types: hydrophilic or polar amino acids and non-polar or hydrophobic amino acids. Each amino acid is abbreviated by three letter word. Polar amino acids can be of two types: acidic (Asp, Glu) which contains more number of carboxyl (COOH) groups in its side chains; whereas, basic (Arg, Lys, His) is composed of more number of amino ($NH_2$) groups in its side chains. Non-polar amino acids (Trp, Ile, Gly, Val, Ala, Leu, Pro, Cys, Phe, Met) contain non-polar carbon atoms as their side-chains. The extensive network of salt-bridges created by interaction of the side chains of polar residues on protein's surface gives thermo-stability in thermophilic organisms and arrest them from denaturation at higher temperatures.[18-19] Amino acids containing the non-polar groups primarily reside inside a protein forming the hydrophobic

core and participate in protein folding process through its van der Waals interactions and disulphide (S-S) bridges.[20-22] Non-polar amino acids are considered as amphiphilic consisting of two parts: (a) a hydrophobic tail part and (b) a head part composed of polar groups. So, structure of proteins is visualized as inner hydrophobic core surrounded by surface layer of hydrophilic groups of amino acid constituents. Protein folding process is mostly studied in aqueous medium[23-25] where, several intermolecular and non-covalent interactions are primarily governed by the specific properties of solvent (water) molecule. Strong interaction between the water molecules results to collapse the hydrophobic moieties of amino acid residues (termed as *hydrophobic interaction*) and by minimizing interface area between hydrophilic surface as well as hydrophobic core, protein gets compact structure and thus the folding occurs.[26-28] Protein folding process is heavily influenced by the hydrophobic effect and the thermodynamic factors behind this is not still understood completely. The strength of hydrophobic effect decreases with lowering of temperature and this is probably the main reason of cold denaturation of proteins.[29]

Both the intracellular and extracellular environments in living cells are considered as heterogeneous on account of several organic and inorganic substances present in it and they are called as "*osmolytes*" due to the maintenance as well as balances of osmotic pressure in living organisms.[30-34] There are large number of macromolecules and other different bio-chemical substances that are inhabited approximately half of the total volume of our living cells.[35-36] Since no single molecule can survive in high concentration, such a densely environment is termed as "*crowded"*. In this crowded milieu, stability and activity of protein are very important because proteins are mainly operative in its folded or native form and unfolding or misfolding or aggregation often create several diseases[37-38] and the collapse of the various part of a living body. For example, several neurodegenerative disorders or diseases like Parkinson, Hungtington, Alzheimer, Hemolytic anemia, Cystic fibrosis etc. originate due to the aggregation or fibrillation of misfolded form of proteins of a particular amino-acid sequence under certain physiological conditions like temperature, pressure, pH etc.[38-41] One of the most regular distinguishing characteristics of those disorders is increment of β-sheet of the secondary structure of protein with simultaneous decrease of the content of α-helices.[42] Studies by different groups showed that certain osmolytes (sugars, polyols, TMAO, amino acids e.g. proline, lysine, arginine) of different specific mixtures can act as therapeutic agents against such particular amyloid aggregates.[43-46] Depending on the protection of living organisms from environmental stress, osmolytes can be

classified into two categories: (a) "*counteracting osmolytes*" (betaine, TMAO) which can modify protein functionality and stability[47], and (b) "*compatible osmolytes*" (sucrose, glycine, proline and some amino acid derivatives) which can only influence the protein stability.[48] Apart from those, there is another special category of osmolytes called "*chemical denaturants*" e.g. urea, guanidinium chloride, guanidinium thiocyanate; which breaks the quaternary, tertiary and secondary structures of native state and as a result, protein loses its biological activity.[49-60] This demands in-vivo study of stability, functionality and activity as well as dynamics of hydration for solvation layers of protein under the nose of different types of co-solutes and osmolytes which is a challenging task. Due to this experimental short-comings, researchers have artificially mimicked (in-vitro study) the protein stability in crowding environment by externally adding chemical denaturants and stabilizing osmolytes. It has been observed that properties of protein such as stability, aggregation and activity are altered significantly in this crowded environment[35, 61-81] and such behavior can be explained mainly by two factors: (a) hard sphere "*excluded volume*" theory[82-86] and (b) soft or preferential interactions.[82, 86-90] In case of hard spherical molecules, the sum of the radii of two closest one allows them to approach one another. It creates an "*excluded volume*" that is defined as the unavailable space or volume of one co-solute due to presence of another co-solute[91]. Owing to substantial co-volume capacity of the unfolded condition compared to the folded one, such volume exclusion can stabilize folded state by destabilizing the denatured state.

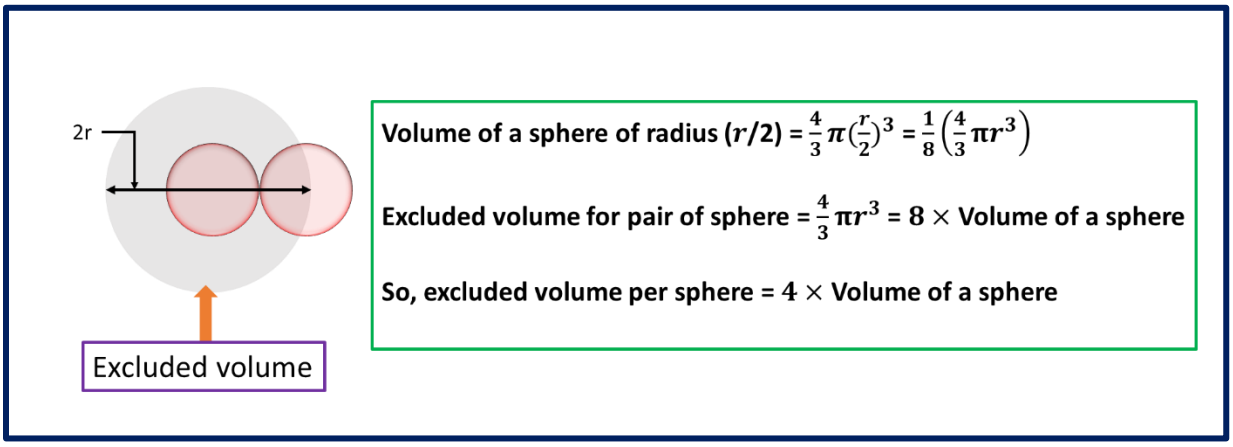


**Figure 1.2:** Schematic diagram of excluded volume and related calculation

In order to comprehend the excluded volume effect in solvated medium, scaled particle theory[92-93] (SPT) is commonly used trustworthy tool to determine the excluded volume segment of the solute which is related to its free energy transfer also. The microscopic and macroscopic hydrophobic effect can be correlated by this SPT which is a practical generalization based on identifying a molecular length serves as a useful radius to connect the macroscopic and microscopic illustrations. Excluded volume theory can be applied on the effect of co-solutes on equilibrium properties of macro-solutes and its preferential interaction with co-solvent, association reactions to form macromolecular complex, diffusive transport of co-solutes and the rate of enzyme catalyzed reactions[94]. Soft chemical interactions can be of two types: non-specific and native-state interactions. Urea, TMAO interact with the protein backbone via non-specific interactions and depending on the extent of interactions, they can destabilize[95] (urea) or stabilize[96] (TMAO) secondary structure of protein. Small molecules (amino acids) stabilize proteins by binding specifically to the native state and such native-state interactions can also change the chemical environment of a particular protein region and have a profound effect on the protein stability in crowded medium[97].

Every proteins generally try to retain its native conformation because of its minimum energy. Perturbation of external environment of protein by several factors like addition of chemical denaturants, increment of temperature, pH of the medium, dehydration can cause denaturation which increases the energy of protein.[98-99] Figure 1.3 showing the energy map of protein clearly dictates that native condition of protein is energetically one of the best stable state. Denaturation unfolds the protein structure gradually passing through molten globule state intermediate which is the semi-folded conformation of protein and finally leads to the fully unfolded form reaching maximum energy of the energy funnel. The corresponding Gibbs free energy of protein unfolding ($\Delta G_u$) is measured with the following equation 1.1:

$$\Delta G_u = -RT \ln K_u \ldots\ldots\ldots\ldots\ldots\ldots\ldots\ldots (1.1)$$

Here R refers to the universal gas constant, T denotes the kelvin temperature and $K_u$ stands for the equilibrium constant of the two state folding-unfolding operation which is defined as,

$$K_u = \frac{fraction\ of\ the\ unfolded\ protein}{fraction\ of\ the\ native\ protein}$$

The enthalpy change ($\Delta H$) for the two state activity can be estimated from the well-known Gibbs-Helmholtz equation which is following (equation 1.2) :

$$\frac{\partial(\Delta G_u/T)}{\partial(1/T)} = \Delta H \quad \ldots\ldots\ldots\ldots\ldots\ldots (1.2)$$

The corresponding change of entropy($\Delta S$) can be calculated by equation 3:

$$\Delta G_u = \Delta H - T\Delta S \quad \ldots\ldots\ldots\ldots (1.3)$$

From the energy diagram, it is found that the stabilization of the native form of protein is not entropy driven rather it is enthalpy driven since Gibbs free energy will be lowest for native form among the three conformations shown.

Differential scanning calorimetric (DSC) study is one of the most authentic tool to be used to estimate the enthalpy change of the unfolding event. In this technique, area beneath the curve (by integrating) between heat capacity $(C_p)$ and temperature (T) is utilized to compute the calorimetric enthalpy change ($\Delta H_{cal}$) using the equation 1.4:

$$\Delta H_{cal} = \int C_p \, dT \quad \ldots\ldots\ldots\ldots\ldots (1.4)$$

Another most important parameter, the melting temperature/transition temperature of protein, can be obtained from this experiment, is dictated by a particular point of temperature at which the surplus heat capacity reaches its extreme value. The associated van't Hoff enthalpy change ($\Delta H_{vh}$) is also be determined by using the following equation 1.5:

$$\Delta H_{vh}(T_m) = 4RT_m^2 \frac{\Delta C_p(T_m)}{\Delta H_{cal}} \quad \ldots\ldots\ldots\ldots\ldots\ldots\ldots (1.5)$$

Where, $\Delta C_p(T_m)$ is the corresponding heat capacity value at the melting point $(T_m)$ of the two state operation. From this change of the heat capacity ($\Delta C_p$) value, the change of entropy ($\Delta S$) for this process can be evaluated by integrating $C_p$ versus T curve which is given by,

$$\Delta S = \int \frac{C_p}{T} \, dT \quad \ldots\ldots\ldots\ldots\ldots\ldots (1.6)$$

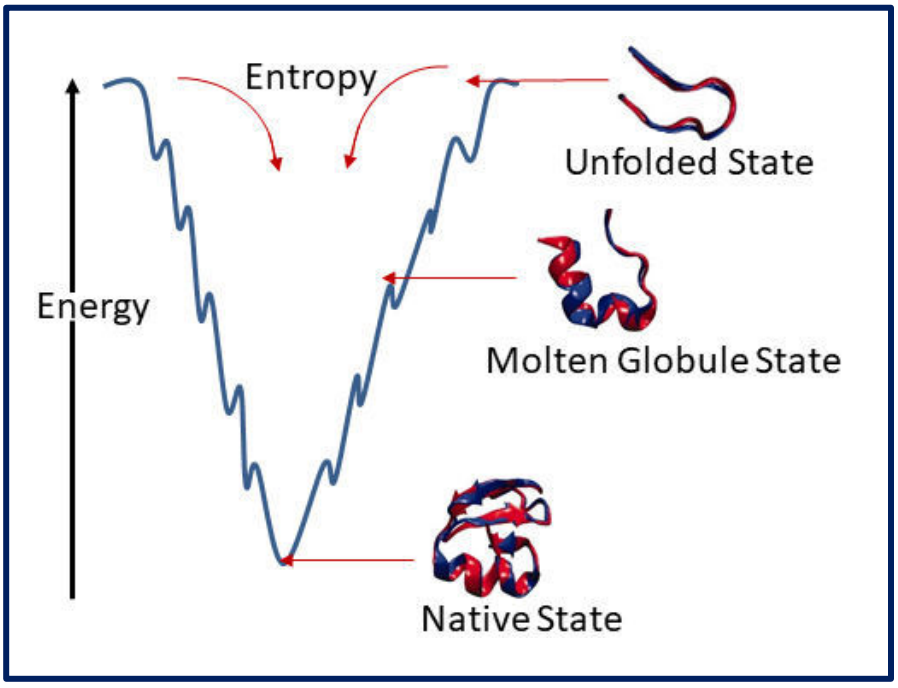


**Figure 1.3:** Energy landscape of folding-unfolding process of protein

Among various crowding agents, proteins and several bio-chemical molecules like amino acids, nucleic acids, peptides are capable to produce good crowding habitat to mimic the cellular environment.[100-107] From earlier studies it has been observed that amino acid can also be treated as stabilizer of protein folding process.[108-110] This motivates me to explore the role of amino acids as macromolecular crowders in the protein folding unfolding pathway. From the previous studies, it has been also found that several characteristics of protein e.g. folding-unfolding mechanism, aggregation, activity and hydration dynamics are largely modulated with the increase of hydrophobicity of the co-solutes.[111-113] In this regard, we have chosen a series of hydrophobic amino acids to investigate their effect on protein stability.

Since protein is biologically most active in its native state, the study of stability and activity of protein in various conditions is of immense importance. Proteins often act as biological catalyst (termed as *enzyme*) in cellular and tissue metabolism processes; in addition it can escalate the rate of biochemical events in living organisms.[114-115] The release of enzyme and the increase of its activity is due to the damage of cells of living body occurring in tissue-breakdown and neuro-muscular diseases.[116] In earlier days, the lock and key model[117-119] has been considered for the

enzymatic action where it is assumed that the appropriate enzyme should have complementary shape in relation to the active site of substrate to properly fit. Nowadays, the induced-fit model[117-121] is more acceptable for enzyme mechanism where the enzymes should be flexible enough to reorganize their shapes accordingly to fit into the substrate. The surface behavior of key residues of enzyme is modulated by different factors like hydrophobic effect, conformational change of enzyme and electrostatic interactions.[122-129] Apart from this, the activity and the selectiveness for a particular substrate can be modulated by proper immobilization of that enzyme.[130-133] Over the few decades, much effort was given to observe the importance of hydrophobic effect on enzymatic activity[134-135]. Lien et.al[136] illustrated that hydrophobic interactions plays vital role in enzyme inhibition process by applying on several enzymes. Alkema et.al[137] studied the role of hydrophobic residues on the catalytic activity of penicillin acylase on the hydrolysis of β-lactam by mutating the active site with Tyr, Trp, Ala and Leu and found 40% decrease in activity in case of Tyr and Trp, whereas, 3% increment for Ala and Leu. The importance of hydrophobicity of Trp moiety residing in the active site of chicken lysozyme to maintain the function, stability, structure of enzyme and efficient binding with substrate was explained by Imoto et.al[138]. In this context, externally adding hydrophobic amino acids as a crowding agent is a much demanded topic of research to observe the enzyme activity and also the temperature dependence of activity.

The main perspective of this thesis is to examine protein folding and unfolding pathway and its accompanied thermodynamic properties (melting temperature, free energy, enthalpy, heat capacity and entropy change), structural perturbation in presence of externally added osmolytes with variable hydrophobicity and some chemical denaturants. The secondary and tertiary structure of model protein molecules (e.g. serum albumin of bovine and human, lysozyme, Ribonuclease-A etc.) in presence of osmolytes (amino acids with different chain-length) and some chemical denaturants (urea, guanidinium salts) has been investigated with the circular dichroism (CD) spectroscopic measurement. The above mentioned thermodynamic parameters and the associated energetic cost of the protein folding-unfolding phenomena is calculated with the help of differential scanning calorimetry (DSC) instrument and temperature dependent CD measurement. Local environment of the protein molecules is measured by observing the change of Trp (intrinsic fluorescence) moiety. Activity of protein (enzyme) and temperature dependent kinetics have been observed by UV-visible spectrophotometer.

The characteristics of water at the surface of protein are very discrete from the bulk which control several activities of protein like binding, recognition, catalysis, denaturation etc. Numerous studies have been performed by various groups to explore the hydration dynamics around protein though most of them are contradicting to each other.[139-141] On the flip side, GdmCl has been recognized as a commonly studied denaturing representative of protein[51] though the actual reason for this denaturation on the basis of hydration dynamics is still debatable. It is believed that the guanidinium cation ($Gdm^+$) directly interacts with the backbone of protein and this is the primary cause of strong denaturation behavior of GdmCl; even though in recent days, several groups claimed that planarity and high surface propensity of $Gdm^+$ is the main reason. But the unusual stabilizing behavior of $Gdm_2SO_4$ on protein structure is still elusive though both contain the same cation. An earlier report by Hippel and Wong showed that addition of $Gdm_2SO_4$ solution increases the melting temperature ($T_m$) of Ribonuclease; whereas, it goes opposite direction with the concentration of GdmCl.[142] Later, the stabilizing activity of $Gdm_2SO_4$ to the native state of globular protein was comprehensively authenticated by applying action on several proteins by Mitra and co-workers.[143] Arakawa and Timasheff manifested that the preferential interaction parameter of BSA (i.e. preferential hydration) increased linearly with $Gdm_2SO_4$ concentration, whereas, GdmCl showed increment of the preferential binding of salt with its concentration.[144] Gordon experimentally observed that the capacity of GdmCl to solubilize of a model peptide named as N-acetyltetraglycine ethyl ester in water increased with its continuous addition; but the solubility was steadily decreased with the concentration of $Gdm_2SO_4$.[57] In the same manner, GdmCl elevates critical micellar concentration (CMC) of a non-ionized detergent called Triton X-100, while $Gdm_2SO_4$ lowers it and stabilizes micelles.[145] Another interesting qualitative difference between those two guanidinium salts was noticed by Kumar et al. where the group dictated that aqueous GdmCl solutions hinder the Diels-Alder reaction rate between methylacrylate and cyclopentadiene system and diminish the yield of the major endo products, in comparison to the accelerating effect of aqueous $Gdm_2SO_4$ solutions.[146] To unravel the ambiguity regarding these contrasting behavior of GdmCl and $Gdm_2SO_4$ and the role of water dynamics on the denaturation process of proteins, another part of this thesis depicts the oscillations of water molecules around a model protein (HSA) in front of guanidinium salts (GdmCl, $Gdm_2SO_4$) as well as two inorganic salts (NaCl, $Na_2SO_4$) using terahertz spectroscopic techniques and Fourier transform infrared (FTIR) measurements.

## Outline of the thesis:

The dissertation is formulated in the following chapters (*Ch*) apart from this introductory section:

**Chapter 2** describes the different techniques used for performing the whole work done of the thesis. The information about the materials used for the entire study has been also provided here.

**Chapter 3** inspects the impact of several L-amino acids (Gly, Ala, Pro, Arg) on thermal strength of a globular protein BSA as well as urea-mediated partial denaturation. We observed that amino acids can adjust the folding-unfolding pathway of BSA without ensuing a specific pattern on solvent accessible surface area (SASA) or hydrophobicity of those amino acids.

**Chapter 4** demonstrates the effect of different non-polar hydrophobic amino acids on different proteins (HSA, lysozyme and RNase-A) containing varying helicity and found that amino acids stabilize the secondary structure of proteins to various extents. From the results we have also found that the conformational stability and the associated thermodynamic parameters do not depend on the hydrophobicity of amino acids; rather, these are protein specific and the α-helicity of the protein plays significant role in it.

**Chapter 5** discusses about the enzymatic activity of model enzyme lysozyme on a dead cell bacteria Micrococcus lysodeikticus (M. Lys.) in association with different non-polar hydrophobic amino acids and found unusual trend where activity increases with increasing concentration for Glycine and Isoleucine; but activity decreases at high concentration in presence of Alanine, Valine and Leucine.

**Chapter 6** examines the contrasting hydration behavior of GdmCl and $Gdm_2SO_4$ on a model protein HSA explained by THz spectroscopy and Mid-infrared FTIR measurement technique.

**Chapter 7** provides the summary and future outlook of this thesis.

## 1.2 Bibliography


1. Berg, J. M.; Tymoczko, J. L.; Stryer, L., Biochemistry, 5th edition. **2002**.
2. Quick, M.; Javitch, J. A., Monitoring the function of membrane transport proteins in detergent-solubilized form. *Proc. Natl. Acad. Sci.* **2007,** *104*, 3603-3608.
3. Hurrell, R. F.; Finot, P. A., Food processing and storage as a determinant of protein and amino acid availability. *Experientia. Suppl.* **1983,** *44*, 135-156.
4. Erbersdobler, H. F., Protein reactions during food processing and storage--their relevance to human nutrition. *Bibl. Nutr. Dieta.* **1989,** (43), 140-155.
5. Rosenbaum, D. M.; Rasmussen, S. G. F.; Kobilka, B. K., The structure and function of G-protein-coupled receptors. *Nature* **2009,** *459*, 356-363.
6. Vaidehi, N.; Floriano, W. B.; Trabanino, R.; Hall, S. E.; Freddolino, P.; Choi, E. J.; Zamanakos, G.; Goddard, W. A., III, Prediction of structure and function of G protein-coupled receptors. *Proc. Natl. Acad. Sci.* **2002,** *99*, 12622-12627.
7. Schenk, P. W.; Snaar-Jagalska, B. E., Signal perception and transduction: the role of protein kinases. *Biochim. Biophys. Acta* **1999,** *1449*, 1-24.
8. Lee, M. J.; Yaffe, M. B., Protein Regulation in Signal Transduction. *Cold Spring Harb. Perspect. Biol.* **2016,** *8*, 1-19.
9. Agarwal, P. K., A Biophysical Perspective on Enzyme Catalysis. *Biochemistry* **2019,** *58*, 438-449.
10. Callender, R.; Dyer, R. B., The Dynamical Nature of Enzymatic Catalysis. *Acc. Chem. Res.* **2015,** *48*, 407-413.
11. Wu, S.; Snajdrova, R.; Moore, J. C.; Baldenius, K.; Bornscheuer, U. T., Biocatalysis: Enzymatic Synthesis for Industrial Applications. *Angew. Chem. Int. Ed.* **2021,** *60*, 88-119.
12. Watson, P. D., Modeling the effects of proteins on pH in plasma. *J. Appl. Physiol.* **1999,** *86*, 1421-1427.
13. Talley, K.; Alexov, E., On the pH-optimum of activity and stability of proteins. *Proteins* **2010,** *78*, 2699-2706.
14. Sanvictores, T.; Farci, F., Biochemistry, Primary Protein Structure. In *StatPearls*, 2021.
15. Rehman, I.; Farooq, M.; Botelho, S., Biochemistry, Secondary Protein Structure. In *StatPearls*, 2021.
16. Rehman, I.; Kerndt, C. C.; Botelho, S., Biochemistry, Tertiary Protein Structure. In *StatPearls*, 2021.
17. Janin, J.; Bahadur, R. P.; Chakrabarti, P., Protein-protein interaction and quaternary structure. *Q. Rev. Biophys.* **2008,** *41*, 133-180.
18. Razvi, A.; Scholtz, J. M., Lessons in stability from thermophilic proteins. *Protein Sci.* **2006,** *15*, 1569-1578.
19. Hollien, J.; Marqusee, S., Structural distribution of stability in a thermophilic enzyme. *Proc. Natl. Acad. Sci* **1999,** *96*, 13674-13678.

20. Camilloni, C.; Bonetti, D.; Morrone, A.; Giri, R.; Dobson, C. M.; Brunori, M.; Gianni, S.; Vendruscolo, M., Towards a structural biology of the hydrophobic effect in protein folding. *Sci Rep.* **2016,** *6*, 28285.
21. Dyson, H. J.; Wright, P. E.; Scheraga, H. A., The role of hydrophobic interactions in initiation and propagation of protein folding. *Proc. Natl. Acad. Sci* **2006,** *103*, 13057-13061.
22. Ibal, G.; Oye, B.; Joo, H.; Tsai, J., Hydrophobic Effect: The Entropic Structure of the Protein Hydration Interface. *Biophys. J* **2018,** *114*, 49A.
23. Dill, K. A.; Ozkan, S. B.; Shell, M. S.; Weikl, T. R., The Protein Folding Problem. *Annu. Rev. Biophys* **2008,** *37*, 289-316.
24. Ben-Naim, A., One-dimensional model for water and aqueous solutions. IV. A study of "hydrophobic interactions". *J. Chem. Phys.* **2008,** *129*, 104506.
25. Ben-Naim, A., Theoretical aspects of self-assembly of proteins: A Kirkwood-Buff-theory approach. *J. Chem. Phys.* **2013,** *138*, 224906.
26. Mattos, C.; Clark, A. C., Minimizing frustration by folding in an aqueous environment. *Arch. Biochem. Biophys.* **2008,** *469*, 118-131.
27. Gadzała, M.; Dułak, D.; Kalinowska, B.; Baster, Z.; Bryliński, M.; Konieczny, L.; Banach, M.; Roterman, I., The aqueous environment as an active participant in the protein folding process. *J. Mol. Graph. Model.* **2019,** *87*, 227-239.
28. Ben-Naim, A., Myths and verities in protein folding theories: From Frank and Evans iceberg-conjecture to explanation of the hydrophobic effect. *J. Chem. Phys.* **2013,** *139*, 165105.
29. Tsai, C. J.; Maizel, J. V., Jr.; Nussinov, R., The hydrophobic effect: a new insight from cold denaturation and a two-state water structure. *Crit. Rev. Biochem. Mol. Biol.* **2002,** *37*, 55-69.
30. Kinne, R. K., The role of organic osmolytes in osmoregulation: from bacteria to mammals. *J. Exp. Zool.* **1993,** *265* (4), 346-355.
31. Csonka, L. N., Physiological and genetic responses of bacteria to osmotic stress. *Microbiol. Rev.* **1989,** *53* (1), 121-147.
32. Burg, M. B.; Ferraris, J. D., Intracellular organic osmolytes: function and regulation. *J. Biol. Chem.* **2008,** *283*, 7309-7313.
33. Kumar, R., Role of naturally occurring osmolytes in protein folding and stability. *Arch. Biochem. Biophys.* **2009,** *491*, 1-6.
34. Khan, S. H.; Ahmad, N.; Ahmad, F.; Kumar, R., Naturally occurring organic osmolytes: from cell physiology to disease prevention. *IUBMB Life.* **2010,** *62*, 891-895.
35. Ellis, R. J., Macromolecular crowding: obvious but underappreciated. *Trends. Biochem. Sci.* **2001,** *26*, 597-604.
36. Fulton, A. B., How crowded is the cytoplasm? *Cell* **1982,** *30* (2), 345-347.
37. Powers, E. T.; Morimoto, R. I.; Dillin, A.; Kelly, J. W.; Balch, W. E., Biological and chemical approaches to diseases of proteostasis deficiency. *Annu. Rev. Biochem.* **2009,** *78*, 959-991.
38. Soto, C., Protein misfolding and disease; protein refolding and therapy. *FEBS Lett.* **2001,** *498*, 204-207.

39. Warrick, J. M.; Paulson, H. L.; Gray-Board, G. L.; Bui, Q. T.; Fischbeck, K. H.; Pittman, R. N.; Bonini, N. M., Expanded polyglutamine protein forms nuclear inclusions and causes neural degeneration in Drosophila. *Cell* **1998,** *93*, 939-949.
40. Chaudhuri, T. K.; Paul, S., Protein-misfolding diseases and chaperone-based therapeutic approaches. *FEBS J.* **2006,** *273*, 1331-1349.
41. Habchi, J.; Tompa, P.; Longhi, S.; Uversky, V. N., Introducing protein intrinsic disorder. *Chem. Rev.* **2014,** *114*, 6561-6588.
42. Uversky, V. N.; Li, J.; Fink, A. L., Evidence for a partially folded intermediate in alpha-synuclein fibril formation. *J Biol Chem* **2001,** *276*, 10737-44.
43. Uversky, V. N.; Li, J.; Fink, A. L., Trimethylamine-N-oxide-induced folding of alpha-synuclein. *FEBS Lett* **2001,** *509*, 31-5.
44. Tanaka, M.; Machida, Y.; Niu, S.; Ikeda, T.; Jana, N. R.; Doi, H.; Kurosawa, M.; Nekooki, M.; Nukina, N., Trehalose alleviates polyglutamine-mediated pathology in a mouse model of Huntington disease. *Nat Med* **2004,** *10*, 148-54.
45. Samuel, D.; Kumar, T. K.; Ganesh, G.; Jayaraman, G.; Yang, P. W.; Chang, M. M.; Trivedi, V. D.; Wang, S. L.; Hwang, K. C.; Chang, D. K.; Yu, C., Proline inhibits aggregation during protein refolding. *Protein Sci* **2000,** *9*, 344-52.
46. Tanaka, M.; Machida, Y.; Nukina, N., A novel therapeutic strategy for polyglutamine diseases by stabilizing aggregation-prone proteins with small molecules. *J. Mol. Med.* **2005,** *83*, 343-352.
47. Zou, Q.; Bennion, B. J.; Daggett, V.; Murphy, K. P., The Molecular Mechanism of Stabilization of Proteins by TMAO and Its Ability to Counteract the Effects of Urea. *J. Am. Chem. Soc.* **2002,** *124*, 1192-1202.
48. Yancey, P. H.; Clark, M. E.; Hand, S. C.; Bowlus, R. D.; Somero, G. N., Living with water stress: evolution of osmolyte systems. *Science* **1982,** *217*, 1214-22.
49. Rossky, P. J., Protein denaturation by urea: Slash and bond. *Proc. Natl. Acad. Sci.* **2008,** *105*, 16825-16826.
50. Das, A.; Mukhopadhyay, C., Urea-Mediated Protein Denaturation: A Consensus View. *J. Phys. Chem. B* **2009,** *113*, 12816-12824.
51. Camilloni, C.; Rocco, A. G.; Eberini, I.; Gianazza, E.; Broglia, R. A.; Tiana, G., Urea and guanidinium chloride denature protein L in different ways in molecular dynamics simulations. *Biophys. J.* **2008,** *94*, 4654-4661.
52. Bennion, B. J.; Daggett, V., The molecular basis for the chemical denaturation of proteins by urea. *Proc. Natl. Acad. Sci.* **2003,** *100*, 5142-5147.
53. Hua, L.; Zhou, R.; Thirumalai, D.; Berne, B. J., Urea denaturation by stronger dispersion interactions with proteins than water implies a 2-stage unfolding. *Proc. Natl. Acad. Sci.* **2008,** *105*, 16928-16933.
54. Lim, W. K.; Rösgen, J.; Englander, S. W., Urea, but not guanidinium, destabilizes proteins by forming hydrogen bonds to the peptide group. *Proc. Natl. Acad. Sci.* **2009,** *106*, 2595-2600.

55. Huerta-Viga, A.; Woutersen, S., Protein Denaturation with Guanidinium: A 2D-IR Study. *J. Phys. Chem. Lett.* **2013,** *4*, 3397-3401.
56. Castellino, F. J.; Barker, R., The denaturing effectiveness of guanidinium, carbamoylguanidinium, and guanylguanidinium salts. *Biochemistry* **1968,** *7*, 4135-4138.
57. Gordon, J. A., Denaturation of globular proteins. Interaction of guanidinium salts with three proteins. *Biochemistry* **1972,** *11*, 1862-1870.
58. Chang, J. Y.; Li, L., The unfolding mechanism and the disulfide structures of denatured lysozyme. *FEBS Lett.* **2002,** *511*, 73-78.
59. Meuzelaar, H.; Panman, M. R.; Woutersen, S., Guanidinium-Induced Denaturation by Breaking of Salt Bridges. *Angew. Chem. Int. Ed.* **2015,** *54*, 15255-15259.
60. Ahmad, F., Free energy changes in ribonuclease A denaturation. Effect of urea, guanidine hydrochloride, and lithium salts. *J. Biol. Chem.* **1983,** *258*, 11143-11146.
61. Zhou, H.-X., Influence of crowded cellular environments on protein folding, binding, and oligomerization: Biological consequences and potentials of atomistic modeling. *FEBS Lett.* **2013,** *587*, 1053-1061.
62. Kuznetsova, I. M.; Turoverov, K. K.; Uversky, V. N., What macromolecular crowding can do to a protein. *Int. J. Mol. Sci.* **2014,** *15*, 23090-23140.
63. Wang, Y.; Sarkar, M.; Smith, A. E.; Krois, A. S.; Pielak, G. J., Macromolecular Crowding and Protein Stability. *J. Am. Chem. Soc.* **2012,** *134*, 16614-16618.
64. Christiansen, A.; Wang, Q.; Cheung, M. S.; Wittung-Stafshede, P., Effects of macromolecular crowding agents on protein folding in vitro and in silico. *Biophys. Rev.* **2013,** *5*, 137-145.
65. Nakano, S.; Karimata, H. T.; Kitagawa, Y.; Sugimoto, N., Facilitation of RNA enzyme activity in the molecular crowding media of cosolutes. *J. Am. Chem. Soc.* **2009,** *131*, 16881-16888.
66. White, D. A.; Buell, A. K.; Knowles, T. P.; Welland, M. E.; Dobson, C. M., Protein aggregation in crowded environments. *J. Am. Chem. Soc.* **2010,** *132*, 5170-5175.
67. Schreck, J. S.; Bridstrup, J.; Yuan, J.-M., Investigating the Effects of Molecular Crowding on the Kinetics of Protein Aggregation. *J. Phys. Chem. B* **2020,** *124*, 9829-9839.
68. Breydo, L.; Reddy, K. D.; Piai, A.; Felli, I. C.; Pierattelli, R.; Uversky, V. N., The crowd you're in with: Effects of different types of crowding agents on protein aggregation. *Biochim. Biophys. Acta Proteins Proteom.* **2014,** *1844*, 346-357.
69. Munishkina, L. A.; Ahmad, A.; Fink, A. L.; Uversky, V. N., Guiding protein aggregation with macromolecular crowding. *Biochemistry* **2008,** *47*, 8993-9006.
70. Munishkina, L. A.; Cooper, E. M.; Uversky, V. N.; Fink, A. L., The effect of macromolecular crowding on protein aggregation and amyloid fibril formation. *J. Mol. Recognit.* **2004,** *17*, 456-464.
71. Tokuriki, N.; Kinjo, M.; Negi, S.; Hoshino, M.; Goto, Y.; Urabe, I.; Yomo, T., Protein folding by the effects of macromolecular crowding. *Protein Sci.* **2004,** *13*, 125-133.

72. Aisenbrey, C.; Bechinger, B.; Gröbner, G., Macromolecular crowding at membrane interfaces: adsorption and alignment of membrane peptides. *J. Mol. Biol.* **2008,** *375*, 376-385.
73. Wei, Y.; Mayoral-Delgado, I.; Stewart, N. A.; Dymond, M. K., Macromolecular crowding and membrane binding proteins: The case of phospholipase $A_1$. *Chem. Phys. Lipids.* **2019,** *218*, 91-102.
74. Gomez, D.; Huber, K.; Klumpp, S., On Protein Folding in Crowded Conditions. *J. Phys. Chem. Lett.* **2019,** *10*, 7650-7656.
75. Ådén, J.; Wittung-Stafshede, P., Folding of an Unfolded Protein by Macromolecular Crowding in Vitro. *Biochemistry* **2014,** *53*, 2271-2277.
76. Zimmerman, S. B.; Minton, A. P., Macromolecular crowding: biochemical, biophysical, and physiological consequences. *Annu. Rev. Biophys. Biomol. Struct.* **1993,** *22*, 27-65.
77. Rivas, G.; Minton, A. P., Macromolecular Crowding In Vitro, In Vivo, and In Between. *Trends. Biochem. Sci.* **2016,** *41*, 970-981.
78. Minton, A. P., The influence of macromolecular crowding and macromolecular confinement on biochemical reactions in physiological media. *J. Biol. Chem.* **2001,** *276*, 10577-10580.
79. Deshwal, A.; Maiti, S., Macromolecular Crowding Effect on the Activity of Liposome-Bound Alkaline Phosphatase: A Paradoxical Inhibitory Action. *Langmuir* **2021,** *37*, 7273-7284.
80. Balcells, C.; Pastor, I.; Vilaseca, E.; Madurga, S.; Cascante, M.; Mas, F., Macromolecular Crowding Effect upon in Vitro Enzyme Kinetics: Mixed Activation–Diffusion Control of the Oxidation of NADH by Pyruvate Catalyzed by Lactate Dehydrogenase. *J. Phys. Chem. B* **2014,** *118*, 4062-4068.
81. Ma, B.; Nussinov, R., Structured crowding and its effects on enzyme catalysis. *Top. Curr. Chem.* **2013,** *337*, 123-137.
82. Miklos, A. C.; Li, C.; Sharaf, N. G.; Pielak, G. J., Volume Exclusion and Soft Interaction Effects on Protein Stability under Crowded Conditions. *Biochemistry* **2010,** *49*, 6984-6991.
83. Zhou, H. X.; Rivas, G.; Minton, A. P., Macromolecular crowding and confinement: biochemical, biophysical, and potential physiological consequences. *Annu. Rev. Biophys.* **2008,** *37*, 375-397.
84. Kim, Y. H.; Stites, W. E., Effects of Excluded Volume upon Protein Stability in Covalently Cross-Linked Proteins with Variable Linker Lengths. *Biochemistry* **2008,** *47*, 8804-8814.
85. Kuznetsova, I. M.; Zaslavsky, B. Y.; Breydo, L.; Turoverov, K. K.; Uversky, V. N., Beyond the excluded volume effects: mechanistic complexity of the crowded milieu. *Molecules* **2015,** *20*, 1377-1409.
86. Mukherjee, S. K.; Gautam, S.; Biswas, S.; Kundu, J.; Chowdhury, P. K., Do Macromolecular Crowding Agents Exert Only an Excluded Volume Effect? A Protein Solvation Study. *J. Phys. Chem. B* **2015,** *119*, 14145-14156.

87. Timasheff, S. N., Protein-solvent preferential interactions, protein hydration, and the modulation of biochemical reactions by solvent components. *Proc. Natl. Acad. Sci.* **2002,** *99*, 9721-9726.
88. Schurr, J. M.; Rangel, D. P.; Aragon, S. R., A Contribution to the Theory of Preferential Interaction Coefficients. *Biophys. J.* **2005,** *89*, 2258-2276.
89. Schneider, C. P.; Trout, B. L., Investigation of Cosolute−Protein Preferential Interaction Coefficients: New Insight into the Mechanism by Which Arginine Inhibits Aggregation. *J. Phys. Chem. B* **2009,** *113* (7), 2050-2058.
90. Zhou, H.-X.; Dill, K. A., Stabilization of Proteins in Confined Spaces. *Biochemistry* **2001,** *40*, 11289-11293.
91. Kuznetsova, I. M.; Zaslavsky, B. Y.; Breydo, L.; Turoverov, K. K.; Uversky, V. N., Beyond the excluded volume effects: mechanistic complexity of the crowded milieu. *Molecules* **2015,** *20*, 1377-409.
92. Tang, K. E.; Bloomfield, V. A., Excluded volume in solvation: sensitivity of scaled-particle theory to solvent size and density. *Biophys. J.* **2000,** *79*, 2222-2234.
93. Reiss, H.; Frisch, H. L.; Lebowitz, J. L., Statistical Mechanics of Rigid Spheres. *J. Chem. Phys.* **1959,** *31*, 369-380.
94. Zimmerman, S. B.; Minton, A. P., Macromolecular crowding: biochemical, biophysical, and physiological consequences. *Annu. Rev. Biophys. Biomol. Struct* **1993,** *22*, 27-65.
95. Lim, W. K.; Rösgen, J.; Englander, S. W., Urea, but not guanidinium, destabilizes proteins by forming hydrogen bonds to the peptide group. *Proc. Natl. Acad. Sci* **2009,** *106*, 2595-600.
96. Doan-Nguyen, V.; Loria, J. P., The effects of cosolutes on protein dynamics: the reversal of denaturant-induced protein fluctuations by trimethylamine N-oxide. *Protein Sci* **2007,** *16*, 20-9.
97. Miklos, A. C.; Li, C.; Sharaf, N. G.; Pielak, G. J., Volume exclusion and soft interaction effects on protein stability under crowded conditions. *Biochemistry* **2010,** *49*, 6984-91.
98. Mallamace, F.; Corsaro, C.; Mallamace, D.; Vasi, S.; Vasi, C.; Baglioni, P.; Buldyrev, S. V.; Chen, S.-H.; Stanley, H. E., Energy landscape in protein folding and unfolding. *Proc. Natl. Acad. Sci.* **2016,** *113*, 3159-3163.
99. Wang, S.; Gu, J.; Larson, S. A.; Whitten, S. T.; Hilser, V. J., Denatured-state energy landscapes of a protein structural database reveal the energetic determinants of a framework model for folding. *J. Mol. Biol.* **2008,** *381*, 1184-1201.
100. Tyrrell, J.; Weeks, K. M.; Pielak, G. J., Challenge of Mimicking the Influences of the Cellular Environment on RNA Structure by PEG-Induced Macromolecular Crowding. *Biochemistry* **2015,** *54*, 6447-6453.
101. Gnutt, D.; Ebbinghaus, S., The macromolecular crowding effect--from in vitro into the cell. *Biol. Chem.* **2016,** *397*, 37-44.
102. Despa, F.; Orgill, D. P.; Lee, R. C., Molecular crowding effects on protein stability. *Ann. N.Y. Acad. Sci.* **2005,** *1066*, 54-66.

103. Feig, M.; Sugita, Y., Variable Interactions between Protein Crowders and Biomolecular Solutes Are Important in Understanding Cellular Crowding. *J. Phys. Chem. B* **2012,** *116*, 599-605.
104. Ghaemmaghami, S.; Oas, T. G., Quantitative protein stability measurement in vivo. *Nat. Struct. Biol.* **2001,** *8*, 879-882.
105. Dix, J. A.; Verkman, A. S., Crowding effects on diffusion in solutions and cells. *Annu. Rev. Biophys.* **2008,** *37*, 247-263.
106. Spitzer, J.; Poolman, B., How crowded is the prokaryotic cytoplasm? *FEBS Lett.* **2013,** *587*, 2094-2098.
107. Harada, R.; Tochio, N.; Kigawa, T.; Sugita, Y.; Feig, M., Reduced Native State Stability in Crowded Cellular Environment Due to Protein–Protein Interactions. *J. Am. Chem. Soc.* **2013,** *135*, 3696-3701.
108. Rumbley, J.; Hoang, L.; Mayne, L.; Englander, S. W., An amino acid code for protein folding. *Proc. Natl. Acad. Sci.*

**2001,** *98*, 105-112.
109. Taneja, S.; Ahmad, F., Increased thermal stability of proteins in the presence of amino acids. *Biochem. J.* **1994,** *303*, 147-153.
110. Yancey, P. H.; Clark, M. E.; Hand, S. C.; Bowlus, R. D.; Somero, G. N., Living with water stress: evolution of osmolyte systems. *Science* **1982,** *217*, 1214-1222.
111. Di Michele, A.; Freda, M.; Onori, G.; Paolantoni, M.; Santucci, A.; Sassi, P., Modulation of hydrophobic effect by cosolutes. *J. Phys. Chem. B* **2006,** *110*, 21077-21085.
112. Calamai, M.; Taddei, N.; Stefani, M.; Ramponi, G.; Chiti, F., Relative influence of hydrophobicity and net charge in the aggregation of two homologous proteins. *Biochemistry* **2003,** *42*, 15078-15083.
113. van der Vegt, N. F. A.; Nayar, D., The Hydrophobic Effect and the Role of Cosolvents. *J. Phys. Chem. B* **2017,** *121*, 9986-9998.
114. Robinson, P. K., Enzymes: principles and biotechnological applications. *Essays. Biochem.* **2015,** *59*, 1-41.
115. Adamson, C.; Kanai, M., Integrating abiotic chemical catalysis and enzymatic catalysis in living cells. *Org. Biomol. Chem.* **2021,** *19*, 37-45.
116. Schmidt, E.; Schmidt, F. W.; Horn, H. D.; Gerlach, U., The Importance of the Measurement of Enzyme Activity in Medicine. Academic Press: 1965; pp 651-712.
117. Koshland Jr., D. E., The Key–Lock Theory and the Induced Fit Theory. *Angew. Chem. Int. Ed.* **1995,** *33*, 2375-2378.
118. Holyoak, T., Molecular Recognition: Lock-and-Key, Induced Fit, and Conformational Selection. In *Encyclopedia of Biophysics*, Springer: 2013; pp 1584-1588.
119. Koshland, D. E., Application of a Theory of Enzyme Specificity to Protein Synthesis. *Proc. Natl. Acad. Sci.* **1958,** *44*, 98-104.
120. Tripathi, A.; Bankaitis, V. A., Molecular Docking: From Lock and Key to Combination Lock. *J. Mol. Med. Clin. Appl.* **2017,** *2*, 1-19.

121. Schmitt, E.; Tanrikulu, I. C.; Yoo, T. H.; Panvert, M.; Tirrell, D. A.; Mechulam, Y., Switching from an induced-fit to a lock-and-key mechanism in an aminoacyl-tRNA synthetase with modified specificity. *J. Mol. Biol.* **2009,** *394*, 843-851.
122. Baek, I.; Choi, H.; Yoon, S.; Na, S., Effects of the Hydrophobicity of Key Residues on the Characteristics and Stability of Glucose Oxidase on a Graphene Surface. *ACS Biomater. Sci. Eng.* **2020,** *6*, 1899-1908.
123. Hammes-Schiffer, S.; Benkovic, S. J., Relating Protein Motion to Catalysis. *Annu. Rev. Biochem.* **2006,** *75*, 519-541.
124. Henzler-Wildman, K. A.; Lei, M.; Thai, V.; Kerns, S. J.; Karplus, M.; Kern, D., A hierarchy of timescales in protein dynamics is linked to enzyme catalysis. *Nature* **2007,** *450* (7171), 913-916.
125. Osuna, S.; Jiménez-Osés, G.; Noey, E. L.; Houk, K. N., Molecular Dynamics Explorations of Active Site Structure in Designed and Evolved Enzymes. *Acc. Chem. Res.* **2015,** *48*, 1080-1089.
126. Saleh, T.; Kalodimos, C. G., Enzymes at work are enzymes in motion. *Science* **2017,** *355*, 247-248.
127. Zhou, H.-X.; Pang, X., Electrostatic Interactions in Protein Structure, Folding, Binding, and Condensation. *Chem. Rev.* **2018,** *118*, 1691-1741.
128. Vascon, F.; Gasparotto, M.; Giacomello, M.; Cendron, L.; Bergantino, E.; Filippini, F.; Righetto, I., Protein electrostatics: From computational and structural analysis to discovery of functional fingerprints and biotechnological design. *Comput. Struct. Biotechnol. J.* **2020,** *18*, 1774-1789.
129. Mader, S. L.; Lopez, A.; Lawatscheck, J.; Luo, Q.; Rutz, D. A.; Gamiz-Hernandez, A. P.; Sattler, M.; Buchner, J.; Kaila, V. R. I., Conformational dynamics modulate the catalytic activity of the molecular chaperone Hsp90. *Nat. Commun.* **2020,** *11*, 1-12.
130. Rodrigues, R. C.; Ortiz, C.; Berenguer-Murcia, Á.; Torres, R.; Fernández-Lafuente, R., Modifying enzyme activity and selectivity by immobilization. *Chem. Soc. Rev.* **2013,** *42*, 6290-6307.
131. Hanefeld, U.; Gardossi, L.; Magner, E., Understanding enzyme immobilisation. *Chem. Soc. Rev.* **2009,** *38*, 453-468.
132. Mateo, C.; Palomo, J. M.; Fernandez-Lorente, G.; Guisan, J. M.; Fernandez-Lafuente, R., Improvement of enzyme activity, stability and selectivity via immobilization techniques. *Enzyme Microb. Technol.* **2007,** *40*, 1451-1463.
133. Garcia-Galan, C.; Berenguer-Murcia, Á.; Fernandez-Lafuente, R.; Rodrigues, R. C., Potential of Different Enzyme Immobilization Strategies to Improve Enzyme Performance. *Adv. Synth. Catal.* **2011,** *353*, 2885-2904.
134. Némethy, G., Hydrophobic Interactions. *Angew. Chem* **1967,** *6*, 195-206.
135. Mitsuda, H.; Yasumoto, K.; Yamamoto, A., Inhibition of lipoxygenase by saturated monohydric alcohols through hydrophobic bondings. *Arch. Biochem. Biophys* **1967,** *118*, 664-669.

136. Lien, E. J.; Hussain, M.; Tong, G. L., Role of Hydrophobic Interactions in Enzyme Inhibition by Drugs. *Journal of Pharmaceutical Sciences* **1970,** *59*, 865-868.
137. Alkema, W. B. L.; Dijkhuis, A. J.; de Vries, E.; Janssen, D. B., The role of hydrophobic active-site residues in substrate specificity and acyl transfer activity of penicillin acylase. *Eur. J. Biochem.* **2002,** *269*, 2093-2100.
138. Inoue, M.; Yamada, H.; Yasukochi, T.; Kuroki, R.; Miki, T.; Horiuchi, T.; Imoto, T., Multiple role of hydrophobicity of tryptophan-108 in chicken lysozyme: structural stability, saccharide binding ability, and abnormal pKa of glutamic acid-35. *Biochemistry* **1992,** *31*, 5545-5553.
139. Kuntz, I. D., Jr.; Kauzmann, W., Hydration of proteins and polypeptides. *Adv. Protein Chem.* **1974,** *28*, 239-345.
140. Rupley, J. A.; Careri, G., Protein hydration and function. *Adv. Protein Chem.* **1991,** *41*, 37-172.
141. Blicharska, B.; Florkowski, Z.; Hennel, J. W.; Held, G.; Noack, F., Investigation of Protein Hydration by Proton Spin Relaxation Time Measurements. *Biochim. Biophys. Acta.* **1970,** *207*, 381-389.
142. Von Hippel, P. H.; Wong, K. Y., On the conformational stability of globular proteins. The effects of various electrolytes and nonelectrolytes on the thermal ribonuclease transition. *J. Biol. Chem.* **1965,** *240*, 3909-3923.
143. Mitra, L.; Smolin, N.; Ravindra, R.; Royer, C.; Winter, R., Pressure perturbation calorimetric studies of the solvation properties and the thermal unfolding of proteins in solution—experiments and theoretical interpretation. *Phys. Chem. Chem. Phys.* **2006,** *8*, 1249-1265.
144. Arakawa, T.; Timasheff, S. N., Protein stabilization and destabilization by guanidinium salts. *Biochemistry* **1984,** *23*, 5924-5929.
145. Gratzer, W. B.; Beaven, G. H., Effect of protein denaturation on micelle stability. *J. Phys. Chem.* **1969,** *73*, 2270-2273.
146. Kumar, A.; Phalgune, U. D.; Pawar, S. S., Contrasting effect of guanidinium salts on kinetics of the Diels–Alder reaction. *J. Phys. Org. Chem.* **2002,** *15*, 131-138.

# Chapter 2

## Experimental Techniques and Materials

## 2.1 Absorption Spectroscopy

Shimadzu UV-2600 absorption spectrometer is employed to measure absorption spectra in the ultraviolet and visible region. The schematics of a single beam spectrophotometer is shown in Figure 2.1. The baseline was recorded by taking air as reference. A tungsten lamp and a deuterated lamp are worked as visible and ultraviolet light source, respectively. A photomultiplier tube (PMT) is used as detector. The absorption of a molecule happens owing to its energetic transition from ground state to the higher energy excited state.[1] The absorbance of a molecule follows the Lambert-Beer's law as given below,

$$A = log\frac{I_0}{I} = \varepsilon cl \quad \text{..... [2.1]}$$

In this equation, A refers to absorbance of the sample, $I_0$ and I are intensity for the incident radiation and of the transmitted one respectively, $\varepsilon$ is the molar extinction coefficient for a particular wavelength at a fixed temperature, $c$ denotes the solution's concentration, $l$ indicates the path length of cuvette.

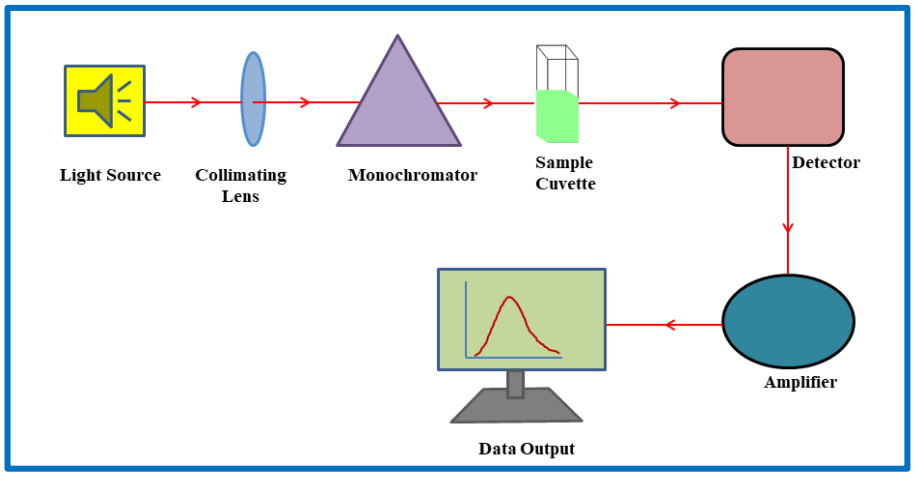


***Figure 2.1*** *Schematics of single beam UV-Visible spectrophotometer instrument.*

## 2.2 Fluorescence Spectroscopy

The time independent fluorescence signal has been recorded using HORIBA Fluorolog 3, Jobin Yvon. The schematics of the instrument is shown in Figure 2.2. The light source is ozone free xenon arc lamp; one excitation and one emission monochromator are used having reflector grating of 1200 grooves per mm accessed with 350 nm to excite sample and 520 nm for emission purpose. Both the excitation and emission slit width were kept fixed. All the spectra taken were corrected for the wavelength dependencies of each optical component. After excitation molecules reach to various excited states according to the frequency of light absorbed. Then they get back to their lowest excited state releasing energy as radiationless decay called internal conversion. Next the molecules jump to their ground energy state from the lowest excited state by emitting energy as the form of radiation known as fluorescence.[1]

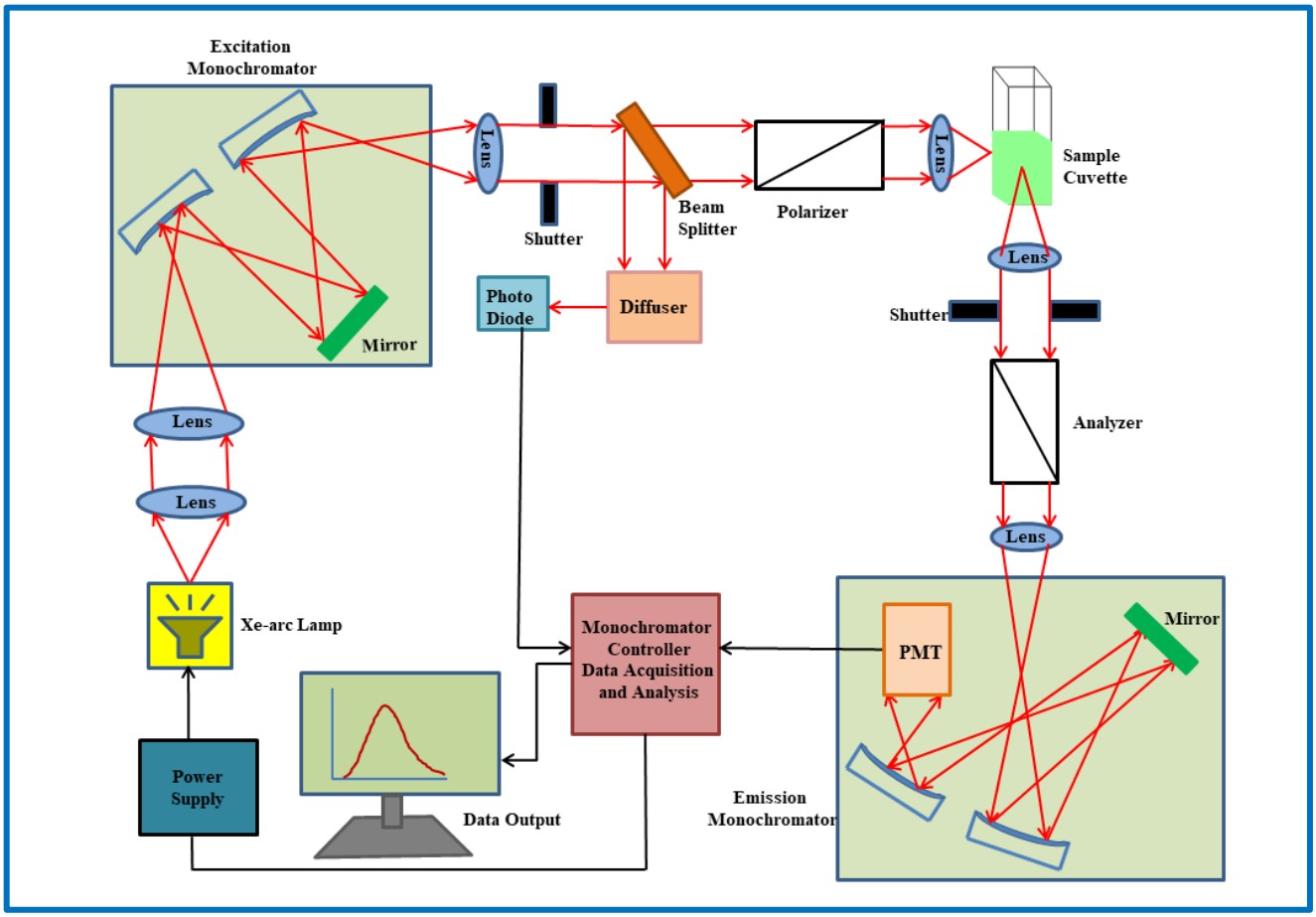


***Figure 2.2*** *Schematics of single beam steady state spectrofluorometer instrument.*

## 2.3 Circular Dichroism (CD) Spectroscopy

The conformational perturbation of protein at constant temperature in various environment is monitored using JASCO J-815 spectrometer attached with a chiller. To measure temperature induced experiments, a Peltier has been attached with the main instrumentation set-up. The experimental solutions are taken in a quartz cell cuvette having path-length of 0.1 cm. Light source of this instrument is a xenon lamp and nitrogen gas is purged to make it ozone free. The schematics of the instrument is shown in figure 2.3. Circular dichroism (CD) is described as the difference in absorption between left-handed (L) and right handed (R) circularly polarized light and creates signal if the sample comprises of at least one chiral centre.

$$\text{CD} = A_L(\lambda) - A_R(\lambda)$$

Molar ellipticity is superior unit compared to CD value because the former removes the concentration impact of protein. It is denoted by:

$$Molar\ ellipticity = \frac{observed\ CD\ value\ (mdeg)}{10 \times\ pathlength\ of\ cuvette(cm) \times\ concentration\ of\ protein\ (M)}$$

Here, a conventional two-state folding-unfolding pathway of protein is followed amidst native form 'N' and unfolded form 'U'. The equilibrium constant (K) at any given temperature (T) for this process is described as:

$$K(T) = \frac{[U]}{[N]} \quad \text{.....} \quad [2.2]$$

In this case, [U] and [N] are the molar concentrations of the unfolded and the native conditions, respectively. The native fraction (φ) designated as the fraction of native form is as follows:

$$\varphi = \frac{[N]}{[N]+[U]} \quad \text{.....} \quad [2.3]$$

$$K = \frac{(1-\varphi)}{\varphi} \quad \text{.....} \quad [2.4]$$

The temperature dependent native fraction, φ(T) is defined as:

$$\varphi(T) = \frac{([\theta]_T - [\theta]_U)}{([\theta]_N - [\theta]_U)} \quad \ldots\ldots\ldots\ldots\ldots\ldots\ldots\ldots\ldots\ldots\ldots\ldots \quad [2.5]$$

Here, $[\theta]_T$ , $[\theta]_N$ *and* $[\theta]_U$ signify the corresponding ellipticity values at every temperature, for the native and unfolded condition, respectively. One important parameter called $T_m$ is identified as the melting temperature of protein where free energy change for the above mentioned two state operation becomes zero. In most of the cases, φ(T) versus T plot looks like a sigmoidal curve and $T_m$ is the point at which φ(T) = 0.5.

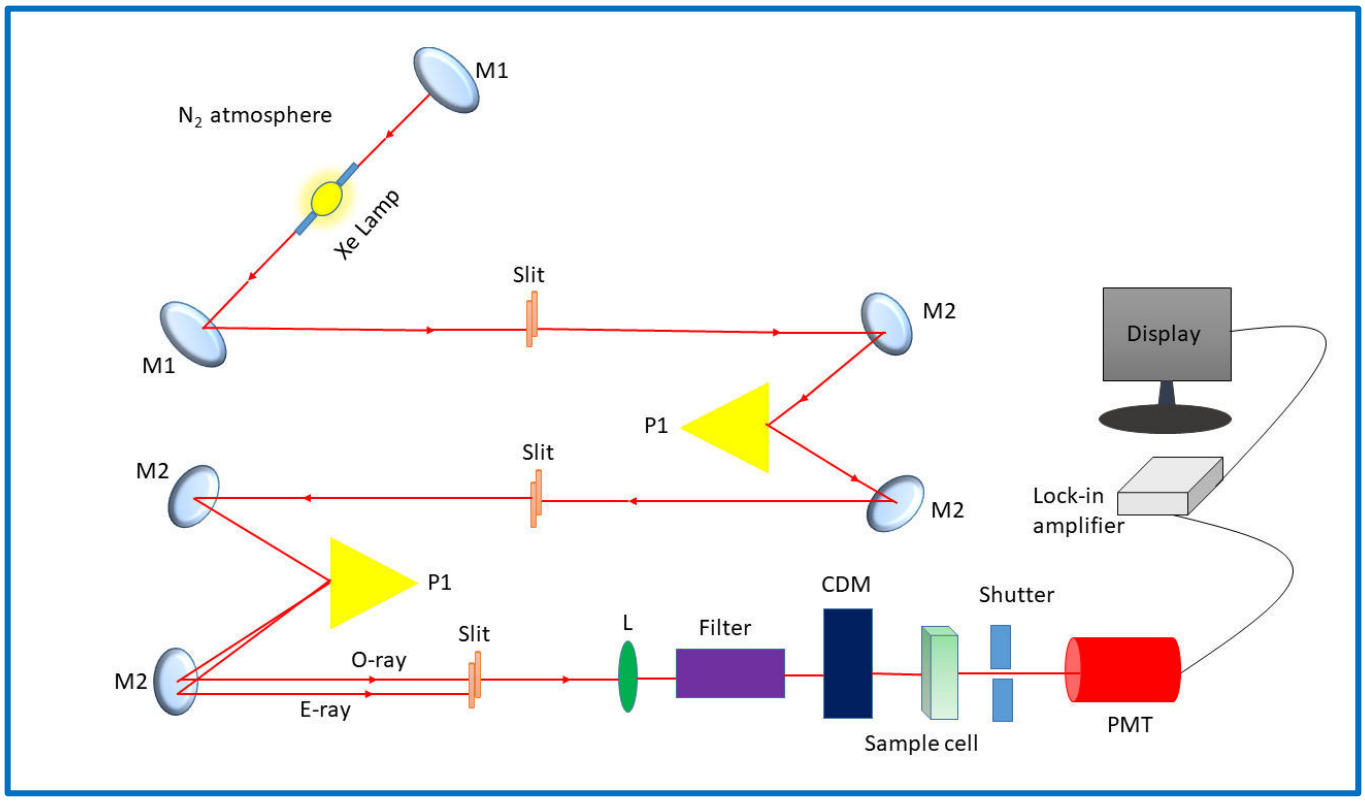


***Figure 2.3*** *Schematics of circular dichroism (CD) spectrometer instrument.*

## 2.4 Differential Scanning Calorimetry (DSC)

Several thermodynamic parameters like enthalpy, entropy, free energy, heat capacity were estimated using MicroCal PEAQ-DSC instrument of Malvern Panalytical (in collaboration with Institute for Physical and Theoretical Chemistry, Braunschweig, Germany) at the scanning speed of 90 ºC/hour (in absence of feedback method) in the temperature span of 20-95 ºC. The schematic diagram of this instrument is shown in figure 2.6. Regular same pressure is supplied to the measuring liquid in reference as well as in sample cell to prevent evaporation or boiling of the liquids. The temperature dependent structural transitions of protein were also monitored using DSC spectroscopy. To check the reproducibility of the data, various buffer-buffer or cosolute-cosolute sample record in the identical situations before every measurement of the protein sample and the last scan is utilized for baseline corrections. The calorimetric enthalpy ($\Delta H_{cal}$) value is estimated by integrating the curve between surplus molar heat capacity ($C_p$) and temperature (T) of every transformation.

$$\Delta H_{cal} = \int C_p \, dT \quad \text{..... [2.6]}$$

This is true regardless of any method. The correlated van't Hoff enthalpy ($\Delta H_v$) is calculated as

$$\Delta H_v(T_m) = 4RT_m^2 \frac{\Delta C_p(T_m)}{\Delta H_{cal}} \quad \text{..... [2.7]}$$

All the data were analyzed with Microcal PEAQ-DSC software which applies a non-linear equation with the help of Levenberg-Marquardt least-square procedures to fit the temperature dependent heat capacity data. The fitting equation represented by equation 2.8 is shown below:

$$C_p(T) = B_0 + B_1(T) + \left[\frac{K(T)\Delta C_p}{1+K(T)} + \frac{K(T)\Delta H_v(T)\Delta H_{cal}(T)}{(1+K(T))^2 RT^2}\right] \quad \text{..... [2.8]}$$

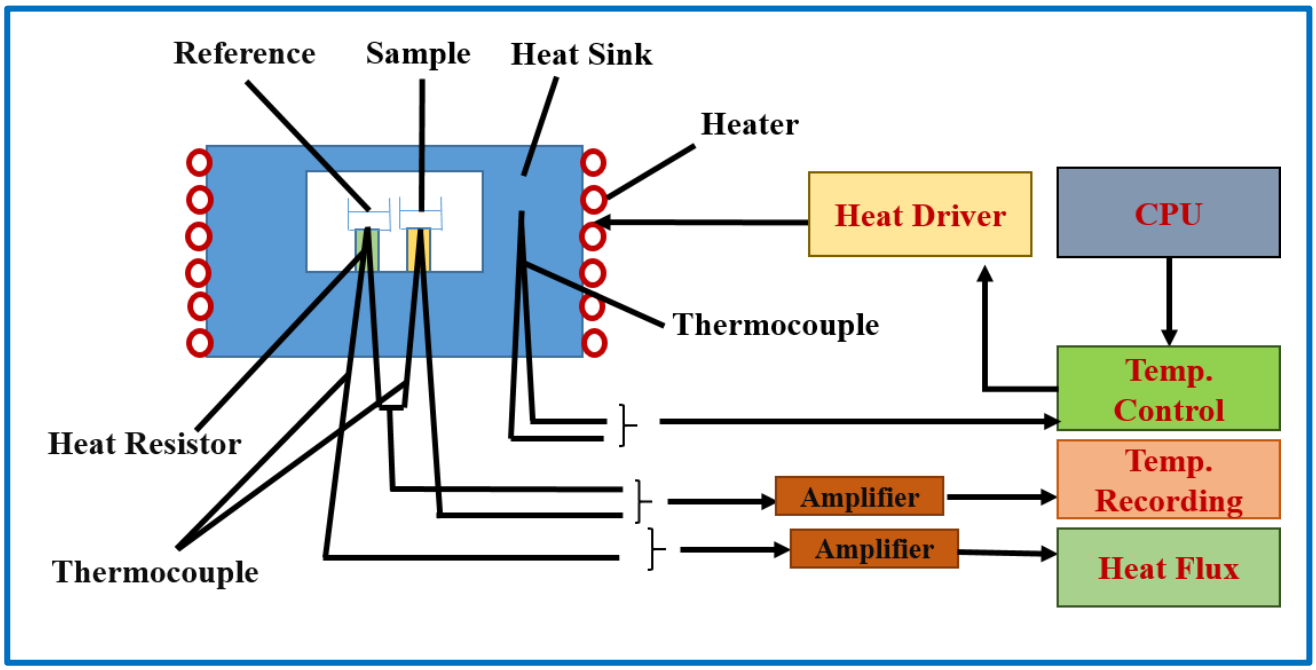


***Figure 2.4*** *Schematics of differential scanning calorimeter (DSC) instrument*

## 2.5 Fourier Transform Infrared (FTIR) Spectroscopy

The FTIR spectra has been recorded by JASCO FTIR-6300 spectrometer (using transmission approach) applying $CaF_2$ window of 2.5 mm thickness with 25 µm spacer thickness. The instrument is constituted with a fixed mirror (M4), a moving mirror (M5) and a beam splitter (BS); the schematics of which is given in figure 2.5. This FTIR spectrometer contains Michelson interferometer.[2] The produced infrared beam is initially transmitted to the moving mirror and then the beam splitter reflected it partly to the fixed mirror. Then mirrors reflect these two beams back towards the beam splitter. Next, these two combined beams is recognized by the detector and relying upon the wavelength of light and difference in their optical path originated by the moving mirror, it can form constructive or destructive interference. The obtained signal popularly known as interferogram is then Fourier transformed to generate the ultimate spectrum. Relative population of various kinds of water molecules including hydrogen bonded water is estimated using dry nitrogen atmosphere with the FTIR spectrometer. We probed the OD stretching frequency of 4% $D_2O$ in $H_2O$ in the wavenumber range of 2200-2800 $cm^{-1}$ using

baseline corrections for every spectra. Each spectrum comprises of 120 scans and 0.6 $cm^{-1}$ power of resolution.

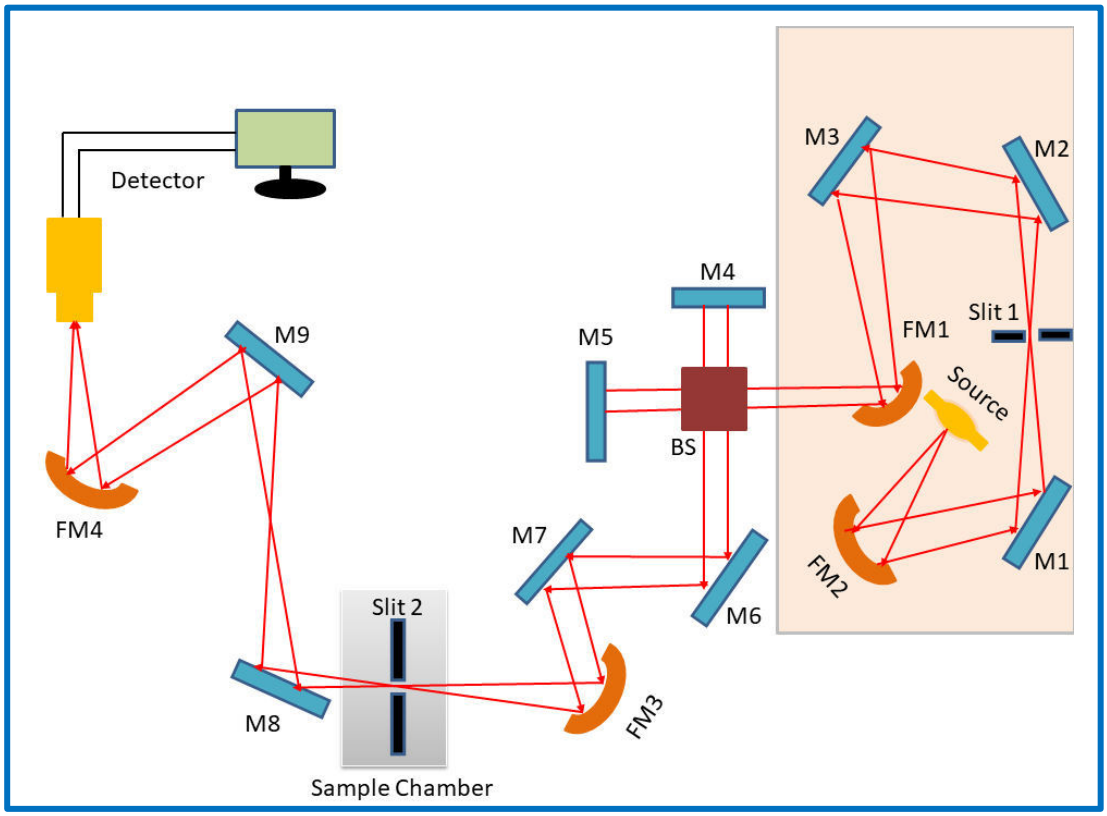


***Figure 2.5*** *Schematics of Fourier Transform Infrared (FTIR) Spectrometer instrument.*

## 2.6 Terahertz Time Domain Spectroscopy (TTDS)

TERA K8, Menlo System spectrophotometer[3-4] was used to measure all terahertz time domain spectra of the samples. A non-linear Er doped fiber laser having excitation wavelength 780 nm and pulse width below 100 fs in addition to the rate of repetition having 100 MHz excites the corresponding antenna to create a terahertz radiation having bandwidth acceptable to 3.0 THz (> 60 dB). The produced THz pulse is then mediated through the measuring solution and finally focused on the THz detector which is barricaded by a probe beam (laser). The THz producing antennas act as dipoles coated with gold having 5 µm dipole gap accumulated on low temperature grown Gallium-arsenide coating of carrier lifetime ~1 ps and mobility ~ 400 cm/s).

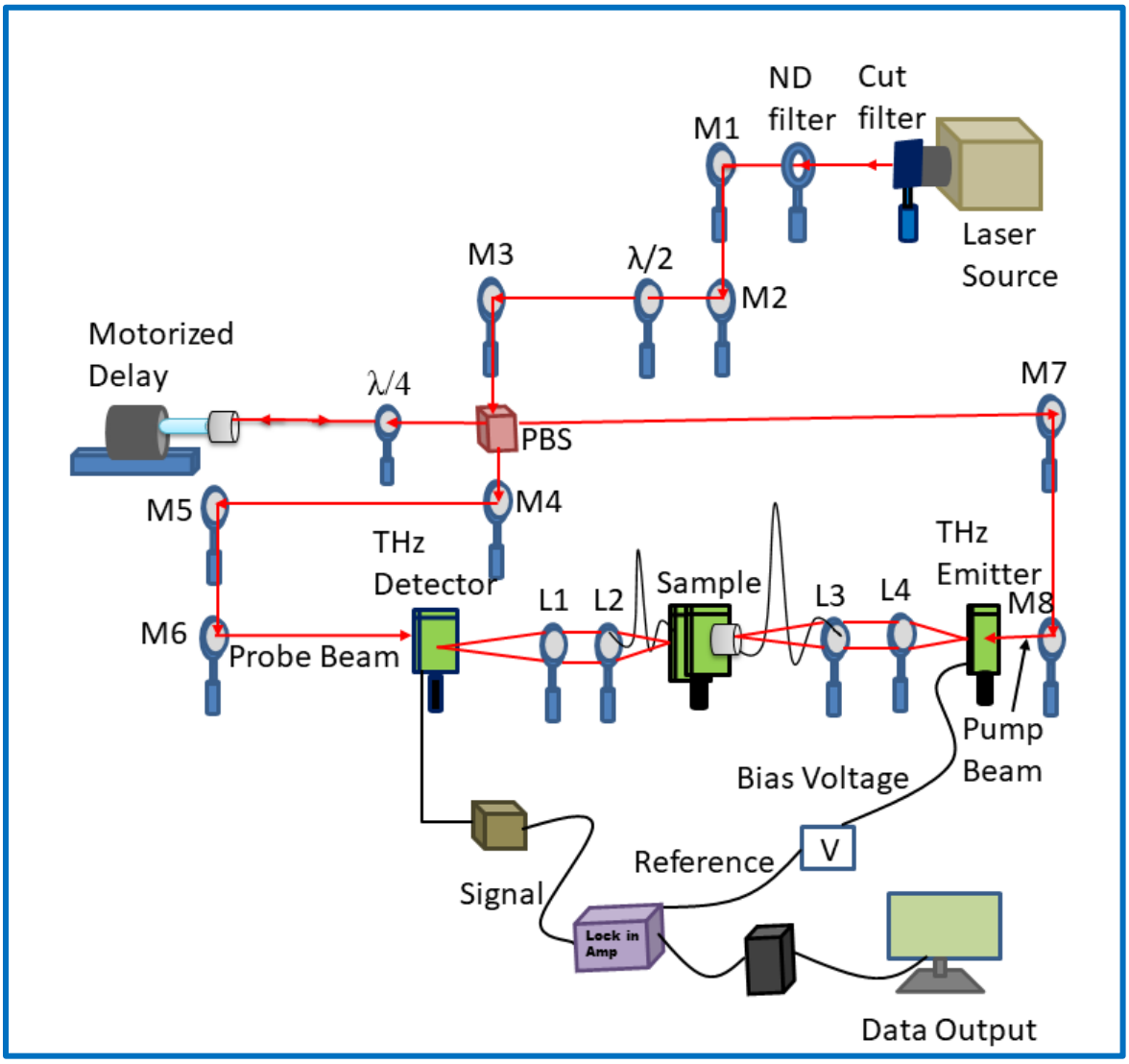


***Figure 2.6*** *Schematics of terahertz time domain spectrometer (TTDS)*

A bias voltage of ~ 20 V and 10 kHz frequency has been applied to store electric energy in the gap area. When the high intensity ultrashort laser pulse hits on the focal point, charge carriers (hole and electron) are generated and then they are speeded-up with the bias voltage to create THz pulse. The fs laser pulses releases the stored electric energy formulated as a time dependent THz electric field, $E_{THz}$ (t) and is correlated with the first derivative of current density J(t).

$$E_{THz}(t) = \frac{1}{4\pi\varepsilon_0}\frac{A}{zc^2}\frac{\partial J(t)}{\partial t} \quad \ldots\ldots\ldots\ldots\ldots\ldots\ldots\ldots\ldots\ldots [2.9]$$

$$J(t) = N(t)e\mu E_b \quad \ldots\ldots\ldots\ldots\ldots\ldots\ldots\ldots\ldots\ldots [2.10]$$

Tuning the path length moved over the probe containing pulse known as time delay, the observed response is consequently estimated with time. The resulting frequency domain signal is computed by Fourier transformation of the quantified electric field, $E_{THz}$ (t).

## 2.7 Materials

### 2.7.I. Protein, Enzyme and cell Bacteria:

***Bovine serum albumin (BSA):*** It is a globular non-glycoprotein available in cow's plasma. This protein consists of 583 amino acid residues; out of those 17 residues come from cysteine group (8 disulphide linkages and one free thiol group). It contains three structurally identical zones (I, II and III), everyone consisting of two sub-regions (A and B). One mole of BSA carries 66.3 kDa weight and its coefficient of molar extinction (ε) at 279 nm[5] is 43,824 $M^{-1}$ $cm^{-1}$. BSA is widely been used in laboratory experiments because of its high capability to enhance signal in assays, absence of side-effects in many biochemical reactions and low cost. Further it is highly water-soluble protein, commercially easily available and well-studied of its crystal structure. Apart from, BSA holds two intrinsic tryptophan Trp-212, Trp-134 moieties[6] (fluorophore) found in subdomain IIA and IB respectively.

***Human serum albumin (HSA):*** It is an extracellular serum albumin, abundantly found in human blood plasma.[7-8] The crystal structure of this heart-shaped protein molecule is almost similar to the BSA structure (~80 % similarity) carrying three analogous helical regions (I, II and III), every zone consists of two sub-regions (A and B).[9] HSA is familiar as a monomeric protein containing 585 amino acid residues. The weight of one mole of HSA is 66.5 kDa and molar absorptivity value (ε) at 280 nm is 36,500 $M^{-1}$ $cm^{-1}$. This serum protein contains a single intrinsic fluorophore tryptophan moiety[10-11](Trp-214) located in the subdomain IIA which is extensively being used as a probe to study the local environment of different domains.

***Hen egg white lysozyme (HEWL):*** Lysozyme composed of a unique chain and is a compact globular protein containing 129 number of amino acid residues. The weight of one mole HEWL is 14.3 kDa[12] and the coefficient[13] of molar extinction (ε) at 280 nm is 36000 $cm^{-1}$ $M^{-1}$. It

accommodates six tryptophan residues[14] (Trp-28, Trp-62, Trp-63, Trp-108, Trp-111 and Trp-123); out of those only three (Trp-62, Trp-63 and Trp-108) are mainly situated in the active site of protein. Moreover, fluorescence emission of lysozyme occurs predominantly due to two Trp moieties[15] (Trp-62 and Trp-108). Moreover, it acts as an antimicrobial enzyme found in nature and behaves as a catalyst in the hydrolysis reaction between N-acetyl muramic acid (NAM) and N-acetyl glucosamine (NAG) present in the peptidoglycan[16-17] component of many gram-positive bacterial cell wall which ultimately causes cell lysis of bacteria. Actually the above mentioned enzyme is particularly capable to break 1, 4-beta glycosidic connection. The amino acids present in the active site of the enzyme are Glu-35 and Asp-52 and bind strongly with many substrates and inhibitors.

***Ribonuclease-A from bovine pancreas (RNase-A):*** It is a relatively small protein containing 124 amino acid residues stabilized by four disulphide (S-S) bonds in its folded form. The native form of this protein are consisted of three α-helices and seven β-strands organized in two layers.[18] It acts as a pancreatic enzyme and plays important role to cleave and hydrolysis of single stranded RNA into its smaller fragments.[19] The molecular weight of this enzyme is 13.7kDa and molar extinction coefficient[20] is 8,640 $M^{-1}$ $cm^{-1}$. It is a well-known model protein generally used to carry out several spectroscopic measurements involving circular dichroism, absorbance, Raman to know about the change of its secondary structure, functionality and activity in presence of various macromolecular crowders.

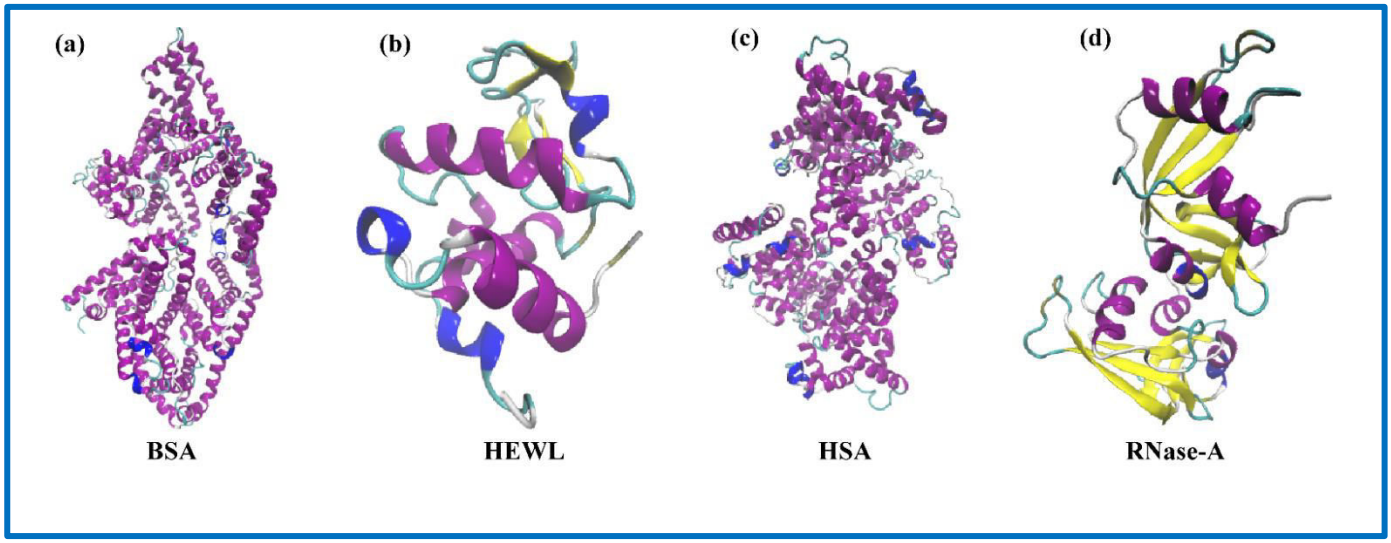


***Figure 2.7.I*** *Tertiary structure of (a) BSA, (b) HEWL, (b) HSA and (d) RNase-A.*

***Micrococcus lysodeikticus cell (substrate of lysozyme enzyme):*** This gram-positive bacterium[21] generally used as a substrate with lysozyme (enzyme) to participate in enzymatic reaction. It mainly exists in water, dust, soil and air. Besides this, it is located in mammalian skin, human mucosae, mouth and oropharynx. This dead cell wall is constituted by N-acetyl muramic acid (NAM) and N-acetyl glucosamine (NAG).

The composition of Micrococcus lysodeikticus cell wall is as follows:

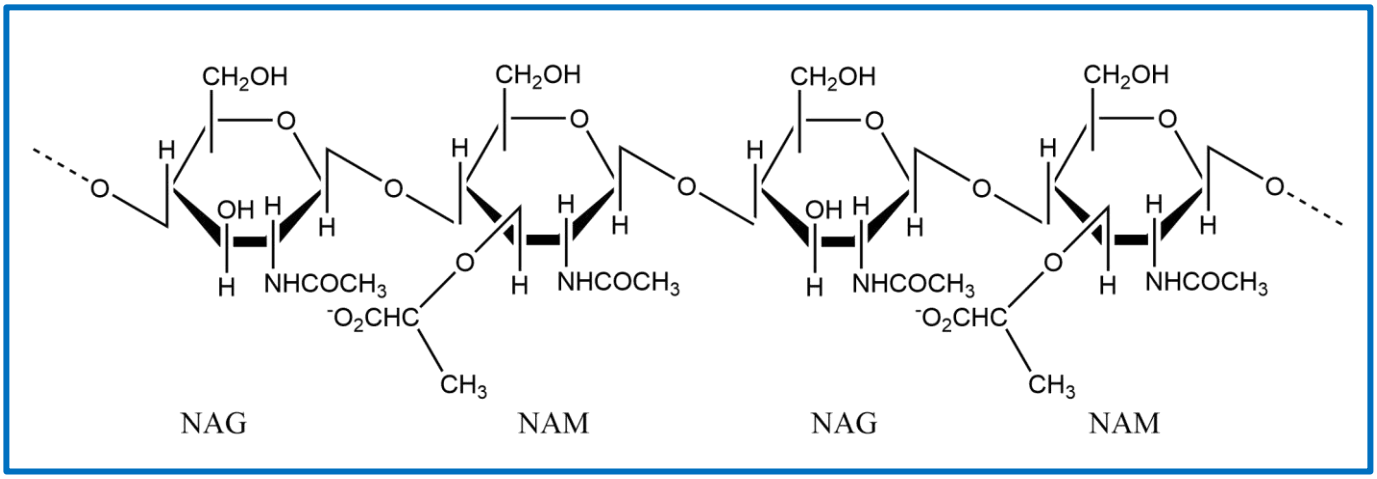


**2.7.II. Amino Acids:** Major portion of this thesis discusses about the effect of various nonpolar hydrophobic amino acids as macromolecular crowders on the stability as well as activity of various proteins. The amino acids used in the entire workdone of this thesis are Glycine (Gly), Alanine (Ala), Arginine (Arg), Proline (Pro), Valine (Val), Leucine (Leu) and Isoleucine (Ile). Among them Gly is the smallest least hydrophobic nonpolar achiral amino acid. The hydrophobicity[22] as well as surface area[23] increases in the order of Ala < Val < Leu < Ile. Proline is the special type of amino acid containing a heterocyclic ring. Arginine is a basic amino acid carrying both hydrophilic and hydrophobic groups; besides it contains some structural similarity with guanidinium chloride. All the required amino acids were procured from Merck and utilized as received. The chemical structures of all the seven amino acids used are as follows:

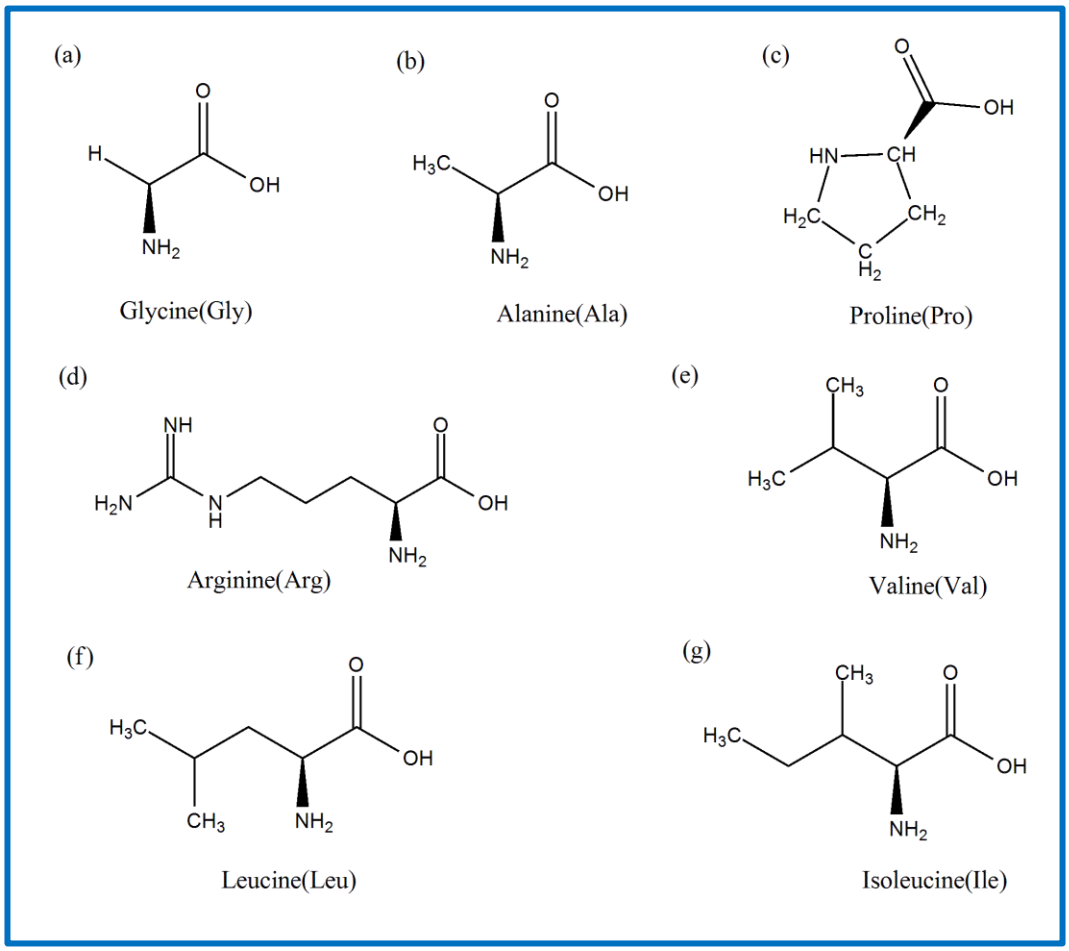


***Figure 2.7.II*** *Chemical structures of various amino acids used in the study. The name of each amino acid has been mentioned below the respective structures.*

**2.7.III. Denaturing Agents:** Urea, Guanidinium chloride (GdmCl) and Guanidium sulphate ($Gdm_2SO_4$) have been used as denaturing agents of the proteins. These materials are applied to unfold the protein partially or completely depending on the experimental situations. All the denaturing agents were bought from Sigma-aldrich. The chemical structures of all the denaturing agents used in this thesis are funished in figure 2.7.III.

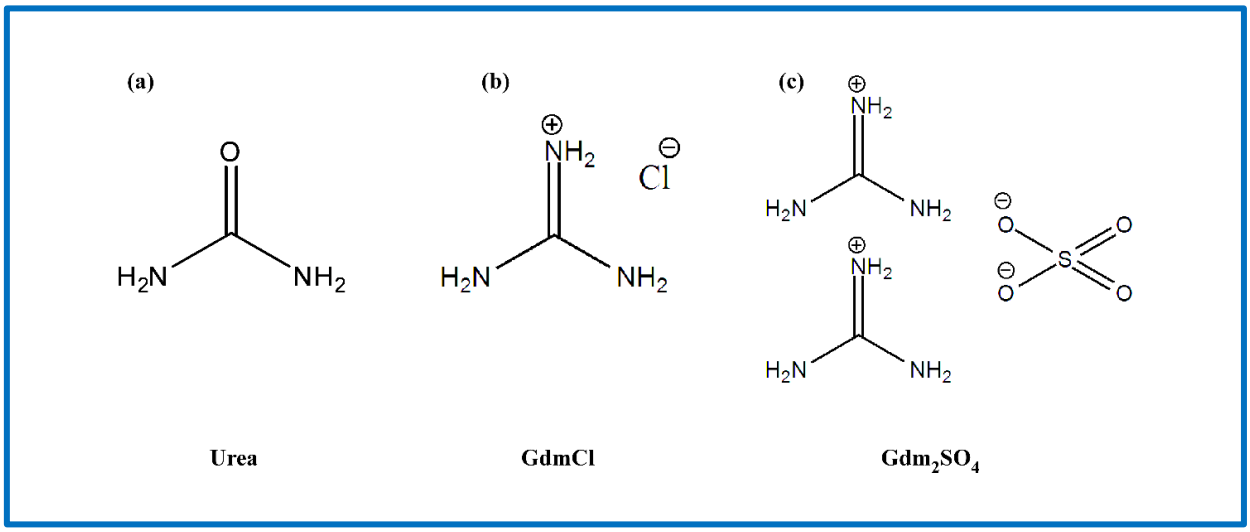


***Figure 2.7.III*** *Chemical structures of (a) Urea, (b) Guanidinium chloride and (c) Guanidinium sulphate.*

## 2.8 Bibliography

1. Lakowicz, J. R., *Principles of Fluorescence Spectroscopy*, Springer Science & Business Media, New York, USA. **2013**.
2. Saptari, V., *Fourier-Transform Spectroscopy Instrumentation Engineering*, SPIE Optical Engineering Press **2004**.
3. Polley, D.; Patra, A.; Mitra, R. K., Dielectric relaxation of the extended hydration sheathe of DNA in the THz frequency region. *Chem. Phys. Lett* **2013,** *586*, 143-147.
4. Polley, D.; Ganguly, A.; Barman, A.; Mitra, R. K., Polarizing effect of aligned nanoparticles in terahertz frequency region. *Opt. Lett* **2013,** *38*, 2754-2756.
5. Pace, C. N.; Vajdos, F.; Fee, L.; Grimsley, G.; Gray, T., How to measure and predict the molar absorption coefficient of a protein. *Protein Sci* **1995,** *4*, 2411-2423.
6. Moriyama, Y.; Ohta, D.; Hachiya, K.; Mitsui, Y.; Takeda, K., Fluorescence behavior of tryptophan residues of bovine and human serum albumins in ionic surfactant solutions: A comparative study of the two and one tryptophan(s) of bovine and human albumins. *J. Protein. Chem* **1996,** *15*, 265-272.

7. Carter, D. C.; Chang, B.; Ho, J. X.; Keeling, K.; Krishnasami, Z., Preliminary crystallographic studies of four crystal forms of serum albumin. *Eur. J. Biochem* **1994,** *226*, 1049-1052.
8. Friedrichs, B., All about Albumin. Biochemistry, Genetics, and Medical Applications. *Food / Nahrung* **1997,** *41*, 382.
9. He, X. M.; Carter, D. C., Atomic structure and chemistry of human serum albumin. *Nature* **1992,** *358*, 209-215.
10. Tayeh, N.; Rungassamy, T.; Albani, J. R., Fluorescence spectral resolution of tryptophan residues in bovine and human serum albumins. *J. Pharm. Biomed. Anal* **2009,** *50*, 107-116.
11. Jankeje, K.; Amiri, M.; Albani, J. R., Relation between Human Serum Albumin Structure and Fluorescence Decay Parameters of Tryptophan Residue 214. pp 1-19.
12. Canfield, R. E., The amino acid sequence of egg white Lysozyme. *J. Biol. Chem* **1963,** *238*, 2698-707.
13. Aune, K. C.; Tanford, C., Thermodynamics of the denaturation of lysozyme by guanidine hydrochloride. I. Depdendence on pH at 25 degrees. *Biochemistry* **1969,** *8*, 4579-4585.
14. Rmoso, C.; Forster, L. S., Tryptophan fluorescence lifetimes in lysozyme. *J. Biol. Chem* **1975,** *250*, 3738-3745.
15. Imoto, T.; Forster, L. S.; Rupley, J. A.; Tanaka, F., Fluorescence of lysozyme: emissions from tryptophan residues 62 and 108 and energy migration. *Proc. Natl. Acad. Sci. USA* **1972,** *69*, 1151-1155.
16. Gorin, G.; Wang, S. F.; Papapavlou, L., Assay of lysozyme by its lytic action on M. lysodeikticus cells. *Anal. Biochem* **1971,** *39*, 113-127.
17. Nash, J. A.; Ballard, T. N.; Weaver, T. E.; Akinbi, H. T., The peptidoglycan-degrading property of lysozyme is not required for bactericidal activity in vivo. *J. Immunol* **2006,** *177*, 519-526.
18. Wyckoff, H. W.; Hardman, K. D.; Allewell, N. M.; Inagami, T.; Johnson, L. N.; Richards, F. M., The structure of ribonuclease-S at 3.5 A resolution. *J. Biol. Chem* **1967,** *242*, 3984-3988.
19. Raines, R. T., Ribonuclease A. *Chem. Rev* **1998,** *98*, 1045-1066.
20. Cuchillo, C. M.; Nogués, M. V.; Raines, R. T., Bovine pancreatic ribonuclease: fifty years of the first enzymatic reaction mechanism. *Biochemistry* **2011,** *50*, 7835-7841.
21. Greenblatt, C. L.; Baum, J.; Klein, B. Y.; Nachshon, S.; Koltunov, V.; Cano, R. J., Micrococcus luteus -- survival in amber. *Microb. Ecol* **2004,** *48*, 120-127.
22. Engelman, D. M.; Steitz, T. A.; Goldman, A., Identifying nonpolar transbilayer helices in amino acid sequences of membrane proteins. *Annu. Rev. Biophys. Biophys. Chem* **1986,** *15*, 321-353.
23. Tien, M. Z.; Meyer, A. G.; Sydykova, D. K.; Spielman, S. J.; Wilke, C. O., Maximum allowed solvent accessibilites of residues in proteins. *PLoS One* **2013,** *8*, e80635.

# Chapter 3

## Thermal Stability Modulation of Native and Chemically Unfolded State of Bovine Serum Albumin by Amino Acids


**Summary**

*Various cosolutes like salts, osmolytes, nucleic acids, peptides, proteins surrounding body cells create crowded environment around cells. The protein folding equilibrium is modulated by these cosolutes in different ways, however, an exact concept remains elusive. To understand the cosolute size-effect, macromolecular crowders are generally compared to their monomeric building blocks (e.g. dextran vs. glucose or polyethylene glycol with different degrees of polymerization) though the molecular level studies for protein crowders are not well reported till now. Hence, how single amino acids modulate the folding equilibrium is still very murky. This chapter discusses the effect of four amino acids glycine, alanine, proline and arginine on the stability of a model globular protein bovine serum albumin (BSA) upon thermal and urea-induced unfolding using fluorescence spectroscopy (as a local site-specific probe), circular dichroism (as a global probe for α-helical structure) and differential scanning calorimetry (to probe the energetics of unfolding). The amino acids modulate BSA stability and unfolding without following a particular trend with either the hydrophobicity scale or the solvent accessible surface area (SASA) of the added amino acids. This study rather suggests that solvation effects play a significant role in understanding the cosolute effect.*

## 3.1 Introduction

Several macromolecules like lipids, sugars, nucleic acids, proteins, amino acids create crowded environment around the cells of the living body.[1] Almost 40% (w/v) of total volume of inner cell is occupied by these macromolecules and co-solutes.[2] Since no individual molecular species is present at high concentration such environment is more commonly known as "crowded" instead of "concentrated".[3] Macromolecular crowding discusses either of the two phenomena: (a) 'excluded volume effect' in which co-solutes like amino acids, sugars cannot penetrate into the volume occupied by the macromolecules[4] and (b) soft interaction which is expressed as preferential binding of co-solute or its preferential hydration with the macromolecule.[5] In such a crowded environment how amino acids modulate the protein folding following a particular energy landscape is much demanded topic of research. The stable protein conformation is achieved by huge number of atomic and non-covalent interactions, such as hydrophobic, di-sulphide, electrostatic, hydrogen-bonding and van der Waals interactions.[6] Any perturbation of such weak interactions results instability of protein. Hence, protein stability is of utmost importance for its various biological functions and can be manifested as the ability of protein to retain its function for long period of time in harsh conditions such as increased temperatures, wide pH environment, in presence of organic co-solvents etc.[7] . In most cases, only the folded conformation is produced in the cell but sometimes a random event occurs and protein molecules follow the wrong track or energy-minimizing funnel and change into a toxic configuration called misfolded form. In all the cases, protein misfolding results in the formation of harmful amyloid.[8] Hooper[9] reported that aggregated/misfolded form of proteins become neurotoxic, e.g. prion protein in mad cow disease. Since the unfolded or misfolded forms of proteins could lead to several diseases like Alzheimer's disease, Parkinson's disease, Huntington's disease, Mad cow disease etc.[10-11] it is very crucial to deal with protein stability. The common feature observed for all these diseases is aggregate formation caused by the destabilization of α-helical structure and the simultaneous formation of a β-sheet.[12] though there is ambiguity whether protein aggregation or oligomer formation due to misfolded proteins induces conformational changes.[13] The protein misfolding and unfolding can be prevented by naturally occurring osmolytes during cellular and environmental stress.[14] For example,

trimethylamine-N-oxide (TMAO) accumulates in marine organisms to counterbalance the denaturing effects of urea.[15]

Although there are various experimental and theoretical work done on the protein folding-unfolding equilibrium in presence of co-solutes available in the literature the exact mechanism remained elusive till now due to the inherent complexity of such systems. "Counteracting" osmolytes[14-15] (e.g. TMAO, glycerophosphorylcholine, betaine, etc.) modulate both stability and functional activity of proteins[16-17] whereas, "compatible" osmolytes[15] like sucrose and some amino acids affect only the stability.[14] Some earlier studies have reported that amino acids can be used as protective osmolytes to stabilize protein structure.[18-19] An earlier report by Shiraki et al. showed that aggregation of lysozyme can be prevented by arginine.[19] Yancey et al.[15] observed that amino acids like glycine, alanine, proline, taurine etc. do not significantly alter the enzymatic activity of pyruvate kinase whereas some basic amino acids like arginine and lysine show significant modulation. In a previous study the role of a series of amino acids on their collective hydration dynamics have been investigated.[20] It has been found that hydration dynamics is modulated with the hydrophobicity of the amino acids as well as solvent accessible surface area (SASA). This also suggested that externally added amino acids could influence hydration dynamics and stability of a protein. This chapter discusses about the effect of four different amino acids, glycine (Gly), alanine (Ala), arginine (Arg) and proline (Pro) on the stability of bovine serum albumin (BSA) (chemical structures are shown in figure 1) which is commonly used as a crowder to mimic the densely crowded cytoplasm.[21] Further, BSA is a commercially available well-studied water soluble globular protein and generally monomeric in physiological condition. The four amino acids chosen have different features like Gly is the smallest and the only achiral amino acid, Ala has one carbon atom more than that in Gly, Pro consists of a five membered nitrogen containing ring, Arg is a basic amino acid containing hydrophilic as well as hydrophobic groups and possesses structural resemblance with guanidinium hydrochloride.

This chapter shows the effect of these amino acids on thermal as well as urea mediated unfolding of BSA using steady state fluorescence spectroscopy to monitor the local environment of the Trp212 moiety in BSA in absence and in presence of amino acids as well as in 4M urea. Temperature dependent circular dichroism measurements were carried out to observe the change

in the secondary and tertiary structures of the protein and to estimate the associated thermodynamic parameters. The melting temperature ($T_m$) and enthalpy ($\Delta H$) of protein unfolding were measured by differential scanning calorimetry (DSC).

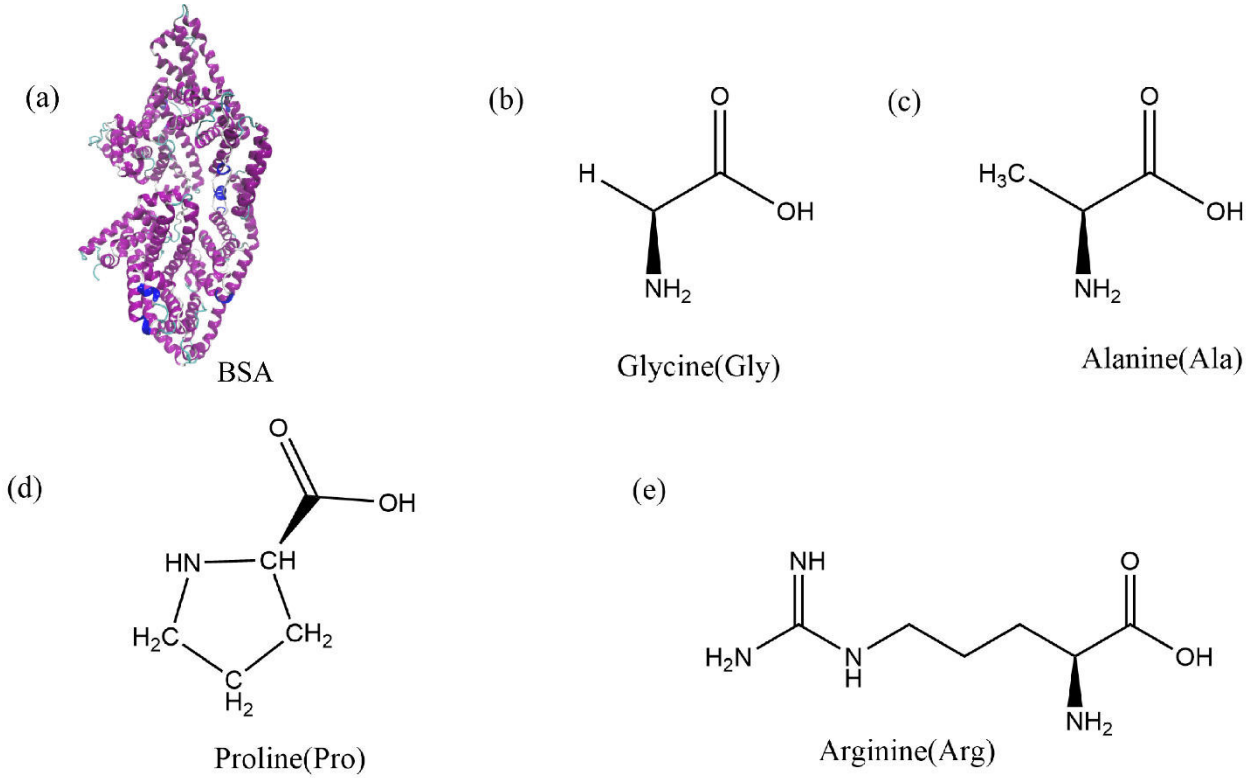


**Figure 3.1:** Structure of (a) Bovine Serum Albumin (BSA), (b-e) different nonpolar amino acids used in the study mentioning the name below of respective chemical structures.

## 3.2 Materials and Methods

BSA (Bovine serum albumin) of molecular weight 66.3 kDa, Glycine, L-alanine, L-proline and L-arginine are purchased from Sigma-Aldrich. All the chemicals are of ~99% purity and have been used without further purification. All the solutions are prepared in aqueous medium (Milli-Q water) in 50 mM sodium phosphate buffer (PBS buffer) at pH 7.4. Protein concentrations are fixed at 10 μM to measure far-UV CD experiments. All the four amino acids are taken of 0.08 M concentrations (limited by the high voltage and signal quality of CD measurements).

**(a) Fluorescence Measurement:** Steady state fluorescence measurements of the protein in presence and in absence of amino acids and urea are performed in Fluorolog 3 (Horiba, Jovin Yvon) instrument. The samples are excited at 295 nm in order to avoid any possible fluorescence contribution from the tyrosine moiety of the protein.

**(b) Circular Dichroism (CD) Measurement:** Far UV (190-260 nm) circular dichroism spectroscopic measurements are performed using a JASCO J-815 spectrometer with a Peltier attachment for the temperature dependent measurements using 0.1 cm path-length quartz cuvette. The secondary structure of the protein has been calculated by CDNN software (http//bioinformatik.biochemtech.uni-halle.de/cdnn).

Temperature dependent CD measurements have been carried to monitor thermal denaturation of BSA both in absence and in presence of amino acids and urea. To eliminate the effect of protein concentration, CD value is calculated in terms of molar ellipticity units using the following relation:

$$Molar\ ellipticity = \frac{observed\ CD\ value\ (mdeg)}{10 \times\ pathlength\ of\ cuvette(cm) \times\ concentration\ of\ protein\ (M)}$$

We assumed a two-state protein folding-unfolding equilibrium model between the native state 'N' and the unfolded state 'U'. At any temperature T the equilibrium constant (K) for this process is given by: $K(T) = \frac{[U]}{[N]}$ where [U] and [N] are the concentrations of the unfolded and the native forms, respectively. The native fraction (φ) present at any temperature T is given by:

$$\varphi = \frac{[N]}{[N]+[U]} \quad \ldots\ldots\ldots\ldots\ldots\ldots\ldots\ldots \quad (3.1)$$

It leads to, $K = \frac{(1-\varphi)}{\varphi}$. In terms of parameters obtained from the CD measurements φ (T) is defined as:

$$\varphi(T) = \frac{([\theta]_T - [\theta]_U)}{([\theta]_N - [\theta]_U)} \quad \ldots\ldots\ldots\ldots\ldots\ldots\ldots \quad (3.2)$$

In this case, $[\theta]_T$ , $[\theta]_N$ $and$ $[\theta]_U$ are the observed ellipticity at T, for the native form and for the unfolded form respectively. $T_m$ is the melting temperature at which activity of native and

unfolded form of protein is equal. A simple way to obtain $T_m$ is from the φ(T) versus T curve at φ= 0.5.

The Gibbs free energy of unfolding (ΔG) is obtained by the standard equation[22-24]

$$\Delta G(T) = -RTlnK = -RTln\ \frac{(1-\varphi)}{\varphi} \quad \ldots\ldots\ldots\ldots \quad (3.3)$$

The corresponding vant Hoff enthalpy ($\Delta H_{VF}$) of unfolding is estimated using the following non-linear equation,[25-26]

$$\Delta G(T) = \Delta H_{VF}\left(1 - \frac{T}{T_m}\right) - \Delta C_p\left[(T_m - T) + T\ln\frac{T}{T_m}\right] \quad \ldots\ldots\ldots\ldots \quad (3.4)$$

**(c) Differential Scanning Calorimetry (DSC) Measurement:** Thermal stability of BSA in absence and in presence of the amino acids are measured in a MicroCal PEAQ-DSC system (Malvern Panalytical) at a scan rate of 90 ºC/hour (without feedback mode) in the temperature range of 20-90 ºC. The evaporation/boiling of the liquids are prevented by applying a constant pressure over the solution in both the reference and the sample cells (250 µL solution in each). BSA concentration is kept fixed at 10 µM and the amino acid concentration is 0.08 M for all the measurements. Before each scan of the protein sample several buffer-buffer (or amino acid solution-amino acid solution) scans in the same conditions are performed until reproducibility of the data is achieved and the last data has been used for baseline corrections of the protein sample. All the data have been analyzed by Microcal PEAQ-DSC software. The calorimetric enthalpy ($\Delta H_{cal}$) is measured as the area under the curve of the excess molar heat capacity ($C_p$, baseline corrected) of each transition.

$$\Delta H_{cal} = \int C_p\ dT \quad \ldots\ldots\ldots\ldots\ldots\ldots \quad (3.5)$$

This is irrespective of any model. The corresponding van't Hoff enthalpy ($\Delta H_v$) is estimated as

$$\Delta H_v(T_m) = 4RT_m^2\frac{\Delta C_p(T_m)}{\Delta H_{cal}} \quad \ldots\ldots\ldots\ldots\ldots\ldots \quad (3.6)$$

MicroCal PEAQ-DSC software uses Levenberg-Marquardt non-linear least-square methods to fit the $C_p$(T) data in the following model:

$$C_p(T) = B_0 + B_1(T) + \left[\frac{K(T)\Delta C_p}{1+K(T)} + \frac{K(T)\Delta H_v(T)\Delta H_{cal}(T)}{(1+K(T))^2 RT^2}\right] \quad \ldots\ldots\ldots\ldots (3.7)$$

## 3.3 Results

**3.3.1: Circular dichroism (CD) measurements:** Figure 3.2a depicts the far-UV (190-260 nm) CD measurements of BSA in buffer and in presence of four different amino acids at room temperature. The native protein shows two characteristic negative peaks occurring at 208 and 222 nm recognizing the abundance of its α-helical structures.[27] The negative signal arising at 222 nm originates from the peptide n→π* transition, while the 208 nm band comes out from the excitonic splitting of the lowest peptide π→π* transition.[28-29] The CD data are noisy in the <205 nm region in presence of Arg and Pro solution, while it is only reasonably detectable up to 210 nm in Ala medium. We, therefore, constrain our discussions based on the data recovered at 222 nm.[30]

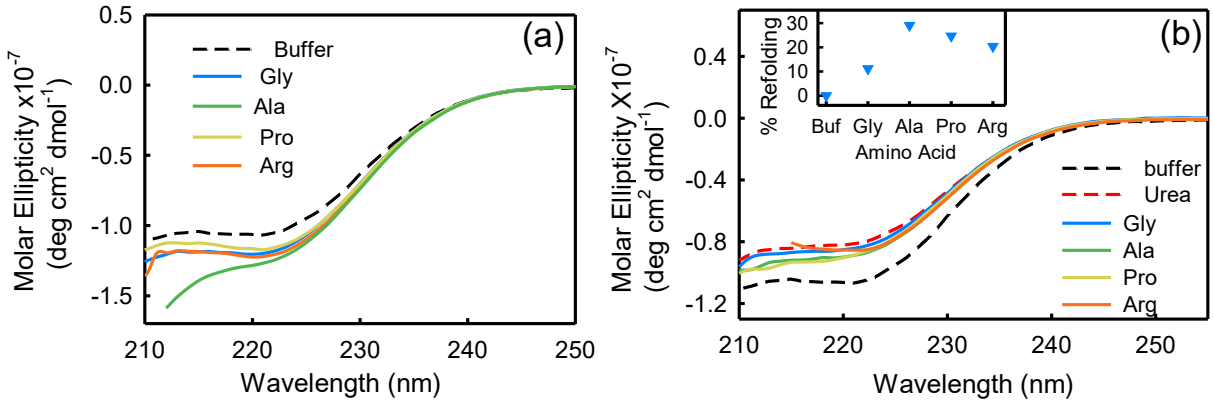


**Figure 3.2:** Plot of far-UV CD spectrum of BSA (10 μM) in presence of (a) various amino acids (0.08 M) in 50 mM phosphate buffer of pH 7.0 and (b) in presence of 4M urea with and without various amino acids (0.08 M). The inset plot indicates 0.08 M amino acid induced refolding percentage curve after 4M urea-mediated unfolding.

We observe that the CD signal is more negative in presence of the added amino acids suggesting an increment of the α-helical content of BSA (table 3.1). We then have calculated percentage of all the secondary structural elements (viz. α-helix, β-sheet, β-turn, random coil)[31] of BSA in buffer and in presence of amino acid. For BSA-buffer, the helix percentage is ~68% which is comparable as given by Reed et al.[27] Helical content increases up-to 10% in presence of added

amino acids which is primarily being converted from the random coil structure. This analysis infers that amino acids make the BSA to attain more folded structure.

**3.3.2: Fluorescence measurements:** We excite the protein at 295 nm in order to eliminate any fluorescence signal obtained from the large number of Tyr and Phe residues present in the protein. The fluorescence signal obtained from BSA (295 nm excitation) emanates predominantly from the Trp212 residue.[32] We notice a distinct emission peak of the protein at 350 nm in buffer. All the amino acids are found to reduce the fluorescence intensity of protein, however, with negligible effect on the emission peak (figure 3.3a). We plot the relative change in fluorescence intensity as a function of 0.08 M amino acids in figure 3.3a, inset. The intensity changes are within 10% error bar with the maximum quenching being occurred in Ala medium and minimum quenching in presence of Arg solution. The fluorescence measurements allude that amino acids instigate minimal effect on the immediate environment of the Trp212 containing domain of the protein. We also monitor temperature-induced unfolding-refolding process of BSA in presence of amino acids using fluorescence measurements. Previous studies on time-resolved fluorescence and FRET measurements clearly indicate that human serum albumin (HSA) forms a distinct intermediate structure below 338 K and the protein undergoes global unfolding beyond 348 K.[33] From the THz measurements, it also argued that the hydration dynamics of protein changes according to the same temperature behavior.[34] Since HSA and BSA are structurally much analogous with respect to its amino acid sequence as well as secondary and tertiary structure[35] such two-step unfolding could also be apprehended in case of BSA. We record the emission profile of BSA at various temperatures in presence of amino acids (a representative plot for BSA in presence of Gly is provided in figure 3.3b). For BSA in buffer, emission intensity quenches with the rise of temperature; this might be due to the enhancement of the non-radiative decay channels of Trp[36] as we also observe this in bare Trp in buffer solutions (figure 3.4a). Up to 328 K, the emission peak does not experience any noticeable change, however, beyond that it suffers a blue shift. Such blue shift is not clearly evident in case of bare Trp in water (figure 3.4a). Upon temperature-induced unfolding, the protein exposes its otherwise buried hydrophobic moieties towards the Trp environment, and correspondingly the emission peak shifts to smaller wavelength. An analogous nature is observed in the presence of amino acids also, although the extent of the change in the emission intensity (at the peak), is different for different amino acids (figure 3.3b). The slope of the relative intensity ($I/I_0$) as a function of

temperature changes significantly beyond 328 K (figure 3.3b, inset). It can be noted here that the temperature induced change in $I/I_0$ of Trp in buffer is relatively high compared to that of Trp in BSA (figure 3.4b). This suggests that the Trp moiety of protein is not entirely exposed towards the solvent during unfolding.

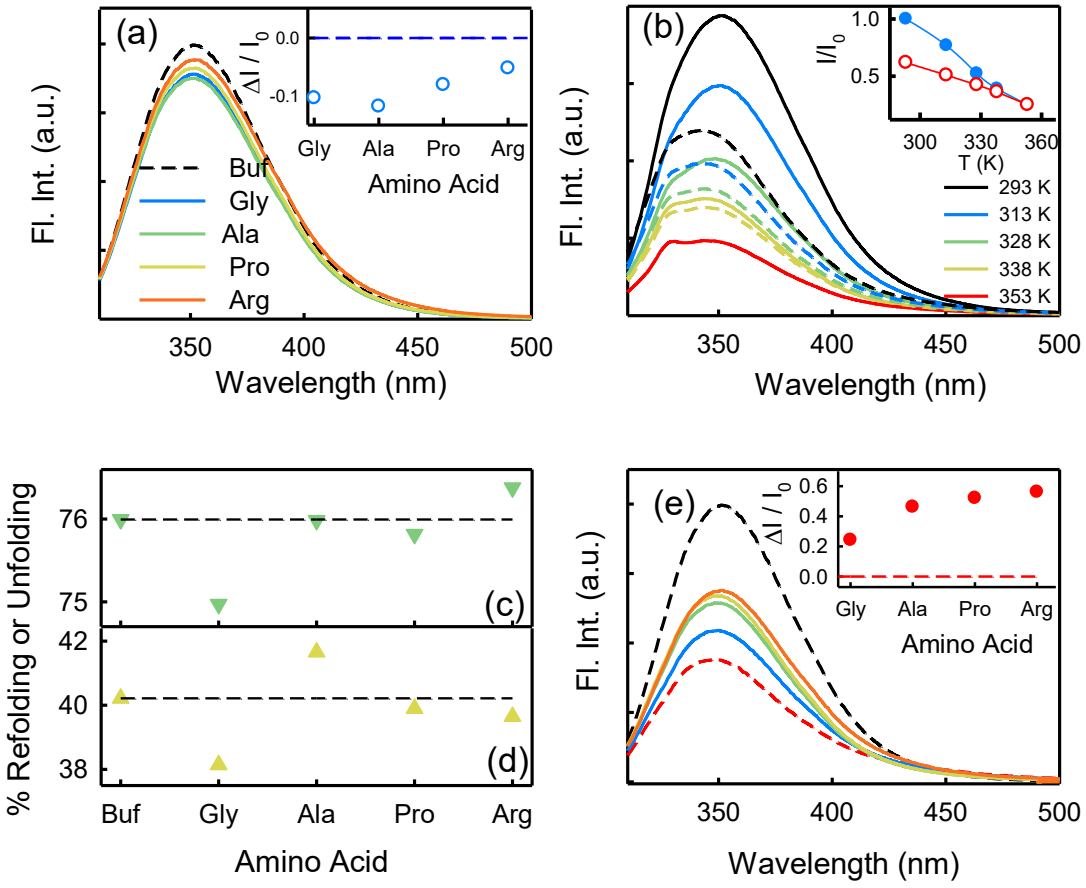


**Figure 3.3.** (a) Plot of emission spectra of 2 μM BSA in presence of buffer (shown by black broken line) and also in presence of 0.08 M amino acids. The inset indicates the plot of relative change of fluorescence peak intensity taken at 350 nm with respect to amino acids. (b) Plot of emission spectra of 2 μM BSA in presence of 0.08 M Gly at various temperatures. The solid and broken lines denote the heating and cooling processes, respectively. The inset indicates the plot of relative fluorescence peak intensity with respect to temperature. The forward heating process has been denoted by the blue solid symbols, whereas, the backward cooling process has been shown by the red hollow symbols. (c) Plot of percentage of relative change of emission peak intensity $[\frac{(\frac{I}{I_0})_{293}-(\frac{I}{I_0})_{353}}{(\frac{I}{I_0})_{293}} \times 100]$ due to unfolding process with respect to amino acids. (d) Plot of percentage of relative change of the native emission peak intensity $[\frac{(\frac{I}{I_0})^{native}_{293}-(\frac{I}{I_0})^{refolded}_{293}}{(\frac{I}{I_0})^{native}_{293}} \times 100]$ upon refolding (recovery) process with respect to amino acids. (e) Plot of emission spectra of 2 μM BSA in presence of buffer (shown by black broken line), in the presence of 4M urea (shown by red broken line) and in presence of 0.08 M amino acids after the addition of 4M urea. The inset indicates the plot of relative change of fluorescence peak intensity with respect to amino acids.

We then analyze the decrease in the relative intensity $[\frac{\left(\frac{I}{I_0}\right)_{293}-\left(\frac{I}{I_0}\right)_{353}}{\left(\frac{I}{I_0}\right)_{293}} \times 100]$ in the native (293 K) and unfolded (353 K) states as a function of amino acid (figure 3.3c). It is found that in the buffer the decrease is ~76%. The decrease is comparable to that of buffer in presence of Ala, Arg and Pro, however, the value is slightly less in Gly solution. This result suggests that the local environment of subdomain IIA of BSA is partially stabilized in Gly medium. We also monitor the refolding process as the temperature is raised first to 353 K and then cooled back to 293 K. We observe that both the intensity as well as the emission peak do not recover to their native values (figure 3.3b, broken lines) and this unfolding-refolding process is irreversible in nature. In presence of buffer, the emission intensity is recovered up to 60% while the peak remains mainly blue shifted. A similar behavior is observed in presence of the different added amino acids. We plot the change in relative intensity at 293 K due to refolding process $[\frac{(\frac{I}{I_0})_{293}^{native}-(\frac{I}{I_0})_{293}^{refolded}}{(\frac{I}{I_0})_{293}^{native}} \times 100]$ as a function of different amino acids (figure 3.3d). We find that amino acids induce the refolding process with decreasing efficiency in the order: Gly>Arg>Pro, whereas, Ala does not show any such effect.

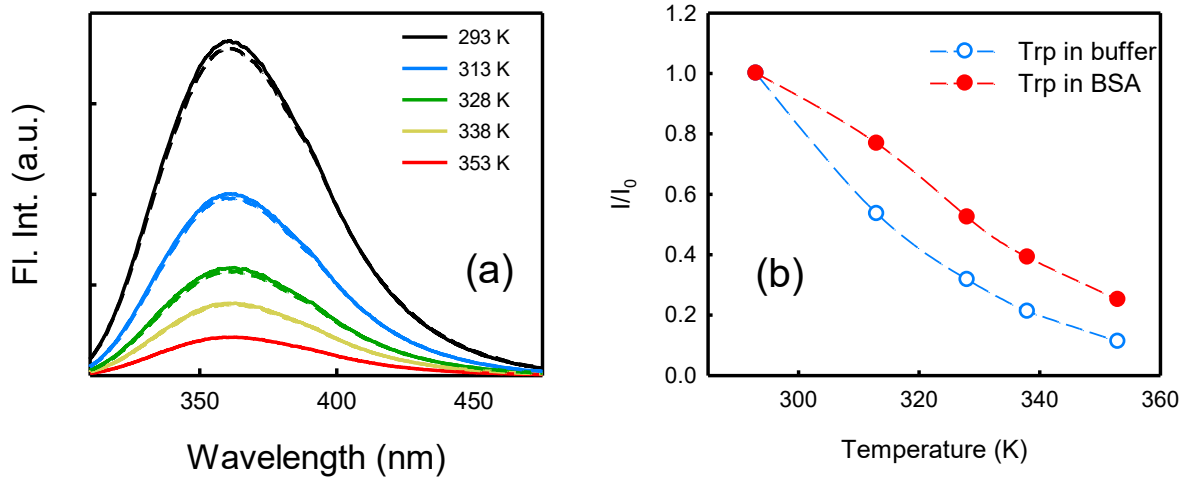


**Figure 3.4.** (a) Emission spectrum of 0.08 M concentration of Trp in buffer at various temperatures. The heating process of Trp in buffer has been denoted by the solid lines while the re-cooled process has been shown by the dotted lines. (b) $I/I_0$ (at the peak) vs. temperature profile of Trp emission in buffer (blue hollow symbol) and in BSA (red filled symbol).

**3.3.3: Temperature dependent circular dichroism measurements:** Effect of temperature on the secondary structure of BSA has been observed using CD spectroscopic analysis. The native fraction of the protein retained at a particular temperature (φ(T)) is calculated by monitoring the CD signal at 222 nm (equation 3.1) as a function of temperature. The melting temperatures ($T_m$) obtained at φ=0.5 are shown in table 3.2. Usually φ(T) follows a sigmoidal pattern defined as:

$$\varphi(T) = \frac{a}{1+e^{-b(T-Tm)}} \qquad \text{..... (3.8)}$$

Where, *a, b* are constants. A representative fit for BSA in presence of buffer and different amino acids individually is shown in figure 3.5a. The fitted parameter *a* lies within 0.95-0.99 range (~1).

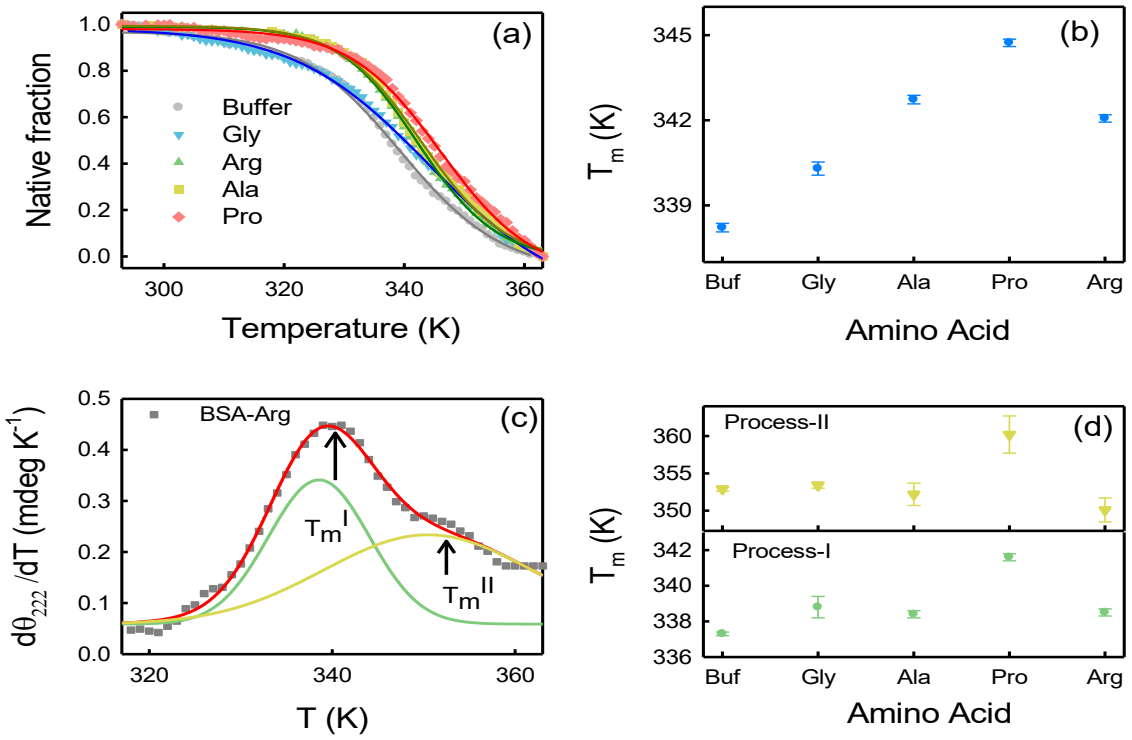


**Figure 3.5.** (a) Plot of native fraction of BSA in presence of buffer and in different amino acids of 0.08 M concentration as a function of temperature. The solid lines indicate the sigmoidal fitting curves. (b) Plot of melting temperature ($T_m$) of BSA in presence of buffer and in different amino acids (obtained by the sigmoidal fitting) as a function of amino acids. (c) A representative plot of first derivative (the main experimental curve has been filtered by the well-known Savitzky-Golay least square procedure) of molar ellipticity taken at 222 nm with respect to temperature for the BSA-Arg mixture. The main experimental data points (shown by grey symbol) has been deconvoluted into two sub-Gaussian curves which indicates the two melting temperatures suggesting the non-two state model of unfolding : (I) green and (II) yellow. The overall fitting curve has been denoted by the red solid line. (d) Plot of two melting temperatures obtained by the non-two unfolding model as a function of amino acids.

It has been observed that the value of $T_m$ calculated from equation 3.8 is in good agreement with that obtained from $T_m$ at φ=0.5 (table 3.2). The $T_m$ value obtained for the native protein is 338.2 K which is in very close agreement with the previous reports.[37] All the amino acids are found to enhance $T_m$ values with various extents (table 3.2).

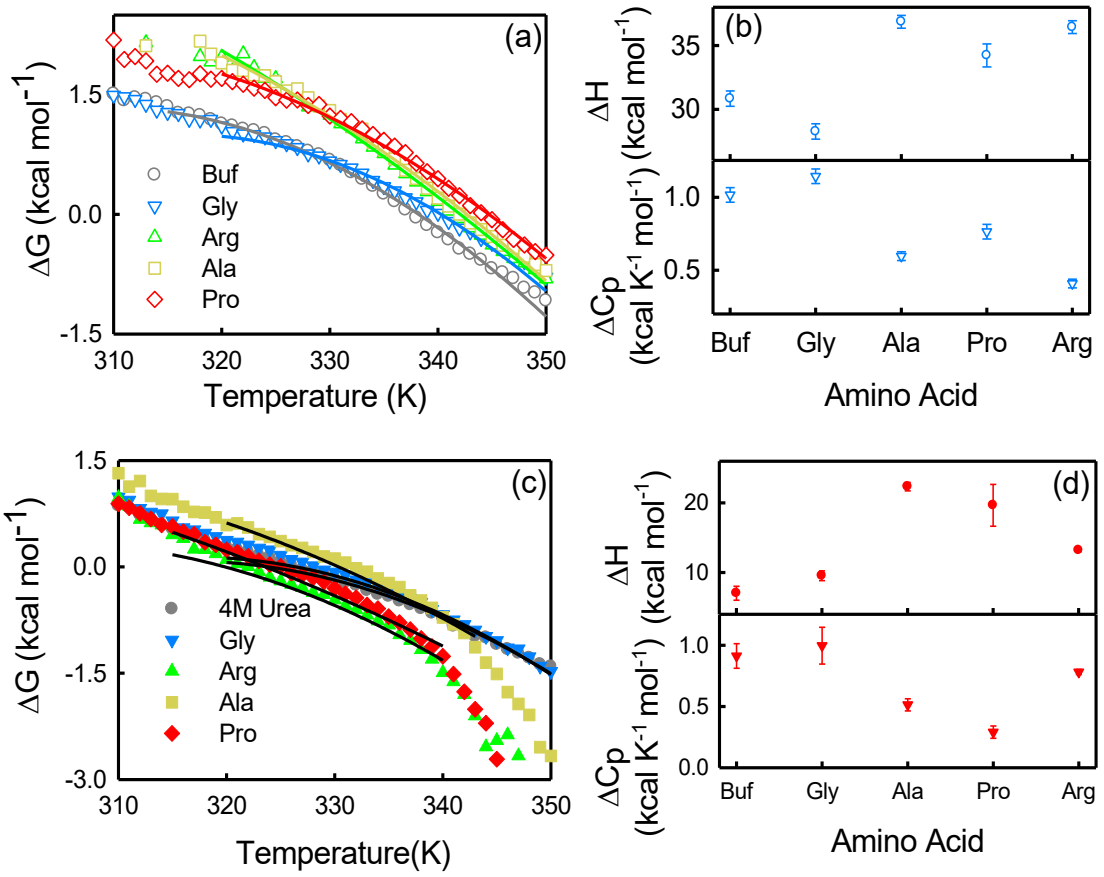


**Figure 3.6.** Plot of Gibbs free energy change of BSA in presence of buffer and in different amino acids as a function of temperature in absence (a) and in presence (c) of 4 M urea. The solid lines indicates the non-linear fitting curves (see equation 4). (b) Plot of van't-Hoff enthalpy (ΔH) at $T = T_m$ and the heat capacity change ($\Delta C_p$) of BSA in presence of buffer and in different amino acids. ΔH and $\Delta C_p$ has been calculated in kcal $mol^{-1}$ and kcal $K^{-1}$ $mol^{-1}$ units respectively. (d) Plot of van't-Hoff enthalpy (ΔH) at $T = T_m$ and the heat capacity change ($\Delta C_p$) of BSA in presence of buffer and in different amino acids in presence of 4M urea. ΔH and $\Delta C_p$ has been calculated in kcal $mol^{-1}$ and kcal $K^{-1}$ $mol^{-1}$ units respectively.

The energetics of thermal unfolding of BSA is calculated by fitting the CD signals at 222 nm using equation 3.4. We fit the ΔG(T) vs. T curves near $T_m$[25] and obtain reasonably good fits (figure 3.6a). The fitted parameters $\Delta H_{VF}$ and $\Delta C_p$ values are presented in table 3.4 and figure

3.6b (open symbols). For BSA we obtain $\Delta H_{VF}$ = 30.8±0.6 kcal $mol^{-1}$ and $\Delta C_p$=1.01±0.05 kcal $K^{-1}$ $mol^{-1}$; these values are in comparable agreement with those for previously reported globular proteins using CD measurements.[38] Upon the addition of amino acids, $\Delta H_{VF}$ of unfolding increases in presence of Ala, Pro and Arg while its value decreases modestly for Gly medium.

Interestingly, when we plot the first derivative of $\theta_{222}$ of BSA in buffer with respect to T (CD data has been smoothened by using a well-known Savitzky-Golay least square procedure[39]) we do not observe a sharp peak as is expected for a two-state unfolding model, and instead an additional hump is observed at a relatively higher temperature (figure 3.7a) . We deconvolute the $d\theta_{222}/dT$ curve into two Gaussians curves and identify two transition temperatures $T_m^I$ and $T_m^{II}$ corresponding to two unfolding processes. Appearance of two such peaks is also evident in case of amino acids also, and the corresponding deconvolution curves in presence of amino acids have been depicted in figure 3.5c and figure 3.7b-3.7d. Such non-two state unfolding for BSA has also been reported in earlier studies.[40-41] In buffer, we obtain $T_m^I$ ~337.3 K and $T_m^{II}$ ~352.9 K. Both $T_m^I$ and $T_m^{II}$ increase in various extents in presence of amino acids except for Ala solution ($T_m^{II}$ decreases for Ala compared to buffer) (figure 3.5d); the trend is comparable to that of $T_m$ (figure 3.5b).

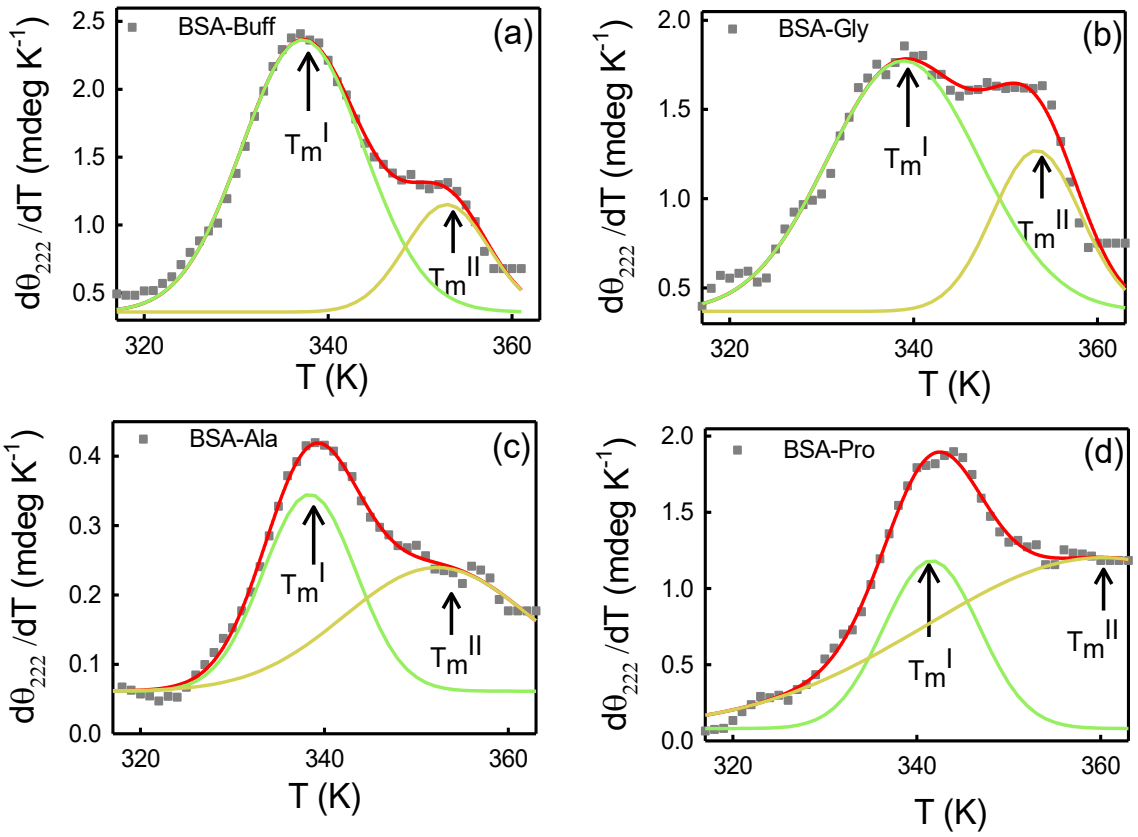


**Figure 3.7.** Plot of first derivative (the curve has been filtered by the well-known Savitzky-Golay least square procedure) of molar ellipticity collected at 222 nm as a function of temperature for the BSA-buffer and BSA-amino acid samples. The main experimental data points (indicated by the grey circles) has been deconvoluted into two sub-Gaussian curves which denotes the two melting temperatures indicating the non-two state model of unfolding : (I) green and (II) yellow. The overall fitting curves has been denoted by the red solid line.

**3.3.4: Differential scanning calorimetry:** DSC measurement techniques have been used to measure the global thermal unfolding properties of the protein in presence of the different amino acids. The thermodynamic parameters due to unfolding of protein obtained by this method provide information about the changes in the hydration behavior of polar and non-polar amino acids upon unfolding and the changes in the corresponding internal interactions (van der Waals, hydrogen bonding etc.) and conformational entropy. A representative $C_p$ vs. T curve is shown in presence of BSA-Arg mixture in figure 3.8a. We observe the presence of two distinct peaks in the DSC profile. Previously Michnik et al.[40, 42] reported the existence of such two definite peaks for defatted BSA in buffer and the peaks have been accredited to the melting of structurally

independent parts of the protein generated after the crevice formation in the proximity region of domains I and II.[32] Such multiple conformational unfolding phenomenon in BSA was also observed by Murayama et al.[41] by temperature-dependent FTIR measurement.

We deconvolute the $C_p$ vs. T curve into two sub-Gaussian curves (figure 3.8a) and from those we obtain the corresponding melting temperatures $T_m^I$ and $T_m^{II}$ for the two unfolding processes. The $T_m^i$ values for BSA in buffer extracted from the thermograms (table 3.5) are ~336 K and ~350 K which are of comparable agreement with those obtained in previously reported values.[42-43] Earlier studies have confirmed that carboxyl-terminal fragment, which consists of mainly domain III and II, melts at a lower temperature (process-I) while the amino-terminal fragment, composed of mostly domain I and a relatively small portion of domain II, unfolds at a comparatively higher temperature (process-II).[32, 40, 43] As the amino acids are added into the protein, both $T_m^I$ and $T_m^{II}$ change in different extents. The corresponding $T_m^I$ and $T_m^{II}$ values for different amino acids have been demonstrated in figure 3.8b and in table 3.5. It has been observed that $T_m^I$ decreases modestly when Gly is added, however, in presence of Ala solution (which has only one extra methyl group compared to that of Gly) $T_m^I$ enhances by ~ 1.6 K with respect to that in buffer. Such an increment in the protein stability in a more hydrophobic environment was also observed by Nick Pace et al.[44] The largest increase in $T_m^I$ was observed in presence of Arg medium (338.0±0.2K), whereas, Pro exhibit a $T_m^I$ (336.0±0.1) comparable to that of buffer (336.1±0.2). In comparison to $T_m^I$, $T_m^{II}$ indicates very marginal shifts in presence of the added amino. The additions of Gly and Arg lead to comparable $T_m^{II}$ values (350.6 K) which are slightly higher than that in buffer while $T_m^{II}$ shows largest value in presence of Ala (350.9±0.3K). The trend in $T_m^I$ values indicates that maximum thermal stability of domain II is achieved in presence of Arg solution, followed by Ala; while, for the domain I, the stability follows the order: Ala > Arg ~ Gly > Pro.

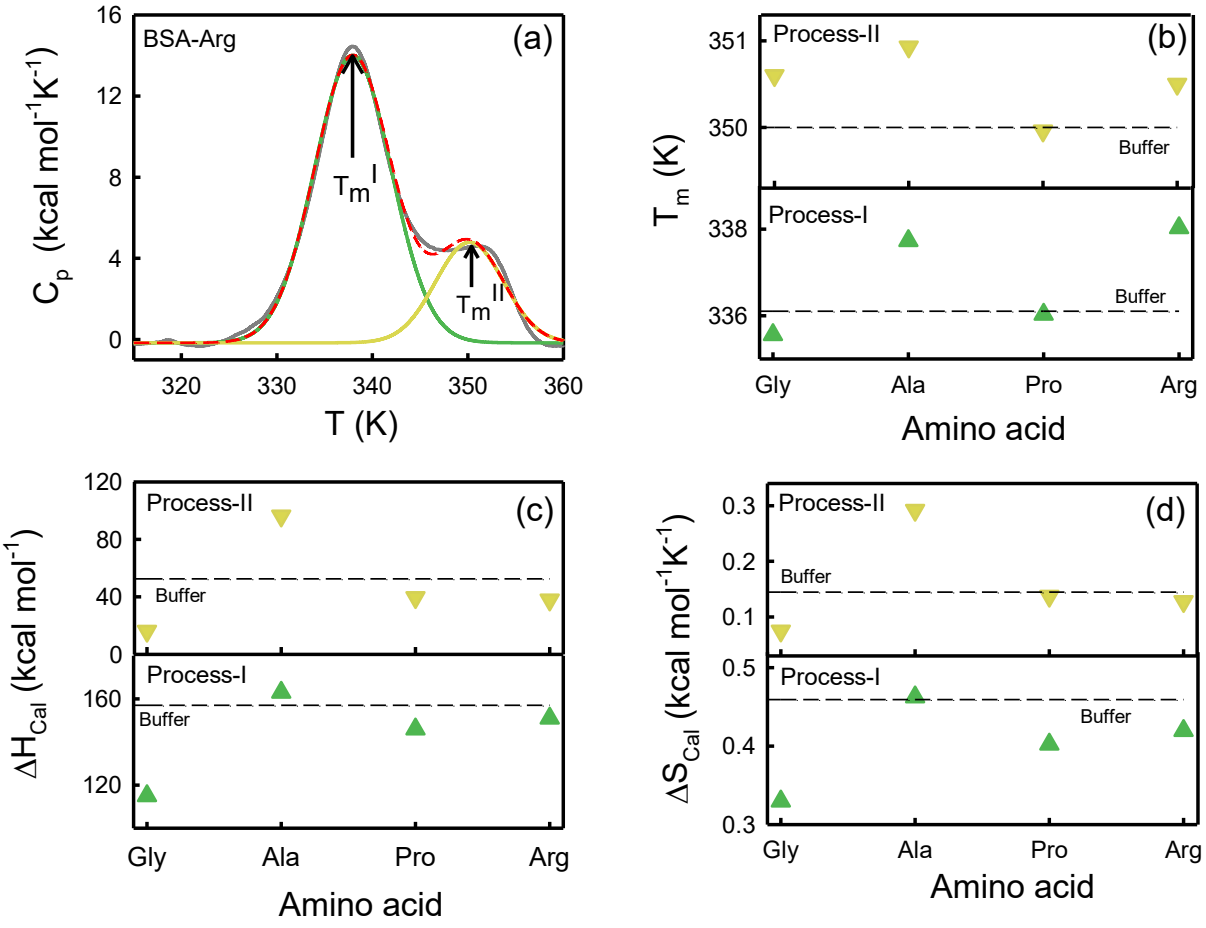


**Figure 3.8.** (a) Molar heat capacity (solid grey line) of BSA and 0.08 M Arg mixture in 50 mM PBS buffer (pH 7.4) obtained at constant pressure ($C_p$) with respect to temperature. The main experimental curve has been deconvoluted into two sub-Gaussian curves which indicates the two melting temperatures $T_m^I$ (shown by green points) and $T_m^{II}$ (shown by yellow points). The red broken line indicates the overall fitting curves. (b) Plot of melting temperatures for the thermal unfolding processes of two different domains as function of amino acids. The melting temperature in presence of buffer has been shown by the black broken line. (c) Plot of calorimetric enthalpies for the two melting processes due to thermal unfolding of two different domains with respect to amino acids. The calorimetric enthalpy in presence of buffer has been denoted by the black broken line. (d) Plot of calorimetric entropies for the two melting processes due to thermal unfolding of two different domains as a function of amino acids. The calorimetric entropy in presence of buffer has been indicated by the black broken line.

The corresponding calorimetric enthalpies ($\Delta H_{cal}^I$ and $\Delta H_{cal}^{II}$) are calculated by fitting the experimental $C_p$ vs T curves to a non-two state model using the well-known Marquardt non-linear least-squares methods (equation 3.7,) and deconvoluting the area under the double humped curves of $C_p$ vs. T. The obtained enthalpies are presented in table 3.5 and figure 3.8c. It has been observed that in presence of Ala solution, $\Delta H_{cal}^I$ increases by ~ 6 kcal mol$^{-1}$ with respect to that

in buffer, while its value is reduced when Gly, Pro and Arg are added individually in the protein solution following the order of $\Delta H_{cal}^{I}$ as: Gly >> Pro > Arg. We also calculate the change in enthalpy contribution during the unfolding process ($\Delta\Delta H = \Delta H_{protein\text{-}AA} - \Delta H_{protein\text{-}buffer}$) for each amino acid (table 3.5). We find that in Gly medium, the $\Delta\Delta H$ value is highly negative while it is positive in presence of Ala solution. This feature also substantiates the $\Delta\Delta H$ values obtained from the CD measurements (table 3.4).

For process-II, the enhancement of the enthalpy values upon the addition of amino acid is quite noticeable in Ala solution (96.3 kcal $mol^{-1}$). Pro and Arg exhibit a slight decrease in $\Delta H_{cal}^{II}$ value, while a significant increment is observed in Gly medium (16.2 kcal $mol^{-1}$). The corresponding van't Hoff enthalpies are evaluated using equation 3.6 and the values are presented in table 3.5. The values of van't Hoff enthalpies differ significantly from the corresponding calorimetric enthalpies indicating that the latter includes all the contributions from the system including solvent rearrangement while the former does not.[45]

The ratio ($\Delta H_{cal}$:$\Delta H_v$) allows for the consideration of the cooperativity of unfolding.[46] If the ratio is very close to unity, the unfolding process can grossly be approximated by a two-state unfolding model. We found that the ratio is higher than one for process I which clearly indicates that there are several intermediate processes involved in the folding-unfolding equilibrium. The ratio reaches minimum value in Gly solution (1.4) while it shows the highest value in Ala medium (2.3). On the other hand, the ratio is less than unity for process II. We calculate the calorimetric entropy of unfolding ($\Delta S_{cal}$) from the obtained area under the curve of $C_p/T$ vs. T for each transition (figure 3.8d). The entropic effect in protein folding-unfolding process in aqueous media primarily comes from the two components: one is configurational entropy which is strongly related to the change of configuration of protein structure during transformation from native to the unfolded state; and the another connected with the change of hydration of polar and non-polar groups.[47] The corresponding change in entropy $\Delta\Delta S = \Delta S_{protein\text{-}AA} - \Delta S_{protein\text{-}buffer}$ has been calculated (table 3.5) which is largely negative in presence of Gly and insignificant in Ala solution. Actually, $\Delta S_i$ is the difference of entropy values between the completely unfolded state (363 K) and the native state (293 K) where "i" is the species (containing protein and buffer/amino acids system). This entropic destabilization in presence of amino acids not only emanates from the protein-amino acids interaction, but also it contains significant contribution

from the associated solvent effect i.e. from the interaction between solvent water and the nonpolar side chains of proteins as well as the interaction with our externally adding different amino acids.[48-50] We obtain slightly large negative value of ΔΔS in case of BSA-Gly compared to Pro, Arg. This entropic change in presence of Ala solution is almost zero. This calculated entropy values matches quite well with the previous study.[51] In the presence of various amino acids, they observed the similar entropic change in thermal stability of Cytochrome c.

**3.3.5: Chemical denaturation by urea:** Next, the effect of amino acids on the secondary structure of BSA has been studied in presence of 4M urea which is a well-known protein denaturant to observe the effect of amino acids on the partially denatured protein.[52-53] It has been observed that the CD signal of BSA decreases significantly in presence of 4M urea (figure 3.2b) which indicates a reduction in the α-helical content and partial unfolding of the secondary structure of the protein (table 3.1). Here it is interesting to be noted that addition of urea decreases the α-helical content of BSA about 14% with simultaneous increment of the random coil percentage which clearly indicates that unfolding of protein occurs. After partial denaturation of protein by urea, when we add amino acids in the solution, it increases α-helical content slightly. We observe that refolding of the urea-mediated unfolded form of protein is induced by the addition of amino acids as is evidenced from the change in molar ellipticity at 222 nm (figure 3.2b). The efficiency of the amino acids to refold the partially unfolded protein has been quantitatively estimated by plotting the relative percentage of refolding (calculated as $\frac{\varepsilon^{222}_{protein-urea-buf}-\varepsilon^{222}_{protein-urea-AA}}{\varepsilon^{222}_{protein-urea-buf}-\varepsilon^{222}_{protein-buf}} \times 100\%$) and the corresponding curve has been shown in figure 3.2b (inset). It has been found that Ala is the most efficient amino acid to refold the partially unfolded form of protein by ~30% followed by Pro>Arg>Gly.

We measure the fluorescence intensity of Trp residue of BSA in presence of 4M urea. It has been observed that the emission intensity quenches drastically in presence of 4M urea solution in comparison to that in buffer (figure 3.3e) suggesting that BSA starts to unfold. The emission intensity of the urea-mediated partially unfolded form of the protein is enhanced after the addition of amino acids. The relative change of fluorescence peak intensity ($\frac{I_{urea-AA}-I_{urea}}{I_{urea}}$) as a function of amino acids has been plotted in figure 3.3e (inset). From the curve, we see that the extent of relative change is higher in Ala solution compared to that in Gly and the Trp peak

intensity of the partially unfolded form of BSA decreases following the order : Arg > Pro > Ala >> Gly.

Further, the temperature dependent CD measurements of BSA has been performed in presence of urea and the added amino acids. It has been found that Ala increases the $T_m^I$ compared to the aqueous solutions (table 3.3). For the other three amino acids, the effect is negligible. The enthalpy ($\Delta H_{VF}$) and change in heat capacity ($\Delta C_p$) values has also been calculated for the two-state folding-unfolding equilibrium process by non-linear fitting of $\Delta G(T)$ versus T curve with the help of equation 3.4, taking the values from $T_m$ to the near neighborhood of $T_m$ (figure 3.6c, table 3.4). The $\Delta H_{VF}$ value is very small in 4M urea solution compared to that in buffer (table 3.4). The value increases in presence of the amino acids indicating their stabilizing role of the protein structure, the effect being the most prominent in Ala.

**Table 3.1**: Secondary structural parameters of BSA in buffer and in presence of different amino acids

| System | α-Helix (%) | β-Antiparallel (%) | β-Parallel (%) | β-Turn (%) | Random Coil (%) |
|---|---|---|---|---|---|
| **Buffer** | 61.18 | 3.49 | 4.29 | 12.57 | 18.46 |
| **Gly** | 68.27 | 2.55 | 3.33 | 11.26 | 14.69 |
| **Arg** | 68.85 | 2.44 | 3.22 | 11.13 | 14.26 |
| **Ala** | 76.97 | 1.62 | 2.19 | 9.42 | 9.90 |
| **Pro** | 77.07 | 1.52 | 2.19 | 9.32 | 9.89 |
| **4M Urea** | | | | | |
| **Buffer** | 47.71 | 5.49 | 6.31 | 14.95 | 25.64 |
| **Gly** | 49.80 | 5.18 | 5.89 | 14.63 | 24.49 |
| **Arg** | 48.88 | 5.29 | 6.10 | 14.73 | 25.00 |
| **Ala** | 52.79 | 4.66 | 5.47 | 14.08 | 22.90 |
| **Pro** | 53.54 | 4.55 | 5.36 | 13.97 | 22.57 |

**Table 3.2.** Fitting parameters for the fit of native fraction of BSA in buffer and in different amino acids by sigmoidal fitting.

| System | In buffer | | | In presence of 4M urea | | |
|---|---|---|---|---|---|---|
| | $T_m$ at φ=0.5 (K) | $T_m$ from Sigmoidal fit (K) | a | $T_m$ at φ=0.5 (K) | $T_m$ from Sigmoidal fit (K) | a |
| **Buffer** | 338 | 338.2±0.2 | 0.96 | 326 | 323.8±0.5 | 1.09 |
| **Gly** | 339 | 340.3±0.2 | 0.96 | 328 | 326.3±0.4 | 1.05 |
| **Ala** | 342 | 342.7±0.2 | 0.99 | 332 | 330.3±0.4 | 0.99 |
| **Pro** | 344 | 344.7±0.1 | 0.97 | 325 | 323.6±0.5 | 1.02 |
| **Arg** | 342 | 342.1±0.1 | 0.98 | 322 | 319.8±0.7 | 1.12 |

**Table 3.3:** $T_m$ values obtained from temperature dependent CD measurements

| System | Buffer | | 4M Urea | |
|---|---|---|---|---|
| | $T_m^I$ (K) | $T_m^{II}$ (K) | $T_m^I$ (K) | $T_m^{II}$ (K) |
| **Buffer** | 337.3±0.1 | 352.9±0.3 | 310.4±0.5 | 333.3±0.6 |
| **Gly** | 338.8±0.6 | 353.4±0.4 | 311.2±0.5 | 335.3±0.6 |
| **Ala** | 338.4±0.2 | 352.3±1.5 | 317.4±1.3 | 340.7±0.7 |
| **Pro** | 341.6±0.2 | 360.2±2.5 | 313.1±0.6 | 336.4±0.6 |
| **Arg** | 338.5±0.2 | 350.1±1.6 | 315.0±0.3 | 336.1±0.4 |

**Table 3.4.** Thermodynamic parameters of BSA thermal unfolding in buffer and in presence of different amino acids obtained from nonlinear equation (3.4)

| Sample | Buffer | | | 4M Urea | | |
|---|---|---|---|---|---|---|
| | $\Delta H_{VF}$ (kcal $mol^{-1}$) | $\Delta\Delta H_{VF}$ (kcal $mol^{-1}$) | $\Delta C_p$ (kcal $K^{-1}$ $mol^{-1}$) | $\Delta H_{VF}$ (kcal $mol^{-1}$) | $\Delta\Delta H_{VF}$ (kcal $mol^{-1}$) | $\Delta C_p$ (kcal $K^{-1}$ $mol^{-1}$) |
| **Buffer** | 30.8±0.6 | - | 1.01±0.05 | 7.0±1.0 | - | 0.91±0.10 |
| **Gly** | 28.3±0.6 | -2.5±0.8 | 1.14±0.05 | 9.5±0.7 | 2.5±1.2 | 0.99±0.15 |
| **Ala** | 36.9±0.5 | 6.1±0.8 | 0.59±0.03 | 22.3±0.6 | 15.3±1.2 | 0.51±0.05 |
| **Pro** | 34.2±0.9 | 3.4±1.1 | 0.76±0.05 | 19.7±3.0 | 12.7±3.2 | 0.29±0.05 |
| **Arg** | 36.4±0.5 | 5.6±0.8 | 0.41±0.03 | 13.2±0.2 | 6.2±1.0 | 0.78±0.02 |

**Table 3.5.** Thermodynamic parameters obtained by fitting in non-two state model of $C_p$ vs temperature curve

| System | $T_m^I$ (K) | $\Delta H_{cal}^I$ (kcal $mol^{-1}$) | $\Delta\Delta H_{cal}$ (kcal $mol^{-1}$) | $\Delta H_V^I$ (kcal $mol^{-1}$) | $\Delta S^I$ (kcal $mol^{-1}K^{-1}$) | $\Delta\Delta S$ (kcal $mol^{-1}K^{-1}$) | $T_m^{II}$ (K) | $\Delta H_{cal}^{II}$ (kcal $mol^{-1}$) | $\Delta H_V^{II}$ (kcal $mol^{-1}$) | $\Delta S^{II}$ (kcal $mol^{-1}$ $K^{-1}$) |
|---|---|---|---|---|---|---|---|---|---|---|
| **Buffer** | 336.1±0.2 | 157±0.3 | - | 69.7 | 0.46 | - | 350.0±0.4 | 52.5±0.3 | 95.2 | 0.14 |
| **Gly** | 335.6±0.1 | 115±0.3 | -42±0.4 | 80.2 | 0.33 | -0.13 | 350.6±0.5 | 16.2±0.2 | 152 | 0.07 |
| **Ala** | 337.7±0.1 | 163±0.6 | 6±0.7 | 70.2 | 0.46 | 0 | 350.9±0.3 | 96.3±0.6 | 88.8 | 0.29 |
| **Pro** | 336.0±0.1 | 146±0.3 | -11±0.4 | 77.4 | 0.40 | -0.06 | 345.0±0.3 | 39.5±0.3 | 109 | 0.14 |
| **Arg** | 338.0±0.2 | 151±0.3 | -6±0.4 | 87.1 | 0.42 | -0.04 | 350.5±0.3 | 37.9±0.2 | 116 | 0.13 |

## 3.4 Discussion

Different spectroscopic tools like fluorescence, circular dichroism, and differential scanning calorimetry have been used to investigate the effect of amino acids on the thermal stability of the model protein BSA. The presence of amino acids neither alter the fluorescence intensity nor the emission maximum noticeably with respect to that of buffer (figure 3.3a), suggesting that the immediate environment of Trp212 in its native state is not perturbed significantly by the amino acids. At elevated temperature, wherein BSA undergoes partial unfolding, quenching of fluorescence peak intensity along with a noticeable spectral shift has been observed (figure 3.3b). This reveals that Trp212 is exposed towards the unfolded hydrophobic moieties near the crevice in domain IIA. Although Gly shows some extent of perturbation of the native form of BSA for other amino acids the effect is marginal.

From the CD measurements it is apparent that all the amino acids increase the helicity content of the protein (figure 3.2a) which could be explained by an excluded volume effect.[3] Since small amount (0.08M) of amino acids used in this experiments the changes observed are only modest. The melting temperature of the protein is obtained by a non-two-state model as it correlates the melting of two different domains though the results are also confirmed by a two-state model (figure 3.5b) and the trends of $T_m$ are identical in both the cases. It is observed that the unfolding of the α-helical content in all the sub-domain of BSA can be grossly resisted with the addition of amino acids, the effect being more prominent in Pro.

DSC study provides the thermodynamics behind the unfolding of the protein which is associated with the changes in hydration behavior of polar and non-polar amino acids as well as changes in

internal interactions (van der Waals, hydrogen bonding etc.) and conformational entropy. Two transitions of BSA has been observed due to the thermal unfolding of two different domains of the protein. Since CD measurements associate changes in the more structured α-helical content only, DSC measurements associate the global unfolding involving less structured secondary motifs also the $T_m^I$ values obtained from DSC measurements are quite lower than those obtained from CD measurements. The van't Hoff enthalpy is smaller compared to the calorimetric one, which illustrates the non-two-state unfolding equilibrium in the protein. The striking difference in both the van't Hoff enthalpy and calorimetric enthalpy of Gly and Ala is intriguing; while Gly significantly lowers it, Ala increases it modestly, the effect being more pronounced in process II. CD measurements reveal that both Gly and Ala increase $T_m^I$ while the DSC thermograms show a marginal decrease in $T_m^I$ for Gly. This apparent contrasting behavior can be explained in the light of their hydration behavior[20] yielding to contrasting solvation energy. One more interesting observation from this overall investigation is that the thermodynamic parameters as well as the protein structural perturbations follow a linear relationship neither with hydrophobicity scale nor with the SASA of the amino acids, thus these parameters are not sufficient to explain the experimental observations.

In order to analyze the amino acid mediated changes in the thermodynamic parameters of the protein it reveals a contrasting behavior between Gly and Ala, though Ala contains only one extra methyl group than Gly. Although Ala produces a positive change in the enthalpy contribution (ΔΔH, table 3.5) the corresponding change in entropy is marginal. It can be argued that enthalpy stabilization (positive ΔΔH), as evidenced in Ala, manifests a classical osmolyte like behavior[54-55] of this amino acid in protein stabilization through a change in the hydration layer of protein mediated by the osmolyte.[56] On the other hand, a negative ΔΔH and a large negative ΔΔS value is obtained for Gly implying that it acts as a non-conventional osmolyte. The negative ΔΔH value obtained is comparable to that observed in a protein denaturant molecule urea suggesting a direct interaction of protein-osmolyte.[25] It is more demanding to consider the individual hydration behavior of the cosolutes to investigate their individual effect on protein stabilization. Previous THz spectroscopic results provide the collective hydrogen bond dynamics of water which have concluded contrasting hydration behavior of Gly as compared to other amino acids; while amino acids in general are water *'structure makers'*, Gly acts as a water

*'structure breaker'*[20] and in that notion it is comparable to urea, which also destabilizes the hydrogen bonded network of water.[57] Being smallest and simplest non-polar amino acid Gly causes minimum steric hindrance compared to other amino acids[58] which leads to better fitting of Gly in this crowded environment and it helps to interact preferably with the protein and solvent. Ala, Arg and Pro have limitations in this regard due to their hydrophobic side chains; this effect has been reflected in their less negative magnitude of ΔΔS or zero compared to Gly. This chapter invokes the idea that stabilization/ destabilization of protein can be induced by osmolyte and the related energetics are correlated with the associated change in the hydration dynamics of both the protein and the added co-solute(s) taken together. Therefore, to generalize the effect of amino acids as macromolecular crowder on protein stability and its functionality more detailed systematic investigation taking amino-acids with varying carbon chain length as well as hydrophobicity scale at different pH condition is much needed.

## 3.5 Bibliography

1. Zimmerman, S. B.; Minton, A. P., Macromolecular Crowding: biochemical, biophysical and physiological consequences. *Annu. Rev. Biophys. Biomol. Struct.* **1993,** *22*, 27-75.
2. Minton, A. P., Implications of macromolecular crowding for protein assembly. *Curr. Op. Struct. Biol.* **2000,** *10*, 34-39.
3. Minton, A. P., Influence of excluded volume upon macromolecular structure and associations in 'crowded" media. *Curr. Op. Biotechnol.* **1997,** *8*, 65-69.
4. Kuznetsova, I.; Turoverov, K.; Uversky, V., What Macromolecular Crowding Can Do to a Protein. *Int. J. Mol. Sci.* **2014,** *15*, 23090-23140.
5. Timasheff, S. N., Protein-solvent preferential interactions, protein hydration, and the modulation of biochemical reactions by solvent components. *Proc. Natl. Acad. Sci. USA* **2002,** *99*, 9721-9726.
6. Gromiha, M. M.; Nagarajan, R.; Selvaraj, S., Protein Structural Bioinformatics: An Overview. In *Encyclopedia of Bioinformatics and Computational Biology*, Ranganathan, S.; Gribskov, M.; Nakai, K.; Schönbach, C., Eds. Academic Press: Oxford, 2019; pp 445-459.
7. Bommarius, A. S.; Paye, M. F., Stabilizing biocatalysts. *Chemical Society Reviews* **2013,** *42* (15), 6534-6565.
8. Cohen, F. E.; Kelly, J. W., Therapeutic approaches to protein-misfolding diseases. *Nature* **2003,** *426* (6968), 905-909.
9. Hooper, N. M., Could inhibition of the proteasome cause mad cow disease? *Trends in Biotechnology* **2003,** *21* (4), 144-145.
10. Chiti, F.; Dobson, C. M., Protein Misfolding, Functional Amyloid, and Human Disease. *Annu. Rev. Biochem.* **2006,** *75*, 333-366.
11. Thirumalai, D.; Klimov, D. K.; Dima, R. I., Emerging ideas on the molecular basis of protein and peptide aggregation. *Curr. Op. Struct. Biol.* **2003,** *13* (2), 146-159.
12. Dobson, C. M., Protein misfolding, evolution and disease. *Trends in Biochemical Sciences* **1999,** *24* (9), 329-332.
13. Soto, C., Protein misfolding and disease; protein refolding and therapy. *FEBS Letters* **2001,** *498* (2), 204-207.
14. Zou, Q.; Bennion, B. J.; Daggett, V.; Murphy, K. P., The Molecular Mechanism of Stabilization of Proteins by TMAO and Its Ability to Counteract the Effects of Urea. *J. Am. Chem. Soc.* **2002,** *124*, 1192-1202.
15. Yancey, P. H.; Clark, M. E.; Hand, S. C.; Bowlus, R. D.; Somero, G. N., Living with water stress: evolution of osmolyte systems. *Science* **1982,** *217* (4566), 1214-1222.
16. Nakanishi, T.; Uyama, O.; Nakahama, H.; Takamitsu, Y.; Sugita, M., Determinants of relative amounts of medullary organic osmolytes: effects of NaCl and urea differ. *Am. J. Physiology-Renal Physiology* **1993,** *264* (3), F472-F479.

17. Bagnasco, S.; Balaban, R.; Fales, H. M.; Yang, Y. M.; Burg, M., Predominant osmotically active organic solutes in rat and rabbit renal medullas. *J. Biol. Chem.* **1986,** *261* (13), 5872-5877.
18. Jamal, S.; Poddar, N. K.; Singh, L. R.; Dar, T. A.; Rishi, V.; Ahmad, F., Relationship between functional activity and protein stability in the presence of all classes of stabilizing osmolytes. *FEBS J.* **2009,** *276*, 6024-6032.
19. Shiraki, K.; Kudou, M.; Fujiwara, S.; Imanaka, T.; Takagi, M., Biophysical Effect of Amino Acids on the Prevention of Protein Aggregation. *J. Biochem.* **2002,** *132*, 591-595.
20. Samanta, N.; Das Mahanta, D.; Choudhury, S.; Barman, A.; Mitra, R. K., Collective hydration dynamics in some amino acid solutions: A combined GHz-THz spectroscopic study. *The Journal of Chemical Physics* **2017,** *146* (12), 125101.
21. Gnutt, D.; Timr, S.; Ahlers, J.; König, B.; Manderfeld, E.; Heyden, M.; Sterpone, F.; Ebbinghaus, S., Stability Effect of Quinary Interactions Reversed by Single Point Mutations. *J. Am. Chem. Soc.* **2019,** *141*, 4660-4669.
22. Tayyab, S.; Siddiqui, M. U.; Ahmad, N., Experimental determination of the free energy of unfolding of proteins. *Biochemical Education* **1995,** *23* (3), 162-164.
23. Seelig, J.; Schönfeld, H.-J., Thermal protein unfolding by differential scanning calorimetry and circular dichroism spectroscopy Two-state model versus sequential unfolding. *Quarterly Reviews of Biophysics* **2016,** *49*, e9.
24. Santoro, M. M.; Bolen, D. W., Unfolding free energy changes determined by the linear extrapolation method. 1. Unfolding of phenylmethanesulfonyl .alpha.-chymotrypsin using different denaturants. *Biochemistry* **1988,** *27* (21), 8063-8068.
25. Senske, M.; Törk, L.; Born, B.; Havenith, M.; Herrmann, C.; Ebbinghaus, S., Protein Stabilization by Macromolecular Crowding through Enthalpy rather than Entropy. *J. Am. Chem. Soc.* **2014,** *136*, 9036-9041.
26. Moulick, R.; Udgaonkar, J. B., Thermodynamic Characterization of the Unfolding of the Prion Protein. *Biophys. J.* **2014** *106*, 410-420.
27. Reed, R. G.; Feldhoff, R. C.; Clute, O. L.; Peters Jr., T., Fragments of bovine serum albumin produced by limited proteolysis. Conformation and ligand binding. *Biochemistry* **1975,** *14*, 4578-4583.
28. Woody, R. W., Optical Rotation of Oriented Helices. III. Calculation of the Rotatory Dispersion and Circular Dichroism of the Alpha- and 310-Helix. *J. Chem. Phys.* **1967,** *46*, 4927-4945.
29. Samanta, N.; Mahanta, D. D.; Hazra, S.; Kumar, G. S.; Mitra, R. K., Short chain polyethylene glycols unusually assist thermal unfolding of human serum albumin. *Biochimie* **2014,** *104*, 81-89.
30. Chen, Y.-H.; Yang, J. T.; Martinez, H. M., Determination of the secondary structures of proteins by circular dichroism and optical rotatory dispersion. *Biochemistry* **1972,** *11*, 4120-4131.

31. Greenfield, N. J., Using circular dichroism spectra to estimate protein secondary structure. *Nature Protocols* **2006,** *1* (6), 2876-2890.
32. Yamasaki, M.; Yano, H.; Aoki, K., Differential scanning calorimetric studies on bovine serum albumin: I. Effects of pH and ionic strength. *Int. J. Biol. Macromol.* **1990,** *12* (4), 263-268.
33. Sinha, S. S.; Mitra, R. K.; Pal, S. K., Temperature Dependent Simultaneous Ligand-binding in Human Serum Albumin. *J. Phys. Chem. B* **2008,** *112*, 4884-4891.
34. Luong, T. Q.; Verma, P. K.; Mitra, R. K.; Havenith, H., Do Hydration Dynamics Follow the Structural Perturbation during Thermal Denaturation of a Protein: A Terahertz Absorption Study. *Biophys. J.* **2011,** *101*, 925-933.
35. Majorek, K. A.; Porebski, P. J.; Dayal, A.; Zimmerman, M. D.; Jablonska, K.; Stewart, A. J.; Chruszcz, M.; Minor, W., Structural and immunologic characterization of bovine, horse, and rabbit serum albumins. *Molecular Immunology* **2012,** *52* (3), 174-182.
36. Kirby, E. P.; Steiner, R. F., Influence of solvent and temperature upon the fluorescence of indole derivatives. *J. Phys. Chem.* **1970,** *74*, 4480-4490.
37. Moriyama, Y.; Kawasaka, Y.; Takeda, K., Protective effect of small amounts of sodium dodecyl sulfate on the helical structure of bovine serum albumin in thermal denaturation. *J Colloid Interface Sci* **2003,** *257* (1), 41-46.
38. Beg, I.; Minton, A. P.; Hassan, M. I.; Islam, A.; Ahmad, F., Thermal Stabilization of Proteins by Mono- and Oligosaccharides: Measurement and Analysis in the Context of an Excluded Volume Model. *Biochemistry* **2015,** *54*, 3594-3603.
39. Savitzky, A.; Golay, M. J. E., Smoothing and Differentiation of Data by Simplified Least Squares Procedures. *Anal. Chem.* **1964,** *36*, 1627-1639.
40. Michnik, A., Thermal stability of bovine serum albumin DSC study. *J. Therm. Anal. Cal.* **2003,** *71*, 509-519.
41. Murayama, K.; Tomida, M., Heat-Induced Secondary Structure and Conformation Change of Bovine Serum Albumin Investigated by Fourier Transform Infrared Spectroscopy. *Biochemistry* **2004,** *43* (36), 11526-11532.
42. Michnik, A.; Michalik, K.; Kluczewska, A.; Drzazga, Z., ComparativeDSC study of human and bovine serum albumin. *J. Therm. Anal. Cal.* **2006,** *84*, 113-117.
43. Precupas, A.; Sandu, R.; Popa, V. T., Quercetin Influence on Thermal Denaturation of Bovine Serum Albumin. *J. Phys. Chem. B* **2016,** *120* (35), 9362-9375.
44. Nick Pace, C.; Scholtz, J. M.; Grimsley, G. R., Forces stabilizing proteins. *FEBS Lett.* **2014,** *588* (14), 2177-2184.
45. Marky, L. A.; Breslauer, K. J., Calculating thermodynamic data for transitions of any molecularity from equilibrium melting curves. *Biopolymers* **1987,** *26* (9), 1601-1620.
46. Malhotra, P.; Udgaonkar, J. B., How cooperative are protein folding and unfolding transitions? *Protein Science* **2016,** *25*, 1924-1941.
47. Makhatadze, G. I.; Privalov, P. L., On the entropy of protein folding. *Protein Science* **1996,** *5* (3), 507-510.

48. Privalov, P. L.; Makhatadze, G. I., Contribution of Hydration to Protein Folding Thermodynamics: II. The Entropy and Gibbs Energy of Hydration. *Journal of Molecular Biology* **1993,** *232* (2), 660-679.
49. Fitter, J., A Measure of Conformational Entropy Change during Thermal Protein Unfolding Using Neutron Spectroscopy. *Biophysical Journal* **2003,** *84* (6), 3924-3930.
50. Sturtevant, J. M., Heat capacity and entropy changes in processes involving proteins. *Proceedings of the National Academy of Sciences* **1977,** *74* (6), 2236-2240.
51. Taneja, S.; Ahmad, F., Increased thermal stability of proteins in the presence of amino acids. *Biochemical Journal* **1994,** *303* (1), 147-153.
52. Guinn, E. J.; Pegram, L. M.; Capp, M. W.; Pollock, M. N.; Record, M. T., Quantifying why urea is a protein denaturant, whereas glycine betaine is a protein stabilizer. *Proc. Nat. Acad. Sci.* **2011,** *108* (41), 16932-16937.
53. Camilloni, C.; Guerini Rocco, A.; Eberini, I.; Gianazza, E.; Broglia, R. A.; Tiana, G., Urea and Guanidinium Chloride Denature Protein L in Different Ways in Molecular Dynamics Simulations. *Biophys. J.* **2008,** *94* (12), 4654-4661.
54. Politia, R.; Harries, D., Enthalpically driven peptide stabilization by protective osmolytes. *Chem. Commun.* **2010,** *46*, 6449-6451.
55. Attri, P.; Venkatesu, P.; Lee, M.-J., Influence of Osmolytes and Denaturants on the Structure and Enzyme Activity of α-Chymotrypsin. *J. Phys Chem. B* **2010,** *114*, 1471-1478.
56. Timasheff, S. N., The Control of Protein Stability and Association by Weak Interactions with Water: How Do Solvents Affect These Processes? *Annu. Rev. Biophys. Biomol. Struct.* **1993,** *22*, 67-97.
57. Samanta, N.; Das Mahanta, D.; Kumar Mitra, R., Does Urea Alter the Collective Hydrogen-Bond Dynamics in Water? A Dielectric Relaxation Study in the Terahertz-Frequency Region. *Chemistry – An Asian Journal* **2014,** *9* (12), 3457-3463.
58. Bhagavan, N. V.; Ha, C. E., Chapter 3 - Amino Acids. In *Essentials of Medical Biochemistry*, Bhagavan, N. V.; Ha, C.-E., Eds. Academic Press: San Diego, **2011**; pp 19-27.

# Chapter 4

## Understanding the Effect of Nonpolar Hydrophobic Amino Acids as Macromolecular Crowders on the Conformational Stability of Globular Proteins


**Summary**

*Macromolecular crowders are added externally for the in vitro study of biomolecules to mimic the interior of the living cells. In this chapter, we intent to investigate the effect of nonpolar hydrophobic amino acids (Gly, L-ala, L-val, L-leu, L-ile) as macromolecular crowding agents on the structural as well as thermal stability of three proteins: human serum albumin (HSA), lysozyme (HEWL) and Ribonuclease-A (RNase-A) of varying α-helical content using circular dichroism (CD) spectroscopic technique. It has been revealed that all these five amino acids aren't capable to amend the secondary structure of any proteins significantly rather they stabilize the native form of every proteins by different extent. Temperature dependent CD measurement explores that the unfolding phenomenon of every proteins is irreversible in nature and the structural loss percentage in buffer during refolding is proportional to the α-helicity of the protein. Estimation of the thermodynamical parameters show that the enthalpic stabilization is protein specific and the added amino acids alter these parameters in different extent for all the three proteins without following any regular trend. Our study affirms that the conformational stability of proteins and the associated thermodynamics do not depend on the hydrophobicity of the crowders (amino acids) rather they are protein specific where α- helicity of the protein has significant role.*

## 4.1 Introduction

Several macromolecules such as nucleic acids, sugars, lipids, proteins, amino acids etc. are densely packed into the inner cellular environments of the living organisms and they can take up to 40% (w/v) of the inner cell. This phenomenon, known as 'macromolecular crowding'[1] performs a crucial part in a variety of processes ensuing in living cell.[2-3] The highly crowded environment of cells is mimicked by macromolecular crowders which offer the "the result of excluded volume" (in which the volume occupied by the crowders becomes unavailable to the other molecules and such effects are mostly offered by Ficoll, Dextran, PEG etc.) or "preferential or soft interaction" (e.g. preferential binding of small co-solutes like amino acids or preferential hydration of protein being acted as a macromolecule itself). Presence of crowders can disrupt protein stability which could lead them to unfold and/or misfold and could cause several diseases like Parkinson, Alzheimer etc. Naturally occurring bio-protective osmolytes like sugars, polyols or methylamines can stabilize the folded shape of globular proteins as in compared to its unfolded one under harsh conditions like pH variations, dehydration, high temperature and lofty concentrations of chemical denaturants.[4-5] For example, betaine, sarcosine and trimethylamine-N-oxide (TMAO) can stabilize proteins and mitigate the disruptive actions of urea via favourable indirect interaction with the particular residues or functional domains of protein through augmentation of the water structure[6-7]

Despite the fact that several experimental and theoretical studies are obtained in the literature on the consequence of macromolecular co-solutes on protein folding-unfolding phenomenon, the exact molecular mechanism and its thermodynamic fingerprints remain evasive due to the inherent complexity of such systems. In this context, small molecules like amino acids can behave as a chemically stabilizing osmolytes and they are familiar as building elements for proteins and are present in plentiful amount in cellular environment. They are familiar not only to stabilize proteins[8-9], but they can also persuade refolding of misfolded proteins[10-11] and eliminate protein aggregation.[12] A previous analysis by Wang et al. have concluded that proline and glycine can act as compatible or counteracting osmolytes and increase the stability of lactate dehydrogenase[13]. Hydrophobicity of amino acids is considered to be a vital framework that can adjust several phenomena like protein folding-unfolding, aggregation, protein-co-solute interaction, activity and protein hydration in aqueous environments[14-16]. Several efforts have

been carried out both experimentally and theoretically to address the hydrophobicity of amino acids[17-19] along with the stability, structure and solvent contribution on different amino acids[20-21] . In the previous chapter, we have established that amino acids can modulate the thermal stability together with the urea induced partially unfolded state of serum albumin, the effects being found to be amino acid specific [22]. A systematic approach, however, is needed to investigate whether the effects is dependent on the amino acid specificity, more specifically on the amino acid hydrophobicity. In the present chapter, we investigate the effects of five different L-isomers of non-polar hydrophobic amino acids with increasing side-chains: glycine (Gly), alanine (Ala), valine (Val), leucine (Leu) and isoleucine (Ile) on three different proteins: human serum albumin (HSA), lysozyme (HEWL) and Ribonuclease-A (RNase-A) containing varying α-helical content. Gly is the smallest and achiral amino acid while rest of the amino acids chosen are chiral and the side-chains vis-à-vis their hydrophobicity increases gradually from Gly to Ile. HSA is an extracellular water soluble globular protein containing 585 amino acids, mostly abundant in blood plasma, comprised of three structurally identical domains (I, II and III), each containing two sub-domains (A and B) and stabilized by 17 di-sulphide bridges.[23-24] It balances the transport and accessibility of hormones, fatty acids and various compounds through blood stream[25]. Hen egg-white lysozyme (HEWL) is a naturally occurring anti-microbial enzyme found in many biological organisms[26-27] containing a single chain polypeptide consisting of 129 amino acids cross-linked with four di-sulphide bridges[28]. Bovine pancreatic ribonuclease-A (RNase-A) is a small, single-domain protein containing 124 residues with four native di-sulphide bonds, that catalyses the hydrolysis of single stranded RNA into smaller components[29-30]. These proteins differ in their secondary structure composition, especially in the α-helix content (see table S1). We investigate the effect of these amino acids on the native structure as well as thermal unfolding of these proteins using circular dichroism spectroscopy by monitoring the perturbation in their secondary structures. The associated thermodynamic parameters for the unfolding process have been estimated by calculating melting temperatures ($T_m$), enthalpy change ($\Delta H$) and heat capacity of unfolding ($\Delta C_p$).

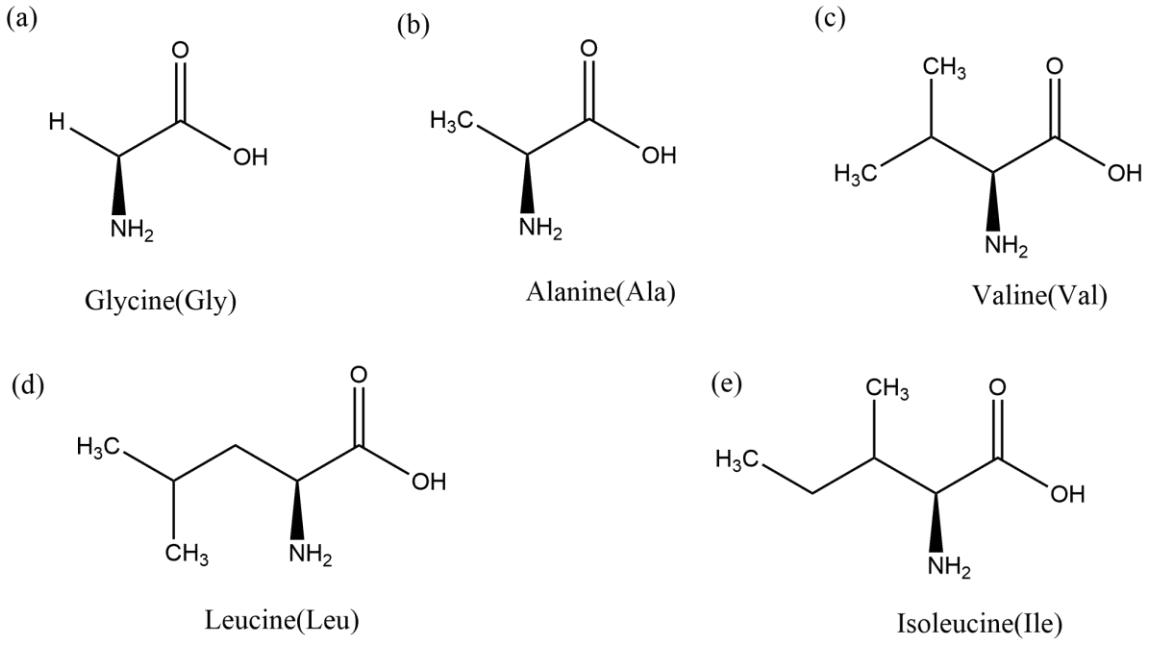


**Figure 4.1:** Different nonpolar amino acids used in the study mentioning the name below of respective chemical structures.

## 4.2 Materials and Methods

Lyophilized powder of human serum albumin (HSA) of molecular weight 66.3 kDa, hen egg white lysozyme (HEWL) of molecular weight 14.3 kDa and Ribonuclease-A from bovine pancreas (RNase-A) of molecular weight 13.7 kDa is procured from Merck. All the chemicals contain highest available purity and are utilized without further purification. All the aqueous solutions are made ready in 10 mM sodium phosphate buffer (PBS buffer) solvated by Milli-Q water (pH 7.4). For far-UV CD measurements 10 μM HSA, 20 μM lysozyme and 20 μM RNase-A are used. The concentrations of all the above mentioned amino acids are kept secured at 0.06 M (restricted by the signal strength of CD measurements). Far UV (190–260 nm) circular dichroism spectroscopic measurements are conducted using JASCO J-815 spectrometer. For the temperature dependent measurements, a peltier is attached with the main instrument. All the solutions are taken in a 0.1 cm path-length quartz cuvette. The CD signal at 222 nm obtained in mili-degree is converted into mean residue ellipticity (MRE) in deg $cm^2$ $dmol^{-1}$, which is given by

$$\text{MRE} = \frac{\theta_{obs}}{10 \times n \times C \times l} \qquad \ldots\ldots\ldots\ldots \qquad (4.1)$$

where, $\theta_{obs}$ is the observed ellipticity in mili-degree, $n$ is the total number of amino acids in the protein, $C$ is the concentration of protein in molar scale and $l$ describes path-length of the cuvette in cm. The percentage of α-helix is enumerated from the MRE values at 222 nm using the following equation 2[31-32]:

$$\%\ \alpha\text{-helix} = \left[\frac{(\text{MRE}_{222} - 2340)}{30300} \times 100\right] \qquad \ldots\ldots\ldots\ldots \qquad (4.2)$$

Thermal denaturation of HSA, lysozyme and RNase-A is monitored by temperature dependent CD measurements both in the absence and in the presence of amino acids. We follow a two-state folding–unfolding pathway between the native form 'N' and the unfolded one 'U' of a protein. At any temperature T, the equilibrium constant (K) for this two-state event is given by: $K(T) = \frac{[U]}{[N]}$, where, [U] and [N] are the equilibrium concentrations of the unfolded and the native states of protein respectively. The native fraction (φ) is designated by:

$$\varphi = \frac{[N]}{[N]+[U]} \qquad \ldots\ldots\ldots\ldots\ldots\ldots \qquad (4.3)$$

It leads to, $K = \frac{(1-\varphi)}{\varphi}$. In the temperature dependent CD measurements φ (T) is described as:

$$\varphi(\text{T}) = \frac{[\theta]_T - [\theta]_U}{[\theta]_N - [\theta]_U} \qquad \ldots\ldots\ldots\ldots\ldots \qquad (4.4)$$

where, $[\theta]_T$, $[\theta]_N$ and $[\theta]_U$ are the measured ellipticity at every particular temperature, for the native state and for the unfolded one, respectively. We designate $T_m$ as the melting temperature beyond which protein begins to unfold. Another straightforward way to assign $T_m$ is from the φ (T) versus T curve at φ = 0.5.

The standard free energy of unfolding ($\Delta G_u^0$) is procured from the equation[33]

$$\Delta G_u^0(\text{T}) = -RT \ln K = -RT \ln \frac{(1-\varphi)}{\varphi} \qquad \ldots\ldots\ldots\ldots\ldots \qquad (4.5)$$

For simplicity, we neglect the superscript ''0'' and subscript ''u'' in the $\Delta G_u^0(\text{T})$ term and use $\Delta G(\text{T})$ henceforth. For the enthalpy (ΔH) and entropy (ΔS) terms also, the similar notations are

used and we avoid the superscript ‘‘0’’ and the subscript ‘‘u’’. The associated van’t-Hoff enthalpy ($\Delta H_{VF}$) for the unfolding process is evaluated using the following non-linear equation[34]:

$$\Delta G(T) = \Delta H_{VF}\left(1 - \frac{T}{T_m}\right) - \Delta C_p[(T_m - T) + T\, ln\, \frac{T}{T_m}] \quad \ldots\ldots\ldots\ldots\ldots \quad (4.6)$$

## 4.3 Results

Far-UV (190–260 nm) CD signals of HSA, lysozyme and RNase-A in buffer and in the presence of five different non-polar amino acids at 293 K are measured and a representative plot for HSA has been shown in figure 4.2a. For the other two proteins the results are shown in figure 4.3a and 4.3b. The protein in its native state shows two characteristic negative peaks at 208 and 222 nm which originates due to the $\pi \rightarrow \pi^*$ and $n \rightarrow \pi^*$ transitions respectively from the peptide bond. In the presence of Val, Leu and Ile, the data are noisy in the < 200 nm region. We, therefore, confine our discussions based on the data recovered at 222 nm which predominantly is correlated with the α-helical content. We calculate the percentage of α -helix from the CD signal obtained at 222 nm [equation 4.1 and 4.2] for these proteins in buffer and in presence of amino acids (figure 4.2b-4.2d and Table 4.1).

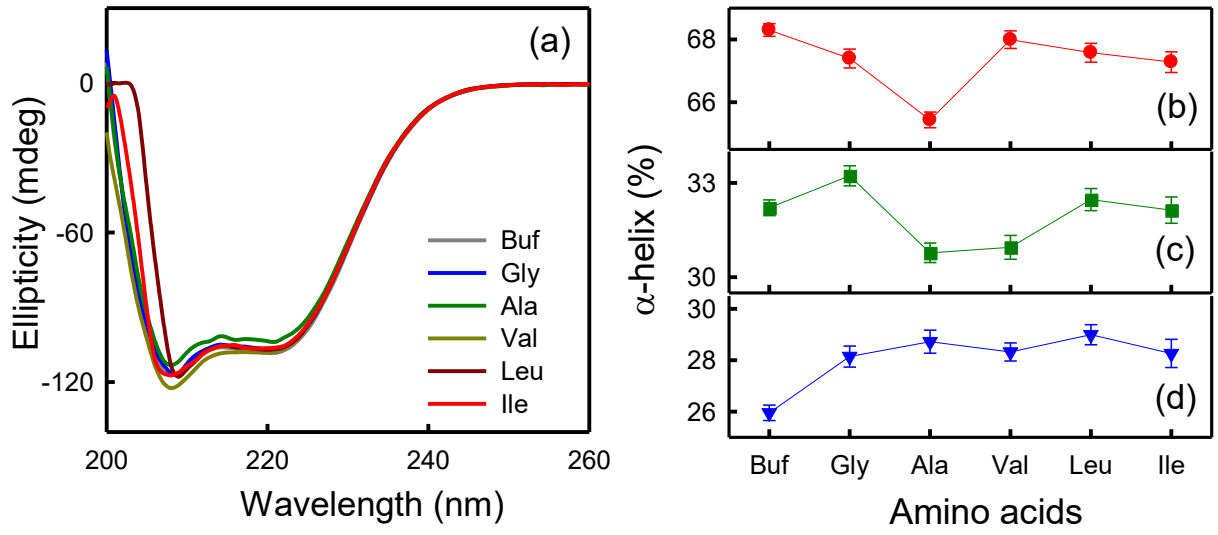


**Figure 4.2:** (a) CD spectra of 10 μM HSA in presence of different amino acids (0.06 M) in 10 mM sodium phosphate buffer (pH 7.0). (b) α-helix content calculated at 222 nm (see equation 2) in presence of different amino acids for (b) HSA (c) lysozyme and (d) RNase-A.

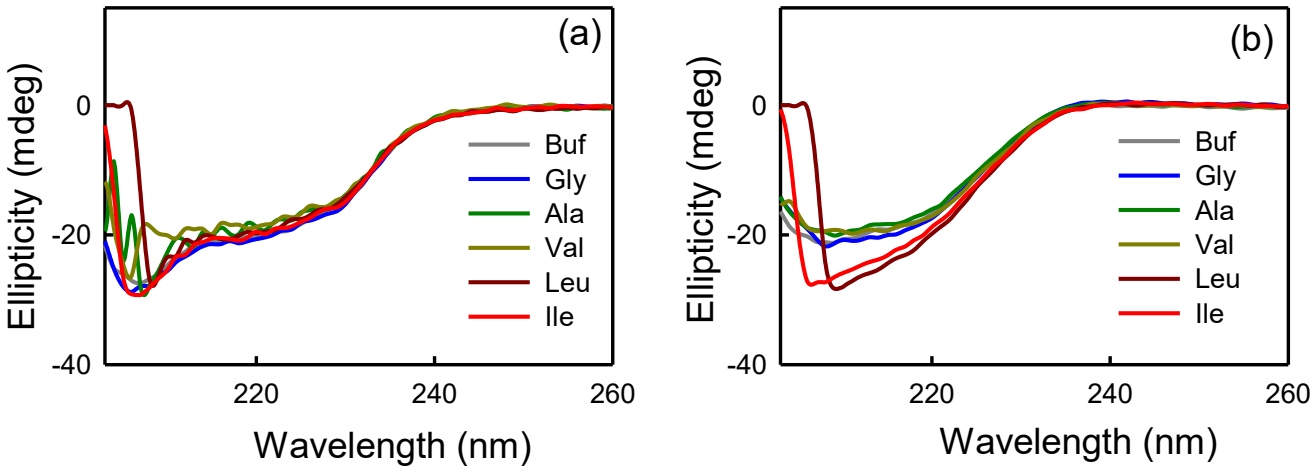


**Figure 4.3.** (a) Room temperature far-UV CD spectrum of (a) HEWL and (b) RNase-A in presence of different amino acids in 10mM sodium phosphate buffer (pH 7.0). The HEWL and RNase-A are of 20 μM concentration each and all amino acids are of 0.06M.

**Table 4.1:** Secondary structural parameters of HSA, HEWL and RNase-A in buffer and in presence of different amino acids.

| Sample | α-Helix (%) for HSA | α-Helix (%) for Lysozyme | α-Helix (%) for RNase-A |
|---|---|---|---|
| Buffer | 68.3 | 32.2 | 25.9 |
| Gly | 67.4 | 33.2 | 28.1 |
| Ala | 65.4 | 30.7 | 28.7 |
| Val | 68.0 | 30.9 | 28.3 |
| Leu | 67.6 | 32.5 | 29.0 |
| Ile | 67.3 | 32.1 | 28.3 |

For HSA in buffer, the helix content is 68.3%, which is in comparable accord with the previous records.[35-36] The value decreases slightly in presence of amino acids with the maximum decrease occurring in presence of Ala (~3% decrease). For lysozyme and RNase-A, the α-helix contents are 32.2% and 25.9%, respectively in buffer, which are in comparable agreement with previous reports.[37-38] The α-helical content of lysozyme increases mildly in presence of Gly, while its value remains mostly unaltered in Leu and Ile and reduces slightly in presence of Ala and Val. For RNase-A, we find that all the amino acids increase the helix percentage to more or less the same extent (~3% increment). This inspection ascertains that amino acids perturbs the secondary structure of protein of varying helicity in different extents.

We also scan temperature instigated unfolding-refolding event of these proteins in presence of different amino acids using temperature dependent CD measurements. To test the reversibility of unfolding, we first increase the temperature up to 368 K followed by a cooling process back to 293 K ($1^0$ C/min for both the heating and the cooling processes). A representative figure for HSA (CD signal monitored at 222 nm) in buffer and in presence of Ile is shown in figure 4.4a and 4.4b respectively. We also obtain the total CD spectra at different temperatures and a representative plot for HSA in buffer and in presence of Gly have been shown in figure 4.5a and 4.5b respectively. Looking at the total spectra as well as at the CD signals at 222 nm, it can unambiguously be inferred that the native secondary structures of any of the three proteins don't recover completely upon cooling. Previous reports by Flora et al.[35] and Moriyama et al.[39] have also confirmed that the process of thermal unfolding of HSA beyond 343 K is irreversible in nature. In order to estimate the extent of irreversibility in the unfolding process, we calculate the loss in the CD signal at 222 nm as the protein refolds back, defined as $\frac{\theta_{293}^{native}-\theta_{293}^{refolded}}{\theta_{293}^{native}} \times 100$ (figure 4.4c). It should be noted here that this is only a rough estimate of the refolding process, and thermal unfolding does not necessarily perturb the helical structure only, however, the parameter could be rationalized with the extent of irreversibility, especially in presence of amino acids. In the buffer medium, the signal is recovered up to 67% for HSA; in presence of amino acids, however, it shows a lower recovery (higher irreversibility) following the order: Ile > Leu > Val > Ala. It seems that the extent of irreversibility increases with increasing hydrophobicity from Ala to Val. The maximum recovery loss is obtained in presence of the smallest amino acid, Gly. In case of lysozyme (figure 4.4d), however, all the amino acids are found to promote higher refolding in comparison to buffer (69.1% recovery in buffer) and their refolding efficiency increases from Gly to Val and does not change much for Leu and Ile. For Ribonuclease-A (figure 4.4e), the recovery percentage is 88% in buffer and except for Gly (92% recovery) all the other amino acids reduce the recovery percentage in the order: Leu > Ala > Ile > Val.

We define the native fraction of proteins (φ(T)) using eqn. 4. Using the temperature dependent profile of φ(T) the melting temperature of protein ($T_m$) is determined at a point where the native fraction becomes half of its original value, (φ = 0.5) (Table 4.2-Table 4.4). φ(T) usually obeys a sigmoidal fashion defined as:

$$\varphi(T) = \frac{a}{1+e^{-b(T-Tm)}} \qquad \ldots\ldots\ldots\ldots\ldots\ldots\ldots\ldots \qquad (4.7)$$

Here, *a* and *b* are constants. $T_m$ can also be obtained by fitting the $\varphi(T)$ curves using equation 4.7. We fit all such profiles and a representative fit for HSA in buffer and in presence of mentioned amino acids are depicted in figure 4.6a. The value of the fitted parameter *'a'* stays in the range of 0.93-0.99, which is very near to the ideal value of 1. We notice that the value of $T_m$ computed from equation 4.7 is in fine accord with the value obtained from $T_m$ at $\varphi$ = 0.5 (Table 4.2-4.4) for all the three proteins in buffer: 338 K, 348.7 K and 339.4 K, respectively; these values are in near agreement with earlier findings.[40-42]As the amino acids are added, $T_m$ increases, the extent of increment being protein specific. In case of HSA, Gly increases $T_m$ by ~ 2.5 K while Ala does it by ~ 3.5 K (with reference to that of buffer). The highest increase in $T_m$ is observed in Leu ($T_m$ ~ 342±0.2, increase by 4.2 K), while Val (340.4±0.2) and Ile (341.0±0.2) show ~ 2K and ~ 3K increment. Amino acids thus provide thermal stability of HSA, specifically in increased hydrophobic environment[43]. For lysozyme, the maximum thermal stability (by ~ 5.5 K) is obtained in the presence of Val (353.8±0.2) followed by Ile (352.3±0.2) and Gly (352.3±0.2) with its thermal stability following the order Val > Ile ~ Gly > Ala > Leu. In RNase-A, the extent of thermal stability offered by amino acids is small and $T_m$ reaches a maximum value in presence of Ile (340.2±0.3). For a better apprehension, we plot the relative change of $T_m$ defined by $\frac{T_{m(AA-buf)}-T_{m(buf)}}{T_{m(buf)}}$ for the three different proteins in presence of amino acids in figure 4.6b. We observe that the increment of $T_m$ does not follow any regular trend.

Measurement of CD signals at 222 nm at different temperatures leads us to calculate various energetic parameters of protein-amino acid interaction. The free energy of unfolding $\Delta$G(T) is obtained by fitting the φ(T) profiles using equation 4.5. $\Delta$G(T) is then used to obtain the other energy parameters: vant Hoff's enthalpy ($\Delta H_{VF}$) and change in heat capacity ($\Delta C_p$) for a two-step thermal unfolding process using the non-linear equation 6. We obtain reasonably good fits in the vicinity of $T_m$ (see figure 4.7a in which representative curves for HSA in buffer and in presence of different amino acids are fitted). The calculated values of $\Delta H_{VF}$ and $\Delta C_p$ for are presented in Table 4.5-Table 4.7. The value of $\Delta H_{VF}$ for HSA, lysozyme and RNase-A in buffer are 22.1±1.0, 60.4 ± 1.5 and 68.7± 4.2 kcal/mol, respectively. It is observed that the van't Hoff enthalpy values obtained in buffer shows reciprocal correlation is inversely proportional to the α-

helical content of proteins. Seelig et al.[44] has previously reported the $\Delta H_{VF}$ values for lysozyme in buffer using a similar approach, and the obtained values by them are comparable to those obtained in the present investigation. There have been reports[45-46] of van't Hoff enthalpies of HSA and RNase-A using DSC measurements; however, the values obtained from DSC measurements are usually higher compared to those measured from CD experiments as the latter considers only the energy associated with the α-helix deformation while the former one manifests the overall change in the protein conformation[22].

We notice that in the presence of Gly, $\Delta H_{VF}$ enhances by ~ 2.5 kcal mol$^{-1}$ with respect to that in buffer in HSA, while its value is slightly reduced in the presence of Ala. In lysozyme such increase is higher (by ~ 19 kcal mol$^{-1}$) with Gly and while it is subtle for Ala (by ~ 1.5 kcal mol$^{-1}$). For a better comparative understanding, we calculate the relative excess enthalpy $[\frac{\Delta H_{protein-AA}-\Delta H_{protein-buf}}{\Delta H_{protein-buf}}]$ and the corresponding relative excess heat capacity $(\frac{\Delta\Delta H}{\Delta H_0})$ $[\frac{\Delta C_{p(protein-AA)}-\Delta C_{p(protein-buf)}}{\Delta C_{p(protein-buf)}}]$ of unfolding (figure 4.7b and 4.7c). This excess thermodynamic parameters are useful tools to explain the stabilization of proteins by different macromolecular co-solutes as has previously been described by Senske et al.[34]. A positive (negative) value of $\frac{\Delta\Delta H}{\Delta H_0}$ indicates protein stabilization (destabilization)[47] by the corresponding co-solutes. In case of HSA, we observe a positive value (0.1) of $\frac{\Delta\Delta H}{\Delta H_0}$ for Gly, whereas, in Ala the value is negative (-0.3). This parameter is found to be the highest in the presence of Leu and it follows the order: Leu > Gly > Val ~ Ile > Ala. In case of lysozyme the trend is comparable to that observed in HSA, however, the extent of stabilization differs, and surprisingly the maximum stability is found in Gly. For RNase-A, the scenario is different as the values are mostly positive (except for Gly and Ala in which the values are close to zero) and it increases with increasing hydrophobicity.

Heat capacity ($\Delta C_p$) of a protein-buffer solution experiencing thermal unfolding is an estimate of the interaction of its aliphatic side chains with water and a positive value of it indicates unfolding of the protein[48-49]. For lysozyme and RNase-A, we obtain the $\Delta C_p$ values of 5.3 ± 0.3 and 5.6 ± 0.8 kcal K$^{-1}$ mol$^{-1}$ in buffer, respectively and the values are in commensurate accordance with the past reported result by Liu et al.[50] $\Delta C_p$ is relatively smaller for HSA (0.28 ± 0.1 kcal K$^{-1}$ mol$^{-1}$) in

buffer and it increases more or less monotonically in presence of the amino acids with increasing side-chains (except Ala). For lysozyme, the trend doesn't follow any particular pattern; the magnitude increases in presence of Ala (7.0 ± 1.3 kcal $K^{-1}$ $mol^{-1}$) and is comparable in Ile with respect to that in the buffer. The value reduces slightly in presence of Leu and Val, while the maximum decrease is observed in Gly. In RNase-A, we observe similar increasing trend in presence of amino acids and the value reaches its maximum in presence of Leu.

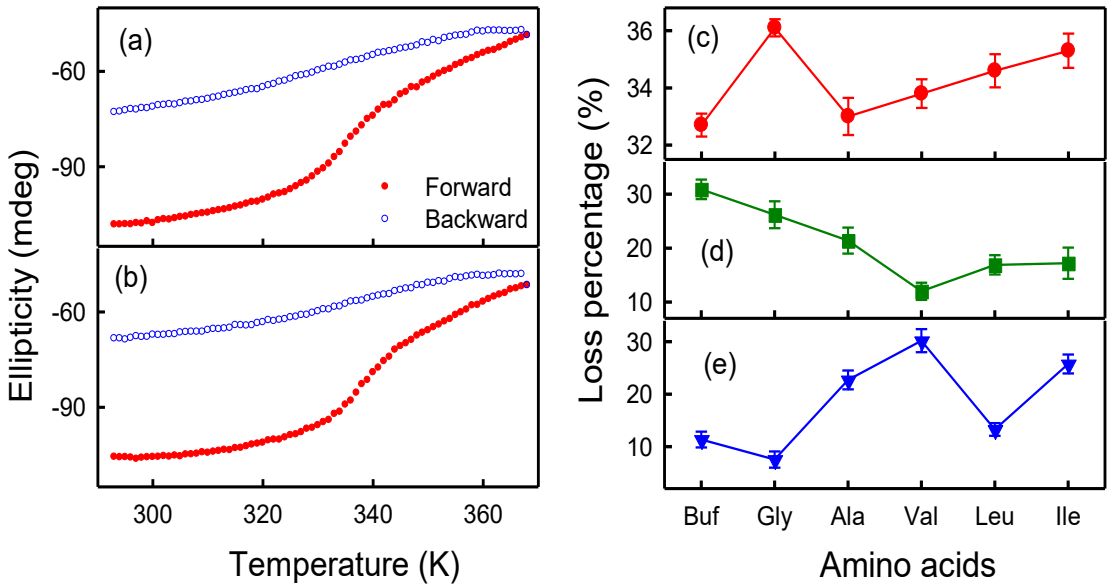


**Figure 4.4.** (a) Temperature dependent CD signal at 222 nm for HSA in buffer and (b) in presence of 0.06 M Isoleucine. The red solid symbols represent forward heating process, the blue hollow symbols represent the backward cooling process. (c-e) Lost percentage of CD signal at 222 nm $\left[\frac{\theta_{293}^{native}-\theta_{293}^{refolded}}{\theta_{293}^{native}} \times 100\right]$ when during refolding of (c) HSA (d) lysozyme and (e) RNase-A in presence of 0.06 M amino acids.

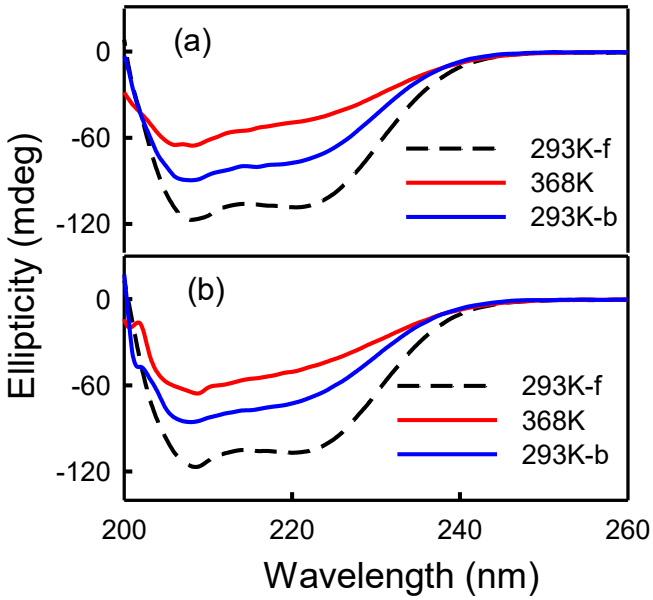


**Figure 4.5.** Representative CD spectra in different temperatures for (a) HSA in buffer and (b) HSA in 0.06M Gly. The black dashed line represent the spectra for the forward process of 293K and blue solid line for 293K backward process; whereas, the red solid line is for 368K.

**Table 4.2:** Fitting parameters for the sigmoidal fit of native fraction of **HSA** in buffer and in different amino acids

| Sample | $T_m$ at φ = 0.5 (K) | $T_m$ from sigmoidal fitting (K) | a | $\Delta T_m/T_m$ (Sigmoidal fitting) |
|---|---|---|---|---|
| Buffer | 337.0 | 338.2 ± 0.2 | 0.99 | 0.000 |
| Gly | 339.4 | 340.8 ± 0.2 | 0.97 | 0.007 |
| Ala | 340.6 | 341.7 ± 0.2 | 0.98 | 0.010 |
| Val | 339.0 | 340.4 ± 0.2 | 0.99 | 0.006 |
| Leu | 341.0 | 342.4 ± 0.2 | 0.98 | 0.012 |
| Ile | 340.0 | 341.0 ± 0.1 | 0.98 | 0.008 |

**Table 4.3:** Fitting parameters for the sigmoidal fit of native fraction of **HEWL** in buffer and in different amino acids

| Sample | $T_m$ at φ = 0.5 (K) | $T_m$ from sigmoidal fitting (K) | a | $\Delta T_m$ / $T_m$ (Sigmoidal fitting) |
|---|---|---|---|---|
| Buffer | 348.6 | 348.7± 0.2 | 0.93 | 0.000 |
| Gly | 352.8 | 352.3± 0.2 | 0.95 | 0.010 |
| Ala | 352.5 | 351.6± 0.3 | 0.92 | 0.008 |
| Val | 355.0 | 353.8± 0.1 | 0.90 | 0.015 |
| Leu | 350.0 | 350.1± 0.1 | 0.90 | 0.004 |
| Ile | 351.9 | 352.3± 0.2 | 0.94 | 0.010 |

**Table 4.4:** Fitting parameters for the sigmoidal fit of native fraction of **RNase-A** in buffer and in different amino acids

| Sample | $T_m$ at φ = 0.5 (K) | $T_m$ from sigmoidal fitting (K) | a | $\Delta T_m / T_m$ (Sigmoidal fitting) |
|---|---|---|---|---|
| Buffer | 339.2 | 339.4± 0.3 | 0.92 | 0.0000 |
| Gly | 340.0 | 340.0± 0.3 | 0.90 | 0.0017 |
| Ala | 339.1 | 339.3± 0.2 | 0.92 | -0.0002 |
| Val | 339.8 | 339.4± 0.3 | 0.90 | 0.0000 |
| Leu | 340.1 | 340.0± 0.3 | 0.91 | 0.0017 |
| Ile | 341.0 | 340.2± 0.3 | 0.93 | 0.00234 |

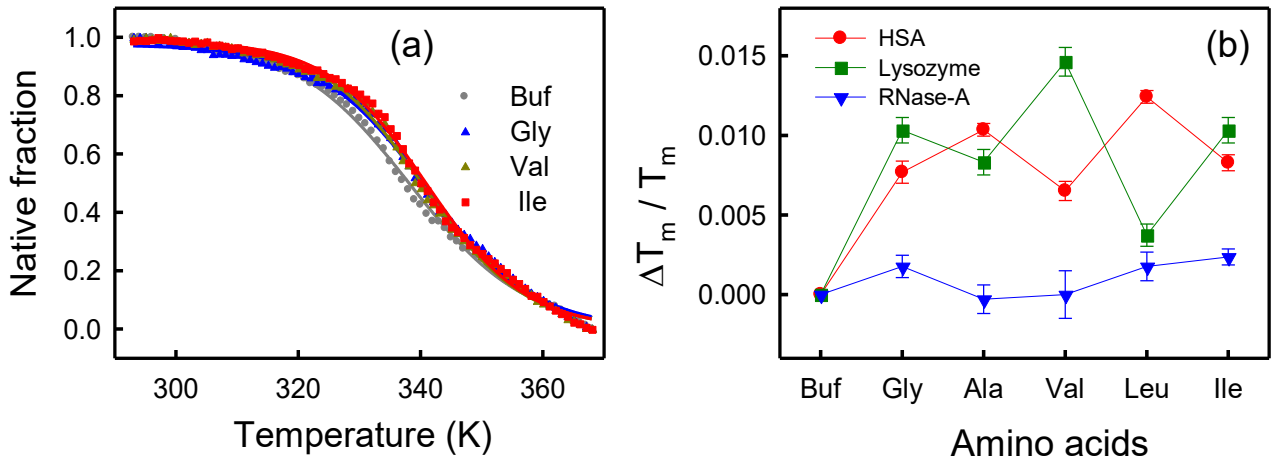


**Figure 4.6.** (a) Relative abundance of the native fraction of HSA as a function of temperature in presence of different amino acids. The solid lines represent sigmoidal fits. (b) Relative change in the melting temperature $[\frac{T_{m(AA-buf)}-T_{m(buf)}}{T_{m(buf)}}]$ of the three different proteins in presence of different amino acids.

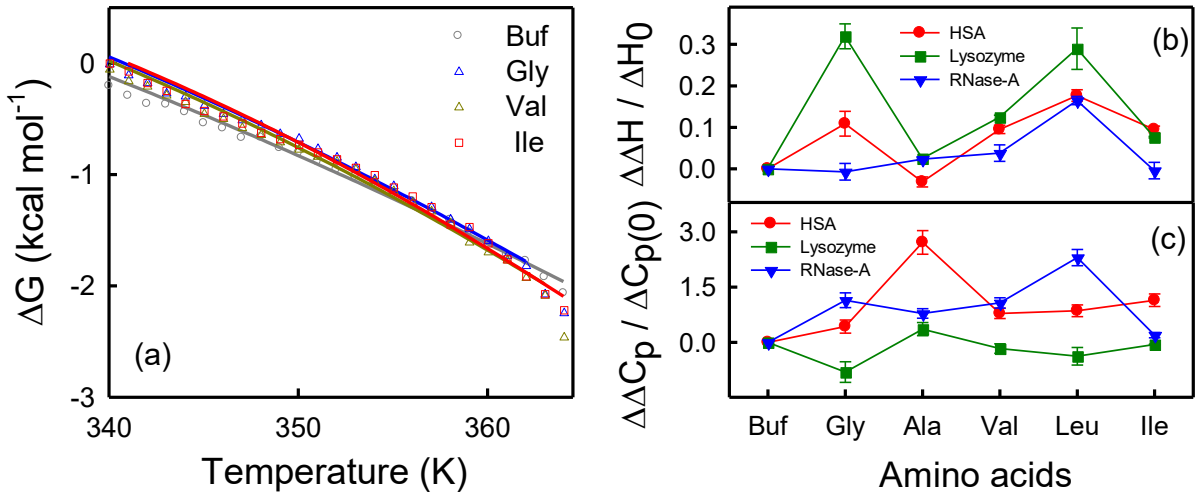


**Figure 4.7.** (a) Change of Gibbs free energy (ΔG) of HSA in buffer and in presence of different amino acids. The solid lines represent non-linear curve fits (see eqn. 6) (b) Relative excess enthalpy change $[\frac{\Delta H_{AA-buf}-\Delta H_{buf}}{\Delta H_{buf}}]$ for three different proteins in presence of different amino acids. (c) Relative excess heat capacity change $[\frac{\Delta C_{p(AA-buf)}-\Delta C_{p(buf)}}{\Delta C_{p(buf)}}]$ for three proteins in presence of different amino acids.

**Table 4.5:** Thermodynamic parameters of **HSA** thermal unfolding in buffer and in presence of different amino acids obtained from nonlinear equation 4.6

| **Sample** | $\Delta H$ **(kcal mol$^{-1}$)** | $\frac{\Delta\Delta H}{\Delta H_0}$ | $\Delta C_p$ **(kcal K$^{-1}$ mol$^{-1}$)** | $\frac{\Delta\Delta C_p}{\Delta C_{p(0)}}$ |
|---|---|---|---|---|
| Buffer | 22.1 ± 1.0 | 0.000 | 0.28 ± 0.1 | 0.00 |
| Gly | 24.5 ± 1.2 | 0.100 | 0.40 ± 0.1 | 0.43 |
| Ala | 21.4 ± 1.3 | -0.030 | 1.04 ± 0.1 | 2.71 |
| Val | 24.2 ± 1.4 | 0.090 | 0.50 ± 0.1 | 0.79 |
| Leu | 26.0 ± 1.6 | 0.180 | 0.52 ± 0.2 | 0.86 |
| Ile | 24.2 ± 1.7 | 0.090 | 0.60 ± 0.2 | 1.14 |

**Table 4.6:** Thermodynamic parameters of **HEWL** thermal unfolding in buffer and in presence of different amino acids obtained from nonlinear equation 4.6

| **Sample** | $\Delta H$ **(kcal mol$^{-1}$)** | $\frac{\Delta\Delta H}{\Delta H_0}$ | $\Delta C_p$ **(kcal K$^{-1}$ mol$^{-1}$)** | $\frac{\Delta\Delta C_p}{\Delta C_{p(0)}}$ |
|---|---|---|---|---|
| Buffer | 60.4 ± 1.5 | 0.00 | 5.30 ± 0.3 | 0.00 |
| Gly | 79.7 ± 7.3 | 0.319 | 1.03 ± 0.3 | -0.80 |
| Ala | 61.9 ± 5.8 | 0.025 | 7.20 ± 1.3 | 0.36 |
| Val | 67.9 ± 6.7 | 0.124 | 4.40 ± 0.7 | -0.17 |
| Leu | 77.9 ± 9.1 | 0.289 | 3.30 ± 0.5 | -0.38 |
| Ile | 65.0 ± 4.4 | 0.076 | 5.00 ± 0.7 | -0.06 |

**Table 4.7:** Thermodynamic parameters of **RNase-A** thermal unfolding in buffer and in presence of different amino acids obtained from nonlinear equation 4.6

| Sample | $\Delta H$ (kcal mol$^{-1}$) | $\frac{\Delta\Delta H}{\Delta H_0}$ | $\Delta C_p$ (kcal K$^{-1}$ mol$^{-1}$) | $\frac{\Delta\Delta C_p}{\Delta C_{p(0)}}$ |
|---|---|---|---|---|
| Buffer | 68.7 ± 4.2 | 0 | 5.6 ± 0.8 | 0.00 |
| Gly | 68.2 ± 7.2 | -0.007 | 12 ± 3.4 | 1.14 |
| Ala | 70.3 ± 3.5 | 0.023 | 10 ± 1.2 | 0.78 |
| Val | 71.3 ± 7.7 | 0.038 | 11.6 ± 3.5 | 1.07 |
| Leu | 80.0 ± 5.8 | 0.164 | 18.5 ± 2.4 | 2.30 |
| Ile | 68.4 ± 4.0 | -0.004 | 6.7 ± 1.5 | 0.20 |

## 4.4 Discussion

The study is aimed to investigate the effect of various nonpolar amino acids as macromolecular crowders on the structural perturbation of three proteins (HSA, lysozyme, RNase-A) of varying helicity using temperature dependent CD measurements. We made a detailed thermodynamic analysis to quantify the various parameters that manifests protein stability and to find if there exists any correlation. On the protein's aspect we varied the α-helical content HSA (68%) > lysozyme (32%) > RNase-A (26%) and on the amino acid perspective we choose to increase the carbon chain length, with special interest towards the ambiguous behavior of Gly[51-53].

All the amino acids are observed to moderately alter the secondary structure content of proteins (Table 4.1, figure 4.2), irrespective of their nature. The change is not remarkable, which indicates that amino acids do not severely perturb the protein structure, at least up to the concentration used. Estimation of the melting temperature ($T_m$) is indicative of the stability of the protein incurred by additives. All the amino acids more or less increase $T_m$ indicating that they render stability towards thermal denaturation in the proteins. A relative effect in the stability is depicted in figure 4.6b. The effect seems noticeable in HSA and lysozyme, while it is only subtle in Ribonuclease-A. The thermal stability incurred by the amino acids HSA and lysozyme is more or less retained in all the amino acids. An interesting trend, however, is found in the reversibility experiments (figure 4.4). The calculated parameter loss percentage indicates the reversibility of the process, the lower the loss percentage the more reversible the process is. In buffer the loss percentage follows the order HSA>lysozyme>RNase-A; it can be correlated that is also

correlates the protein size, for a larger sized protein, unfolding is intrinsically complex involving many secondary structures and therefore less prone to return to their native structure. Barring Gly, the loss percentage increases substantially in Ribonuclease-A while it decreases in lysozyme. With comparable α-helical content, the contrasting behavior in lysozyme and Ribonuclease-A is intriguing.

From the thermodynamic parameters estimated from CD measurements we are unable to obtain any clear pattern in the unfolding-refolding phenomenon, the phenomenon is found to be protein-amino acid pair specific. With comparable α-helicity of lysozyme and RNase-A, they show comparable values of $\Delta H_{VF}$ and $\Delta C_p$ whereas, HSA having higher α-helix offer lower values for these parameters. The excess enthalpic stabilization reveals that it is protein specific since both HSA and lysozyme show very high stabilization in presence of Gly compared to that in buffer whereas in case of RNase-A, Gly slightly destabilizes the protein than buffer. The total magnitude of $\Delta C_p$ emanates from the two contributions (a) due to hydrophobic effect coming out from the change in hydration of non-polar surface area upon unfolding and (b) due to change in intramolecular vibrational modes, hydrogen bonding, electrostatic interactions and conformational entropy upon unfolding[48-49]. Previous reports of the reliance of $\Delta C_p$ on accessible surface area[54] shows that change in the hydration of surface area of non-polar groups of amino acids are the most significant positive contributor to the $\Delta C_p$ of unfolding, while the change in surface area of polar groups makes its magnitude smaller; the negative contributor to the $\Delta C_p$ of unfolding. The higher $\Delta C_p$ in lysozyme and RNase-A compared to HSA-buffer could emanate from the fact that due to the higher helicity of HSA, polar surface area could increase from helix unfolding. However, no clear trend on the effect of amino acid could be extracted from the observation. While the observation are intriguing a detailed investigation involving simulation is demanded to explain them.

## 4.5 Bibliography

1. Minton, A. P., The effect of volume occupancy upon the thermodynamic activity of proteins: some biochemical consequences. *Mol. Cell. Biochem.* **1983,** *55*, 119-140.
2. Ellis, R. J., Macromolecular crowding: an important but neglected aspect of the intracellular environment. *Curr. Opin. Struct. Biol.* **2001,** *11*, 114-119.
3. Zhou, H. X.; Rivas, G.; Minton, A. P., Macromolecular Crowding and Confinement: Biochemical, Biophysical, and Potential Physiological Consequences. *Annu. Rev. Biophys* **2008,** *37*, 375-397.
4. Lippert, K.; Galinski, E. A.; Trüper, H. G., Biosynthesis and function of trehalose inEctothiorhodospira halochloris. *Antonie van Leeuwenhoek* **1993,** *63*, 85-91.
5. Yancey, P. H.; Clark, M. E.; Hand, S. C.; Bowlus, R. D.; Somero, G. N., Living with water stress: evolution of osmolyte systems. *Science* **1982,** *217*, 1214-1222.
6. Yancey, P. H.; Somero, G. N., Methylamine osmoregulatory solutes of elasmobranch fishes counteract urea inhibition of enzymes. *J. Exp. Zool.* **1980,** *212*, 205-213.
7. Zou, Q.; Bennion, B. J.; Daggett, V.; Murphy, K. P., The molecular mechanism of stabilization of proteins by TMAO and its ability to counteract the effects of urea. *J. Am. Chem. Soc.* **2002,** *124*, 1192-1202.
8. Bolen, D. W.; Baskakov, I. V., The osmophobic effect: natural selection of a thermodynamic force in protein folding. *J. Mol. Biol.* **2001,** *310*, 955-963.
9. Timasheff, S. N., Protein-solvent preferential interactions, protein hydration, and the modulation of biochemical reactions by solvent components. *Proc. Natl. Acad.Sci.* **2002,** *99*, 9721-9726.
10. Meng, F.; Park, Y.; Zhou, H., Role of proline, glycerol, and heparin as protein folding aids during refolding of rabbit muscle creatine kinase. *Int. J. Biochem. Cell Biol.* **2001,** *33*, 701-709.
11. Singh, L. R.; Chen, X.; Kozich, V.; Kruger, W. D., Chemical chaperone rescue of mutant human cystathionine beta-synthase. *Mol. Genet. Metab.* **2007,** *91*, 335-342.
12. Tanaka, M.; Machida, Y.; Nukina, N., A novel therapeutic strategy for polyglutamine diseases by stabilizing aggregation-prone proteins with small molecules. *J. Mol. Med.* **2005,** *83*, 343-352.
13. Wang, A.; Bolen, D. W., Effect of proline on lactate dehydrogenase activity: testing the generality and scope of the compatibility paradigm. *Biophys. J.* **1996,** *71*, 2117-2122.
14. Chandler, D., Interfaces and the driving force of hydrophobic assembly. *Nature* **2005,** *437*, 640-647.
15. Estell, D. A.; Graycar, T. P.; Miller, J. V.; Powers, D. B.; Wells, J. A.; Burnier, J. P.; Ng, P. G., Probing steric and hydrophobic effects on enzyme-substrate interactions by protein engineering. *Science* **1986,** *233*, 659-663.
16. Zhou, R.; Huang, X.; Margulis, C. J.; Berne, B. J., Hydrophobic collapse in multidomain protein folding. *Science* **2004,** *305*, 1605-1609.

17. Acharya, H.; Vembanur, S.; Jamadagni, S. N.; Garde, S., Mapping hydrophobicity at the nanoscale: Applications to heterogeneous surfaces and proteins. *Faraday Discuss.* **2010,** *146*, 353-365.
18. Frömmel, C., The apolar surface area of amino acids and its empirical correlation with hydrophobic free energy. *J. Theor. Biol.* **1984,** *111*, 247-260.
19. Kyte, J.; Doolittle, R. F., A simple method for displaying the hydropathic character of a protein. *J. Mol. Biol.* **1982,** *157*, 105-132.
20. Guzzo, A. V., The influence of amino-acid sequence on protein structure. *Biophys. J.* **1965,** *5*, 809-822.
21. Weiss, I. M.; Muth, C.; Drumm, R.; Kirchner, H. O. K., Thermal decomposition of the amino acids glycine, cysteine, aspartic acid, asparagine, glutamic acid, glutamine, arginine and histidine. *BMC Biophys.* **2018,** *11*, 2.
22. Pal, S.; Pyne, P.; Samanta, N.; Ebbinghaus, S.; Mitra, R. K., Thermal stability modulation of the native and chemically-unfolded state of bovine serum albumin by amino acids. *Phys. Chem. Chem. Phys.* **2020,** *22*, 179-188.
23. Friedrichs, B., All about Albumin. Biochemistry, Genetics, and Medical Applications. *Food / Nahrung* **1997,** *41*, 382.
24. He, X. M.; Carter, D. C., Atomic structure and chemistry of human serum albumin. *Nature* **1992,** *358*, 209-215.
25. Lee, P.; Wu, X., Review: modifications of human serum albumin and their binding effect. *Curr. Pharm. Des.* **2015,** *21*, 1862-1865.
26. Jollès, P.; Jollès, J., What's new in lysozyme research? Always a model system, today as yesterday. *Mol. Cell. Biochem.* **1984,** *63*, 165-189.
27. Oliver, W. T.; Wells, J. E., Lysozyme as an alternative to growth promoting antibiotics in swine production. *J. Anim. Sci. Biotechnol.* **2015,** *6*, 35.
28. Jollès, P., Lysozymes: A Chapter of Molecular Biology. *Angew. Chem. Int. Ed.* **1969,** *8*, 227-239.
29. Messmore, J. M.; Fuchs, D. N.; Raines, R. T., Ribonuclease A: Revealing Structure-Function Relationships with Semisynthesis. *J. Am. Chem. Soc.* **1995,** *117*, 8057-8060.
30. Cuchillo, C. M.; Nogués, M. V.; Raines, R. T., Bovine pancreatic ribonuclease: fifty years of the first enzymatic reaction mechanism. *Biochemistry* **2011,** *50*, 7835-7841.
31. Chen, Y.-H.; Yang, J. T.; Martinez, H. M., Determination of the secondary structures of proteins by circular dichroism and optical rotatory dispersion. *Biochemistry* **1972,** *11* (22), 4120-4131.
32. Yasmeen, S.; Riyazuddeen; Rabbani, G., Calorimetric and spectroscopic binding studies of amoxicillin with human serum albumin. *J.Therm.Anal.Calorim.* **2016,** *127*, 1445-1455.
33. Santoro, M. M.; Bolen, D. W., Unfolding free energy changes determined by the linear extrapolation method. 1. Unfolding of phenylmethanesulfonyl .alpha.-chymotrypsin using different denaturants. *Biochemistry* **1988,** *27*, 8063-8068.

34. Senske, M.; Törk, L.; Born, B.; Havenith, M.; Herrmann, C.; Ebbinghaus, S., Protein Stabilization by Macromolecular Crowding through Enthalpy Rather Than Entropy. *J. Am. Chem. Soc* **2014,** *136*, 9036-9041.
35. Flora, K.; Brennan, J. D.; Baker, G. A.; Doody, M. A.; Bright, F. V., Unfolding of acrylodan-labeled human serum albumin probed by steady-state and time-resolved fluorescence methods. *Biophys. J.* **1998,** *75*, 1084-1096.
36. Mitra, R. K.; Sinha, S. S.; Pal, S. K., Hydration in protein folding: thermal unfolding/refolding of human serum albumin. *Langmuir* **2007,** *23*, 10224-10229.
37. Knubovets, T.; Osterhout, J. J.; Connolly, P. J.; Klibanov, A. M., Structure, thermostability, and conformational flexibility of hen egg-white lysozyme dissolved in glycerol. *Proc. Natl. Acad. Sci.* **1999,** *96*, 1262-1267.
38. Kurapkat, G.; Krüger, P.; Wollmer, A.; Fleischhauer, J.; Kramer, B.; Zobel, E.; Koslowski, A.; Botterweck, H.; Woody, R. W., Calculations of the CD spectrum of bovine pancreatic ribonuclease. *Biopolymers* **1997,** *41*, 267-287.
39. Moriyama, Y.; Takeda, K., Protective Effects of Small Amounts of Bis(2-ethylhexyl)sulfosuccinate on the Helical Structures of Human and Bovine Serum Albumins in Their Thermal Denaturations. *Langmuir* **2005,** *21*, 5524-5528.
40. Picó, G. A., Thermodynamic features of the thermal unfolding of human serum albumin. *Int. J. Biol. Macromol.* **1997,** *20*, 63-73.
41. Yan, Y. B.; Zhang, R. Q.; Zhou, H. M., Biphasic reductive unfolding of ribonuclease A is temperature dependent. *Eur. J. Biochem.* **2002,** *269*, 5314-5322.
42. Blumlein, A.; McManus, J. J., Reversible and non-reversible thermal denaturation of lysozyme with varying pH at low ionic strength. *Biochim. Biophys. Acta* **2013,** *1834*, 2064-2070.
43. Mozo-Villarías, A.; Cedano, J.; Querol, E., Hydrophobicity density profiles to predict thermal stability enhancement in proteins. *Protein. J.* **2006,** *25*, 529-535.
44. Li-Blatter, X.; Seelig, J., Thermal and Chemical Unfolding of Lysozyme. Multistate Zimm–Bragg Theory Versus Two-State Model. *J. Phys. Chem. B* **2019,** *123*, 10181-10191.
45. Rabbani, G.; Lee, E. J.; Ahmad, K.; Baig, M. H.; Choi, I., Binding of Tolperisone Hydrochloride with Human Serum Albumin: Effects on the Conformation, Thermodynamics, and Activity of HSA. *Mol. Pharmaceutics* **2018,** *15*, 1445-1456.
46. Stelea, S. D.; Pancoska, P.; Benight, A. S.; Keiderling, T. A., Thermal unfolding of ribonuclease A in phosphate at neutral pH: deviations from the two-state model. *Protein Sci.* **2001,** *10*, 970-978.
47. Senske, M.; Constantinescu-Aruxandei, D.; Havenith, M.; Herrmann, C.; Weingärtner, H.; Ebbinghaus, S., The temperature dependence of the Hofmeister series: thermodynamic fingerprints of cosolute–protein interactions. *Phys. Chem. Chem. Phys.* **2016,** *18*, 29698-29708.
48. Sturtevant, J. M., Heat capacity and entropy changes in processes involving proteins. *Proc. Natl. Acad. Sci.* **1977,** *74*, 2236-2240.
49. Prabhu, N. V.; Sharp, K. A., HEAT CAPACITY IN PROTEINS. *Annu. Rev. Phys. Chem.* **2005,** *56*, 521-548.

50. Liu, Y.; Sturtevant, J. M., The Observed Change in Heat Capacity Accompanying the Thermal Unfolding of Proteins Depends on the Composition of the Solution and on the Method Employed To Change the Temperature of Unfolding. *Biochemistry* **1996,** *35*, 3059-3062.
51. Ellerton, H. D.; Reinfelds, G.; Mulcahy, D. E.; Dunlop, P. J., Activity, Density, and Relative Viscosity Data for Several Amino Acids, Lactamide, and Raffinose in Aqueous Solution at 25°. *J. Phys. Chem.* **1964,** *68*, 398-402.
52. Whitney, P. L.; Tanford, C., Solubility of amino acids in aqueous urea solutions and its implications for the denaturation of proteins by urea. *J. Biol. Chem.* **1962,** *237*, 1735-1737.
53. Tyrrell, H. J. V.; Zaman, M., 1187. Optical studies of the soret effect. Part II. Entropies and heat capacities of transfer of glycine, DL-α-alanine, β-alanine, glycolamide, and lactamide in aqueous solution. *J. Chem. Soc.* **1964**, 6216-6226.
54. Myers, J. K.; Pace, C. N.; Scholtz, J. M., Denaturant m values and heat capacity changes: relation to changes in accessible surface areas of protein unfolding. *Protein Sci.* **1995,** *4*, 2138-2148.

# Chapter 5

## Nonpolar Hydrophobic Amino Acids as Macromolecular Crowding Agents Sharply Tune the Enzymatic Activity of Lysozyme


**Summary**

*In order to mimic the internal cell wall of our body several osmolytes are externally added to protein solution for in vitro study. In this study we have used five nonpolar hydrophobic amino acids (Gly, L-ala, L-val, L-leu, L-ile) as macromolecular crowders to investigate their role on the enzymatic activity of hen egg white lysozyme (HEWL) towards Micrococcus lysodeikticus (M. Lys.) cell as substrate. It has been found that except Ile, all other amino acids show a bell like profile of catalytic efficiency ($k_{cat}/K_m$) of lysozyme with their increasing concentration whereas for Ile the value is gradually increasing. The trend of activation energy ($E_a$) is well correlated with the catalytic efficiency of lysozyme. Several factors like soft interaction, excluded volume effect, viscosity, size, surface area, hydrophobicity compete with each other to modulate the enzymatic activity. This study explores that at low concentration of amino acids soft interaction predominates whereas at higher concentration range excluded volume, viscosity, hydrophobicity combinedly decrease the activity of lysozyme.*

## 5.1 Introduction

The interior of the living cells of our body are crowded with various macromolecules like ribosomes, nucleic acids, microtubules and several co-solutes like glucose, amino acids etc. These macromolecular crowding alter various properties of the protein molecules in the cell.[1-2] Perturbation of external environment of protein can lead to its unfolding[3-4] which may proceed through several pathways, among them the pathway having minimum topological frustration[5-6] is the preferred one. To maintain various biological functions, retaining of the native form of protein is important. Due to destruction of the native form, protein may lose its various activities. Therefore, it is very interesting to study the stability as well as activity of protein along with various factors that influence the conformation of protein. Enzymes are also proteins that have been often used to accelerate the chemical reactions of protein by choosing an alternative pathway of lower activation energy. In many cases, it has been found that enzymes modify the stability as well as activity of protein.[7] Enzymes are generally substrate specific and have high catalytic power to modulate the efficiency of protein.[8] Enzymes fold into their functional conformation through various types of bonding like hydrogen bonding, disulfide bonding, ionic bonding, hydrophobic interactions etc. by achieving minimum unfavorable hydrophobic and hydrophilic interactions between specific parts of protein chains.[9] In literature there are two different theories regarding enzymatic action towards substrate: (a) one is the conventional lock and key model[10] in which enzyme should have the complementary shape with respect to the shape of the active site of the substrate to properly fit, (b) another one is modern induced-fit model[10-12] where the enzymes should be flexible enough to reorganize their shapes accordingly to fit into the substrate. Due to several limitations of the lock and key model, the induced-fit model is more acceptable which recommends that when the substrate binds, the energy of binding helps the enzyme to change its conformation to form a catalytically competent state and after finishing its work the enzyme gets free by producing products.[10]

Lysozyme is a well-known compact globular protein comprising of total 129 residues, four alpha helices and two beta sheets.[13] There are four residues Trp62, Trp63, Asp101, Trp108 of lysozyme which are important for substrate binding whereas Glu35 and Asp52 residues help the substrate to be hydrolyzed.[14] The hydrolysis of beta glycosidic bond between N-acetyl muramic acid (NAM) and N-acetyl glucosamine (NAG) which is the backbone of many bacterial cell walls is catalyzed by lysozyme.[15] Numerous efforts have been given by various groups to study

the enzymatic activity of lysozyme on different cells.[16-18] Addition of various cosolutes externally can influence the folding-unfolding pathways of lysozyme differently.[19-20] Osmolytes (polyols, amino acids, peptides, dextran etc.) are one of the important cosolutes which can affect the stability of the lysozyme by denaturing its native state. Shahid et al.[21] have shown that in presence of dextran 70 and ficoll 70 lysozyme gets stabilized whereas its activity on M. lysodeikticus cell is decreased with the increasing concentration of both the crowders. Previous work from our group[18] has shown a bell like profile of the activity of lysozyme on M. lysodeikticus cell with the increasing concentration of two macromolecular crowders ethylene glycol (EG) and polyethylene glycol (PEG). Singh et al.[22] have reported that addition of trehalose in GdmCl increases the activity of lysozyme by removing the Gdm cation from the active sites of lysozyme. R. Atkin's group[16] has claimed a dramatic influence on the activity and stability of lysozyme in the presence of various ionic liquids. From previous studies it has been found that in general externally added cosolutes work in two ways to influence the protein activity depending on their concentration.[18] In low concentration regime of cosolutes the soft interaction which is basically attractive and nonspecific in nature predominates between protein and cosolutes whereas, in high concentration range of crowders it switches to excluded volume (the volume occupied by the crowder which is impenetrable by the protein molecules) effect which reduces the proximity between protein and substrate molecules and decreases the enzymatic activity of protein towards substrate. Some studies[23-24] have reported that when the enzymatic reaction follows Michaelis-Menten equation, excluded volume effect decreases both the catalytic constant ($k_{cat}$) and Michaelis-Menten constant ($K_m$).

Many groups[25-28] reported that hydrophobic interaction leads to protein stabilization where one or more than one residues of the protein is replaced by hydrophobic residues which stabilizes the folded state of protein. Indeed, the use of nonpolar hydrophobic amino acids as crowding agents to investigate the stability as well as activity of proteins is very limited. Therefore, here we report the effect of hydrophobicity of the amino acids of varying sizes as macromolecular crowders on the enzymatic activity of hen egg white lysozyme (HEWL) towards M. lysodeikticus (M. lys.) cell as substrate.

## 5.2 Materials and Methods

Glycine (Gly), L-alanine (Ala), L-valine (Val), L-leucine (Leu), L-isoleucine (Ile), lyophilized powder of hen egg white lysozyme (HEWL) [$M_w$ 14.3 kDa, molar extinction coefficient at 280 nm ($\varepsilon_{280}$ = 36000 $M^{-1}$ $cm^{-1}$), lyophilized micrococcus lysodeikticus (M. lys) cell were purchased from Sigma-Aldrich and used without further purification. All the solutions and samples were dissolved in 10mM phosphate buffer of pH ~7.4.

Enzymatic activity measurements were performed by turbid metric method using UV visible spectroscopic instrument (Shimadzu UV-2600 spectrophotometer). The decrease in absorption at 450 nm of the turbid solution of M. lys dead cell were recorded immediately after mixing with lysozyme. Temperature dependent activity measurement were performed using a Peltier attachment with the UV visible spectrophotometer to control the temperature. The secondary structure of lysozyme was measured by far-UV (190-260 nm) circular dichroism (CD) spectroscopy using JASCO-J-815 spectrometer with a Peltier attachment for the temperature dependent measurements using a quartz cuvette of 0.1 cm path-length. For CD experiment, 20 µM lysozyme and all the amino acids of 60 mM concentration were taken.

The simplest mechanism of an enzyme (E) kinetic reaction on a substrate (S) to form a product (P) is as follows:

$$E + S \rightleftarrows ES \rightarrow ES^{\#} \rightarrow E + P$$

Where, $ES$ is the enzyme-substrate complex and $ES^{\#}$ is the intermediate transition state before product formation. We measured the initial rate of cell lysis reaction at a fixed lysozyme concentration (0.1µM) by changing the substrate ($S$) concentration and found that it follows Michaelis-Menten equation. We have calculated enzyme catalytic efficiency ($k_{cat}/K_m$) and plotted as a function of amino acids concentration.

## 5.3 Results

The rate of enzyme catalytic reaction is found to vary with the concentration of externally added hydrophobic amino acids from the linear fitting of decrease of substrate concentration of first few seconds (figure 5.1a). For a clear quantitative understanding, we measure the concentration dependent rate of catalytic reaction of substrate by fixing lysozyme concentration (0.1μM) in absence and in presence of amino acids. We obtain reasonably good linear fits of the double reciprocal Lineweaver-Burk (L-B) plots (figure 5.1b) and from the slope and intercept of those curves, the catalytic parameters ($K_m$, $k_{cat}$ and $k_{cat}/K_m$) have been calculated.

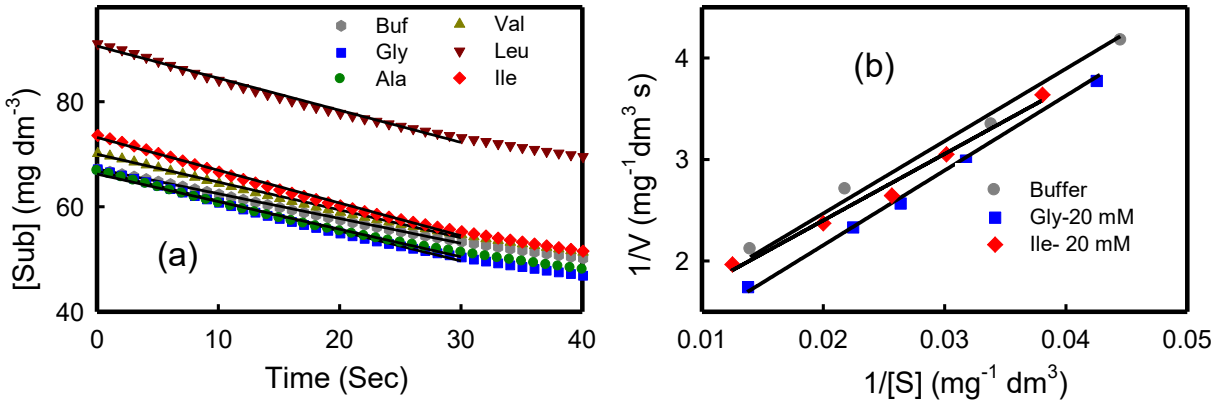


**Figure 5.1:** (a) A representative plot of lysozyme (0.1 μM) catalysed M. Lys. cell concentration decay (obtained from the O.D. at 450 nm) as a function of time in presence of different amino acids at room temperature. The solid lines represent linear fits. (b) Representative Lineweaver Burk (LB) plot for buffer and amino acids of 20 mM concentration.

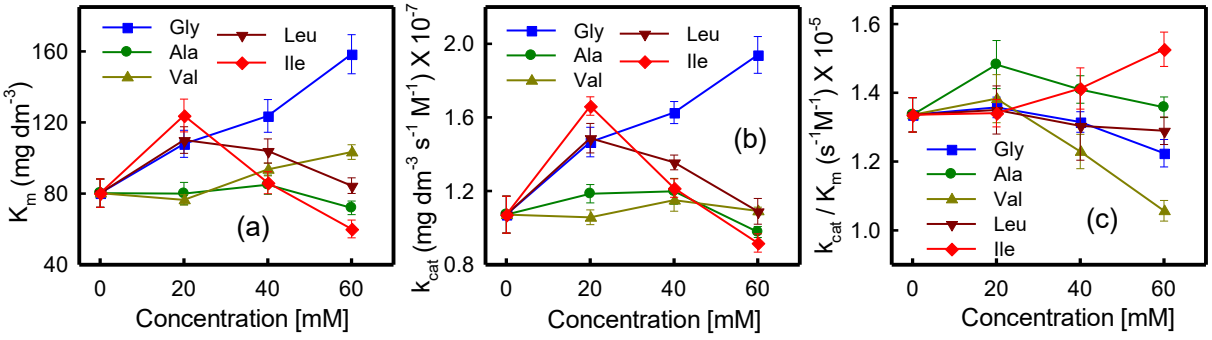


**Figure 5.2.** (a) Plot of Michaelis-menten constant ($K_m$) as a function of amino acids concentration.(b) Turnover number ($k_{cat}$) as a function of concentration of different amino acids. (c) Catalytic efficiency of lysozyme ($k_{cat}/K_m$) in presence of different concentrations of amino acids.

The obtained values of $K_m$ (80.3 mg $dm^{-3}$) and $k_{cat}$ ($1.07\times10^7$ mg $dm^{-3}$ $s^{-1}$ $M^{-1}$) in buffer are in excellent agreement with the previously reported values for the same enzyme-substrate complex.[18] The Michaelis-Menten constant ($K_m$) inversely illustrates the extent of dissociation of enzyme-substrate (E-S) complex; higher is the value of $K_m$, weaker is the binding of E-S complex. We have plotted $K_m$ values in presence of different concentration of amino acids in figure 5.2a. $K_m$ values increase with increasing concentration of Gly solution; this indicates that at low concentration of Gly, stable E-S complex is formed, which gets weaker with increasing concentration of Gly. The same trend is observed in presence of Val also. In presence of Ala medium, the change is very minimal at 20mM and 40mM concentration but at 60mM concentration a sharp decrease is observed. $K_m$ value shows a bell shaped nature in presence of Leu and Ile solution, where it is maximum at 20mM concentration and then it gradually decreases with the increase in concentration of the amino acids. The result clearly indicates that stability of E-S complex gets higher for low concentration of amino acids and also the weakest binding occurs at high concentration of amino acids in case of maximum hydrophobic residues (Leu and Ile).

Another important kinetic parameter is turnover number ($k_{cat}$) and the corresponding plot has been shown in figure 5.2b; it shows that at 20mM concentration of all the amino acids (except Val), its value increases compared to buffer whereas with the rise of concentration of the crowding agents (amino acids) $k_{cat}$ decreases gradually except in Gly solution. The value of $k_{cat}$ is monotonically increased with the increase in concentration of Gly whereas the slope of the reduction curve of $k_{cat}$ is very steep for Leu and Ile solution compared to other amino acids. The catalytic efficiency ($k_{cat}/K_m$) of the enzyme has also been estimated for all the amino acids used and the plot is depicted in figure 5.2c. It has been observed that the catalytic efficiency of the enzyme is increased in presence of amino acids at their 20mM concentration than buffer. With the increase in concentration of amino acids, the efficiency is started to decrease except in Ile medium, where the catalytic efficiency of lysozyme is gradually increased with the rise in concentration of Ile solution. This signifies that except in Ile solution, all other amino acids show a bell shaped feature in their enzymatic efficiency.

### 5.3.1: Energetics associated with the enzyme-kinetics:

The dissociation constant ($K_d$) of the complex $ES$ can be roughly equated to the $K_m$.[29] The corresponding free energy change ($\Delta G_M$) can be written as[30]

$$\Delta G_M = -RT \ln(1/K_d) \approx RT \ln K_m \quad \ldots\ldots\ [5.1]$$

The magnitude of $\Delta G_M$ is correlated to the '*entrance channel*', which modulates the permission of accessing of substrate and solvent towards the active site of enzyme as E and S react to form ES complex[31]. The lower the magnitude of $\Delta G_M$ in comparison to buffer, the interaction between E and S becomes more favorable. $ES$ is then converted to $ES^{\#}$ at the expense of free energy change given as,

$$\Delta G^{\#} = -RTln\left(\frac{h}{k_B T} k_{cat}\right) \quad \ldots\ldots\ldots\ [5.2]$$

Where, $h$ is the Planck's constant ($6.626 \times 10^{-34}$ J.sec) and $k_B$ is the Boltzmann's constant ($1.38 \times 10^{-23}$ J/K). The formation of $ES^{\#}$ indicates the '*exit channel*' which modulates the releasing pathway of unreacted substrate and product formed after the reaction, as $ES^{\#}$ breaks to form products.[32] The net free energy change for the formation of $ES^{\#}$ is given by,

$$\Delta G_t^{\#} = -RTln\left(\frac{h}{k_B T}\frac{k_{cat}}{K_m}\right) \quad \ldots\ldots\ldots\ [5.3]$$

The difference of $\Delta G_M$ between buffer and amino acids denoted as $\Delta\Delta G_M$ ($\Delta G_M^{Amino\ acids} - \Delta G_M^{Buffer}$) is solely dependent on the change of $K_m$, hence, the change of $\Delta\Delta G_M$ follows the same trend of $K_m$ and the corresponding plot has been shown in figure 5.3a. $\Delta\Delta G_M$ is more negative for Ala and Ile of 60mM concentration, for the other amino acids of different concentration its value increases indicating the reaction is disfavored with respect to that of buffer. This implies that entrance channel of the substrate for the formation of $ES^{\#}$ is favored in Ile and Ala solution of 60mM concentration, while the channel is disfavored for all the amino acids at its 40mM and concentration. The exit channel is characterized by the magnitude of $\Delta G^{\#}$ (equation 5.2) and the possibility of the overall reaction towards the product formation is controlled by the difference of the above two energy terms ($\Delta G_t^{\#}$), which is actually equivalent to the activation energy ($E_a$) term. We have calculated $\Delta\Delta G^{\#}$ $[\Delta\Delta G^{\#} = \Delta G^{\#(Amino\ acids)} - \Delta G^{\#(Buffer)}]$ and the

corresponding plot as a function of amino acids concentration has been manifested in figure 5.3b and its positive value indicates disfavoring of the exit channel. We have found that at low and moderate concentrations (20mM and 40mM) of all the amino acids, the exit channel is quantitatively favored, but at high concentration (60mM) of amino acids, only Ala and Ile show disfavoring exit channel.

The net activation energy change ($\Delta\Delta G_t^{\#}$) in presence of amino acids with respect to that of buffer is quantified by,

$$\Delta\Delta G_t^{\#} = \Delta G_t^{\#(Amino\ acids)} - \Delta G_t^{\#(Buffer)} \quad \ldots\ldots\ldots\ldots \quad [5.4]$$

It's variation as a function of amino acid concentration has been expressed in figure 5.3c. At 20mM concentration, $\Delta\Delta G_t^{\#}$ value decreases for all the amino acids indicating the enzyme-substrate reaction is favored in presence of amino acids at low concentration compared to buffer. Except in Ile solution, for all the amino acids $\Delta\Delta G_t^{\#}$ values increase with the rise in concentration of the amino acids suggesting disfavoring of the enzyme-substrate binding at higher concentration of amino acids. In Ile solution, the decrease in the $\Delta\Delta G_t^{\#}$ value with the increase in its concentration indicates more favorable interaction of the substrate with the enzyme. Since $\Delta\Delta G_t^{\#}$ is a rough estimation of activation energy ($E_a$) of the enzyme-substrate reaction pathway, to elucidate various kinetic parameters the temperature dependent activity measurement of the enzyme has been done.

### 5.3.2: Temperature dependent enzymatic activity measurements:

We have studied the temperature dependent lysozyme activity measurements in absence and in presence of 20mM amino acids by measuring catalytic activity at 298K, 303K, 308K and 313K. We have found that turnover number ($k_{cat}$) increases gradually with the rise of temperature as is expected from the following Arrhenius equation:

$$k_{cat} = A\, e^{-E_a/RT} \quad \ldots\ldots\ldots\ldots \quad [5.5]$$

$$\Rightarrow\ ln(k_{cat}) = lnA - \frac{E_a}{RT} \quad \ldots\ldots\ldots \quad [5.6]$$

We have plotted $ln(k_{cat})$ vs. $(1/T)$ for buffer as well as for different amino acids and a representative curve in presence of 20mM Ile solution has been shown in figure 5.4a. From the slope of the linear fitting of this curve, activation energy ($E_a$) for the enzyme catalytic process in absence and in presence of amino acids has been calculated and the plot has been depicted in figure 5.4b. For buffer, the value of $E_a$ is 44.4 kJ mol$^{-1}$ and all the amino acids reduce the $E_a$ values to different extent with respect to that of buffer. In presence of Ala solution, lowest $E_a$ value attains (22.4 kJ mol$^{-1}$) whereas, it reaches maximum (42.8 kJ mol$^{-1}$) in Ile solution. The magnitude of $E_a$ values in different amino acids solutions follow the order: Ile > Gly > Leu > Val > Ala which is well correlated with the hydrophobicity of the amino acids.[33-34] The trend of their $E_a$ values can be correlated to the enzyme catalytic efficiency ($k_{cat}/K_m$) of 20mM amino acid solutions since higher catalytic efficiency dictates lower $E_a$ values. For 20mM concentration, Ala shows highest efficiency among all amino acids, and that is reflected in its lowest $E_a$ value, while lowest value of catalytic efficiency in Ile solution indicates highest magnitude of $E_a$ value.

**5.3.3: Circular dichroism (CD) study:** To investigate the structural perturbation of lysozyme due to addition of these five amino acids we have recorded the far-UV (190-260 nm) CD spectra of lysozyme at room temperature in the presence of each amino acids in their 60 mM concentration and the corresponding spectra are shown in figure 5.5a. We observe that no amino acids perturb the secondary structure of lysozyme. We have also calculated the melting temperature ($T_m$) of lysozyme in presence of amino acids from temperature dependent CD measurements and the plots are shown in figure 5.5b. It has been found that all amino acids increase the melting temperature of lysozyme compared to buffer indicating these hydrophobic amino acids increase the stability of lysozyme without perturbing its native form.

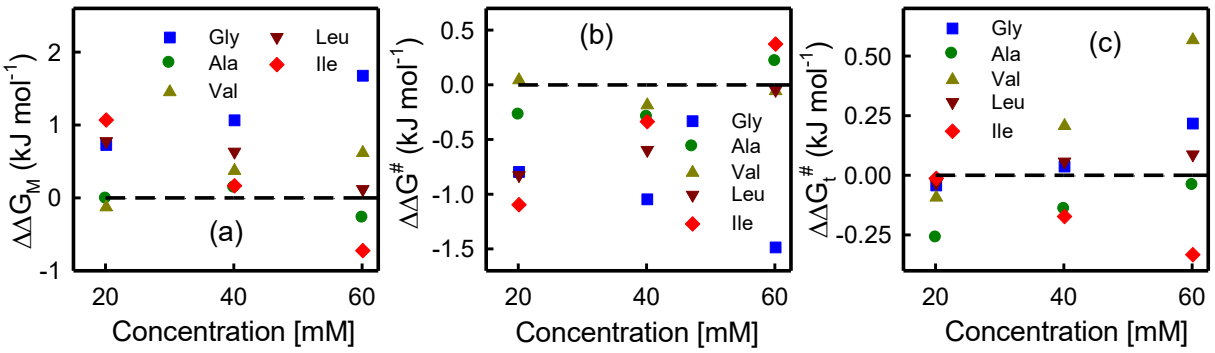


**Figure 5.3.** (a) $\Delta\Delta G_M = \Delta G_M^{Amino\ acids} - \Delta G_M^{Buffer}$ as a function of amino acid concentration. (b) $\Delta\Delta G^{\#} = \Delta G^{\#(Amino\ acids)} - \Delta G^{\#(Buffer)}$ with respect to amino acid concentration. (c) Plot of $\Delta\Delta G_t^{\#} = \Delta G_t^{\#(Amino\ acids)} - \Delta G_t^{\#(Buffer)}$ as a function of amino acid concentration.

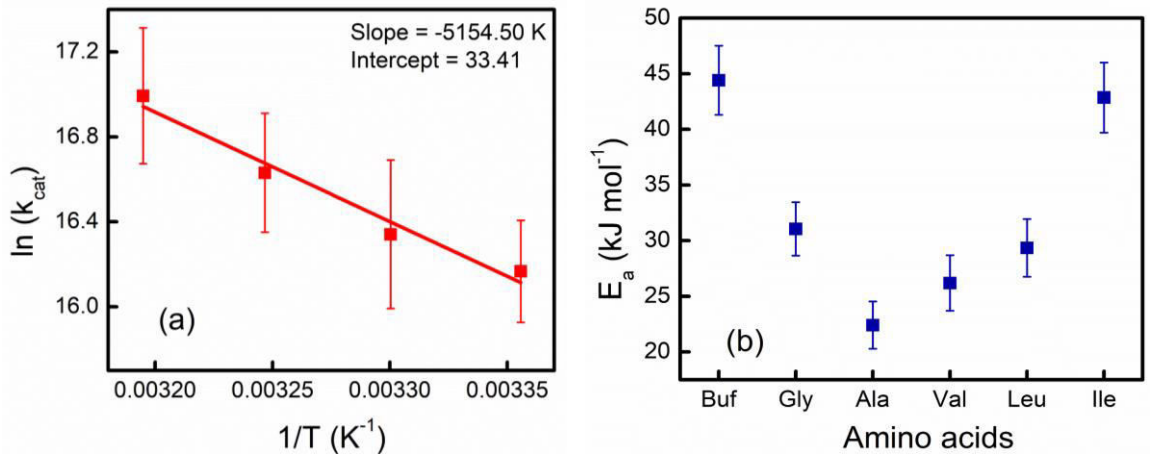


**Figure 5.4:** (a) Representative Arrhenius plot of temperature dependent enzyme-substrate kinetics in presence of 20 mM isoleucine solution. (b) Activation energy ($E_a$) calculated as a function of different amino acids.

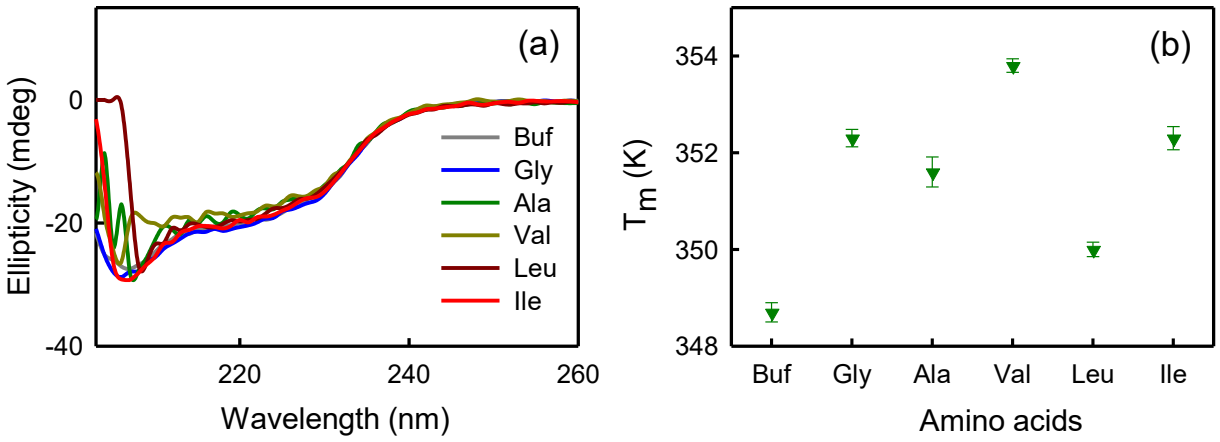


**Figure 5.5.** (a) Far-UV CD spectra of 20μM lysozyme in presence of different amino acids (60 mM) in 10 mM sodium phosphate buffer (pH 7.4). (b) Melting temperatures ($T_m$) of lysozyme in buffer and in presence of different amino acids.

**Table 5.1:** Catalytic parameters of lysozyme in buffer and in presence of amino acids of different concentrations

| Sample | $K_m$ (mg $dm^{-3}$) | $k_{cat} \times 10^{-7}$(mg $dm^{-3}$ $s^{-1}$ $M^{-1}$) | $k_{cat}/K_m \times 10^{-5}$ ($s^{-1}$ $M^{-1}$) |
|---|---|---|---|
| Buffer | 80.24±8 | 1.07±0.10 | 1.33±0.05 |
| 20 mM | | | |
| Gly | 107.99±7.6 | 1.47±0.08 | 1.36±0.03 |
| Ala | 79.98±6.3 | 1.18±0.05 | 1.48±0.07 |
| Val | 76.46±2.9 | 1.06±0.04 | 1.38±0.07 |
| Leu | 110.15±7.5 | 1.49±0.08 | 1.35±0.07 |
| Ile | 123.92±9.2 | 1.66±0.05 | 1.34±0.04 |
| 40 mM | | | |
| Gly | 123.68±9.2 | 1.63±0.06 | 1.31±0.03 |
| Ala | 85.02±5.4 | 1.20±0.07 | 1.41±0.04 |
| Val | 93.59±3.6 | 1.15±0.06 | 1.23±0.05 |
| Leu | 103.96±6.8 | 1.35±0.04 | 1.30±0.1 |
| Ile | 86.08±6.2 | 1.22±0.05 | 1.41±0.06 |
| 60 mM | | | |
| Gly | 158.42±11 | 1.94±0.10 | 1.22±0.04 |
| Ala | 71.98±3.8 | 0.98±0.03 | 1.36±0.03 |
| Val | 103.34±4.1 | 1.09±0.02 | 1.06±0.03 |
| Leu | 84.46±4.4 | 1.09±0.07 | 1.29±0.04 |
| Ile | 60.12±5 | 0.92±0.05 | 1.53±0.05 |

**Table 5.2:** Energetics for the Enzyme (lysozyme) catalyzed reaction in buffer and in presence of amino acids of different concentrations

| Sample | $\Delta G_M$ (kJ/mol) | $\Delta G^{\#}$ (kJ/mol) | $\Delta G_t^{\#}$ (kJ/mol) |
|---|---|---|---|
| Buffer | 10.86 | 32.88 | 43.74 |
| 20 mM | | | |
| Gly | 11.60 | 32.09 | 43.70 |
| Ala | 10.86 | 32.61 | 43.48 |
| Val | 10.74 | 32.93 | 43.65 |
| Leu | 11.65 | 32.06 | 43.71 |
| Ile | 11.94 | 31.79 | 43.73 |
| 40 mM | | | |
| Gly | 11.94 | 31.84 | 43.78 |
| Ala | 11.00 | 32.59 | 43.60 |
| Val | 11.24 | 32.70 | 43.95 |
| Leu | 11.50 | 32.29 | 43.80 |
| Ile | 11.03 | 32.55 | 43.60 |
| 60 mM | | | |
| Gly | 12.55 | 31.40 | 43.96 |
| Ala | 10.59 | 33.10 | 43.70 |
| Val | 11.49 | 32.83 | 44.31 |
| Leu | 10.99 | 32.84 | 43.83 |
| Ile | 10.15 | 33.26 | 43.41 |

**Table 5.3:** Melting temperatures ($T_m$) of lysozyme in buffer and in presence of 60 mM of amino acids obtained by temperature dependent CD measurement

| Sample | $T_m$ (K) |
|---|---|
| Buffer | 348.7±0.20 |
| Gly-60 mM | 352.3±0.18 |
| Ala-60 mM | 351.6±0.31 |
| Val-60 mM | 353.8±0.14 |
| Leu-60 mM | 350.0±0.15 |
| Ile-60 mM | 352.3±0.24 |

**Table 5.4:** Parameters for the Temperature dependent Enzyme (Lysozyme) catalyzed reaction in buffer and in presence of amino acids of 20 mM concentrations

| **Temperature (K)** | $\mathbf{k_{cat} \times 10^{-7}}$**(mg dm$^{-3}$ s$^{-1}$ M$^{-1}$)** | $\boldsymbol{E_a}$ **(kJ/mol)** |
|---|---|---|
| Buffer | | |
| 298 | 1.09±0.15 | 44.41±3.1 |
| 303 | 1.30±0.18 | |
| 308 | 1.75±0.20 | |
| 313 | 2.57±0.20 | |
| Gly-20 mM | | |
| 298 | 1.36±0.14 | 31.05±2.4 |
| 303 | 1.86±0.17 | |
| 308 | 2.21±0.16 | |
| 313 | 2.51±0.17 | |
| Ala-20 mM | | |
| 298 | 1.20±0.12 | 22.40±2.1 |
| 303 | 1.31±0.15 | |
| 308 | 1.57±0.12 | |
| 313 | 1.83±0.17 | |
| Val-20 mM | | |
| 298 | 1.41±0.15 | 26.19±2.5 |
| 303 | 1.65±0.13 | |
| 308 | 1.98±0.15 | |
| 313 | 2.33±0.17 | |
| Leu-20 mM | | |
| 298 | 1.33±0.12 | 29.34±2.6 |
| 303 | 1.63±0.16 | |
| 308 | 1.95±0.14 | |
| 313 | 2.35±0.16 | |
| Ile-20 mM | | |
| 298 | 1.05±0.24 | 42.85±3.1 |
| 303 | 1.25±0.35 | |
| 308 | 1.67±0.28 | |
| 313 | 2.40±0.32 | |

## 5.4 Discussion

The work reported here is an attempt to investigate the effect of various nonpolar hydrophobic amino acids as macromolecular crowders on the catalytic activity of lysozyme in the enzymatic reaction with the M. Lys cell. We observe an interesting trend in the enzymatic efficiency of lysozyme with the substrate in presence of five different amino acids (Gly, Ala, Val, Leu, Ile) with varying hydrophobicity. In order to get insight about the enzymatic activity of lysozyme, double reciprocal plot has been made which reveals that the enzyme obeys Michaelis-Menten equation in presence of all amino acids. It has been observed that change of $K_m$ is very significant in presence of more hydrophobic amino acids Leu and Ile compared to buffer as well as with the change in concentration of the amino acids; whereas, the change is very minimal in presence of Ala and Val solution. Since lower $K_m$ value indicates greater affinity of enzyme towards substrate. It has been understood that in the lower concentration region of crowders, substrate prefers small sized less hydrophobic amino acids to show better binding with the enzyme, whereas, at the high concentration range of crowders greatest affinity between lysozyme and substrate is shown in presence of largest sized most hydrophobic Ile solution.[33-36] Figure 5.2b shows that except for Gly solution, $k_{cat}$ values show a bell shaped profile with concentration of the amino acids added implying that at low concentration of amino acids, the reaction between enzyme and substrate is faster compared to buffer but with the rise of concentration of amino acids enzyme cannot interact well with the substrate. $k_{cat}$ shows subtle variation in presence of Ala and Val whereas, the change is very sharp for Leu and Ile suggesting either size or hydrophobicity or both the properties of the amino acids play an important role to modulate $k_{cat}$. From previous studies, it is apparently understood that at low concentration of crowders, soft or preferential interaction predominates to increase the catalytic efficiency of enzyme-substrate reaction[37-38], whereas, at high concentration excluded volume effect plays significant role to decrease the $k_{cat}$ value of enzyme.[39] Due to the very small size of Gly, probably the excluded volume effect is not so prominent even at its 60mM concentration; as a result, the $k_{cat}$ value is monotonically increasing with the increase in concentration of Gly. Figure 5.2c shows the $k_{cat}/K_m$ values which depicts the catalytic efficiency of lysozyme in binding with substrate. It is noticed that at 20mM concentration of the crowders, the catalytic efficiency of lysozyme decreases with the increasing size/hydrophobicity of the amino acids except in Gly solution although the change is very marginal for Gly, Leu and Ile medium in comparison to buffer. It has

been observed that except in Ile medium, the $k_{cat}/K_m$ value is decreasing with the increase in concentration of amino acids beyond 20mM. Although at low concentration (20mM) of amino acids the $k_{cat}/K_m$ value follows a regular pattern with the size or hydrophobicity of the amino acids; at higher concentration the pattern is very random suggesting that at low concentration, soft interaction predominately controls the efficiency of the enzyme whereas, at higher concentration of amino acids more than one factors are responsible. It has been known that viscosity of the medium, protein stability and flexibility, preferential interaction, volume exclusion - all these factors modulate the enzymatic activity towards substrate.[18, 21, 40-42]. From the CD measurement, it has been found that at 60mM concentration of added amino acids there is no perturbation of the protein structure whereas, the melting temperature of lysozyme is increased than buffer suggesting in presence of 60mM of all the amino acids the stability of lysozyme has been increased keeping its conformation intact. According to induced fit model[43], to bind with the substrate properly the enzyme should be flexible in nature so that it can modulate its shape according to the shape of the binding site of the substrate. Therefore, since higher concentration of amino acids increases the stability of the lysozyme the flexibility of lysozyme should be reduced which decreases the binding capacity of lysozyme with the substrate known as stability-activity trade-off.[44-45] As a result, the catalytic efficiency of lysozyme decreases in presence of high concentration of the added amino acids. Apart from that, viscosity of the medium has a key role in modulating the enzymatic activity. In highly viscous media, the proximity of the enzyme and substrate has been greatly reduced which in turn decreases the enzymatic efficiency. Since the viscosity of the amino acids is increased with the increase in hydrophobicity as well as with the increase in concentration of the amino acids[46-47], there is a possibility of decreasing enzymatic efficiency in presence of Leu and Ile solution comparatively than in Ala and Val solution along with the reduction of efficiency at their high concentration compared to low concentration. In the case of Ile, we observe a different trend which probably due to larger surface area as well as greater hydrophobicity of Ile compared to the other amino acids used. In presence of high concentration of Leu medium, the subtle reduction of catalytic efficiency is observed but the change is very prominent in case of Ala and Val solution. This indicates that with the increase in size and hydrophobicity of amino acids, two opposing factors (efficiency increasing factor and efficiency decreasing factor) compete and balance with each other at high concentration resulting modulation of the overall catalytic activity. It has been

already discussed that at higher concentration of the crowders both viscosity factor and protein stability decrease the enzymatic efficiency. From previous studies[48], it is well understood that size is directly proportional to the excluded volume effect of the crowders which also decreases the catalytic efficiency of the enzyme. On contrary, from previous studies, it has been found that the hydrophobic amino acid Ile forms large cluster at its high concentration.[49] Therefore, in our case, at higher concentration Ile probably forms cluster or aggregates which hinders to enter between enzyme and substrate due to the steric reason. As a result, the proximity between enzyme and substrate is increased leads to stronger interaction between them; consequently the activity of lysozyme increases.

From the experimental data, it is well understood that only Ala and Ile at their 60mM concentration show both favorable entrance channel and exit channel of the substrate. The difference in free energy change of lysozyme in buffer and the added amino acids $\Delta\Delta G_t^{\#}$ shows monotonic increment with the increase in the concentration of the amino acids except for Ile solution which shows a gradual decrease. As $\Delta\Delta G_t^{\#}$ is proportional to the activation energy of the medium the estimated energetic parameters suggest that the enzymatic efficiency is lowered with the concentration of the crowders except Ile which increases the efficiency of the lysozyme monotonically with the increase of its concentration.

The temperature dependent catalytic activity measurement reveals that lysozyme-substrate interaction follows Arrhenius equation in presence of added amino acid solutions. Figure 5.4b reveals that the activation barrier of lysozyme gets lower in presence of 20mM concentration of all amino acids compared to buffer indicating favorable binding interaction between lysozyme and substrate in presence of amino acids. The activation energy is minimum in presence of Ala followed by an increase in activation energy with the increase in size or hydrophobicity of the amino acids suggesting that enzymatic efficiency decreases with the increase in size or hydrophobicity of amino acids except in Gly solution which is in well correlated with the trend of $k_{cat}/K_m$ values estimated at 20mM concentration of amino acids (figure 5.2c). To explore the unusual trend of these catalytic parameters of lysozyme in presence of smallest sized Gly and largest sized Ile medium, hard core theoretical investigation and more detailed studies are on demand in future.

## 5.5 Bibliography

1. Elcock, A. H., Models of macromolecular crowding effects and the need for quantitative comparisons with experiment. *Curr. Opin. Struct. Biol* **2010,** *20*, 196-206.
2. Zimmerman, S. B.; Minton, A. P., Macromolecular crowding: biochemical, biophysical, and physiological consequences. *Annu. Rev. Biophys. Biomol. Struct* **1993,** *22*, 27-65.
3. Roche, J.; Caro, J. A.; Norberto, D. R.; Barthe, P.; Roumestand, C.; Schlessman, J. L.; Garcia, A. E.; García-Moreno, B. E.; Royer, C. A., Cavities determine the pressure unfolding of proteins. *Proc. Natl. Acad. Sci. U.S.A* **2012,** *109*, 6945-6950.
4. Cao, Y.; Li, H., How do chemical denaturants affect the mechanical folding and unfolding of proteins. *J. Mol. Biol* **2008,** *375*, 316-324.
5. Bryngelson, J. D.; Onuchic, J. N.; Socci, N. D.; Wolynes, P. G., Funnels, pathways, and the energy landscape of protein folding: a synthesis. *Proteins* **1995,** *21*, 167-195.
6. Shea, J. E.; Onuchic, J. N.; Brooks, C. L., Exploring the origins of topological frustration: Design of a minimally frustrated model of fragment B of protein A. *Proc. Natl. Acad. Sci. U.S.A* **1999,** *96*, 12512-12517.
7. Shoichet, B. K.; Baase, W. A.; Kuroki, R.; Matthews, B. W., A relationship between protein stability and protein function. *Proc. Natl. Acad. Sci. U.S.A* **1995,** *92*, 452-456.
8. Robinson, P. K., Enzymes: principles and biotechnological applications. *Essays Biochem* **2015,** *59*, 1-41.
9. Drago, G. A.; Gibson, T. D., Enzyme Stability and Stabilisation: Applications and Case Studies. *Engineering and Manufacturing for Biotechnology, Springer* **2001,** *4*, 361-376.
10. Koshland Jr, D. E., The Key–Lock Theory and the Induced Fit Theory. *Angew. Chem. Int. Ed* **1995,** *33*, 2375-2378.
11. Koshland, D. E., Application of a Theory of Enzyme Specificity to Protein Synthesis. *Proc. Natl. Acad. Sci. U.S.A* **1958,** *44* (2), 98-104.
12. Thoma, J. A.; Koshland Jr, D. E., Competitive Inhibition by Substrate during Enzyme Action. Evidence for the Induced-fit Theory. *J. Am. Chem. Soc* **1960,** *82*, 3329-3333.
13. Jollès, P., Lysozymes: A Chapter of Molecular Biology. *Angew. Chem. Int. Ed.* **1969,** *8*, 227-239.
14. Blake, C. C.; Koenig, D. F.; Mair, G. A.; North, A. C.; Phillips, D. C.; Sarma, V. R., Structure of hen egg-white lysozyme. A three-dimensional Fourier synthesis at 2 Angstrom resolution. *Nature* **1965,** *206*, 757-761.
15. Gorin, G.; Wang, S. F.; Papapavlou, L., Assay of lysozyme by its lytic action on M. lysodeikticus cells. *Anal. Biochem* **1971,** *39*, 113-127.
16. Mann, J. P.; McCluskey, A.; Atkin, R., Activity and thermal stability of lysozyme in alkylammonium formate ionic liquids—influence of cation modification. *Green Chem* **2009,** *11*, 785-792.
17. Levashov, P. A.; Matolygina, D. A.; Ovchinnikova, E. D.; Adamova, I. Y.; Gasanova, D. A.; Smirnov, S. A.; Nelyub, V. A.; Belogurova, N. G.; Tishkov, V. I.; Eremeev, N. L.; Levashov, A. V., The bacteriolytic activity of native and covalently immobilized lysozyme against Gram-

positive and Gram-negative bacteria is differentially affected by charged amino acids and glycine. *FEBS Open Bio* **2019,** *9*, 510-518.
18. Samanta, N.; Mahanta, D. D.; Patra, A.; Mitra, R. K., Soft interaction and excluded volume effect compete as polyethylene glycols modulate enzyme activity. *Int. J. Biol. Macromol.* **2018,** *118*, 209-215.
19. Levartovsky, Y.; Shemesh, A.; Asor, R.; Raviv, U., Effect of Weakly Interacting Cosolutes on Lysozyme Conformations. *ACS Omega* **2018,** *3*, 16246-16252.
20. Makhatadze, G. I.; Privalov, P. L., Protein interactions with urea and guanidinium chloride. A calorimetric study. *J. Mol. Biol* **1992,** *226*, 491-505.
21. Shahid, S.; Ahmad, F.; Hassan, M. I.; Islam, A., Relationship between protein stability and functional activity in the presence of macromolecular crowding agents alone and in mixture: An insight into stability-activity trade-off. *Arch. Biochem. Biophys* **2015,** *584*, 42-50.
22. Biswas, B.; Singh, P. C., Molecular level insight into the counteraction of trehalose on the activity as well as denaturation of lysozyme induced by guanidinium chloride. *Chem. Phys* **2019,** *527*, 110489.
23. Laurent, T. C., Enzyme reactions in polymer media. *Eur. J. Biochem* **1971,** *21*, 498-506.
24. Minton, A. P.; Wilf, J., Effect of macromolecular crowding upon the structure and function of an enzyme: glyceraldehyde-3-phosphate dehydrogenase. *Biochemistry* **1981,** *20*, 4821-4826.
25. Eriksson, A. E.; Baase, W. A.; Zhang, X. J.; Heinz, D. W.; Blaber, M.; Baldwin, E. P.; Matthews, B. W., Response of a protein structure to cavity-creating mutations and its relation to the hydrophobic effect. *Science (New York, N.Y.)* **1992,** *255*, 178-183.
26. Kellis, J. T.; Nyberg, K.; S˘ail, D. a.; Fersht, A. R., Contribution of hydrophobic interactions to protein stability. *Nature* **1988,** *333*, 784-786.
27. Shortle, D.; Stites, W. E.; Meeker, A. K., Contributions of the large hydrophobic amino acids to the stability of staphylococcal nuclease. *Biochemistry* **1990,** *29*, 8033-8041.
28. Matsumura, M.; Becktel, W. J.; Matthews, B. W., Hydrophobic stabilization in T4 lysozyme determined directly by multiple substitutions of Ile 3. *Nature* **1988,** *334*, 406-410.
29. Berg, J. M.; Tymoczko, J. L.; Stryer, L., The Michaelis-Menten Model Accounts for the Kinetic Properties of Many Enzymes. *Biochemistry, 5th Edition* **2002**.
30. Fersht, A. R.; Perutz, M. F., Catalysis, binding and enzyme-substrate complementarity. *Proc. Royal. Soc. B* **1974,** *187*, 397-407.
31. Gora, A.; Brezovsky, J.; Damborsky, J., Gates of Enzymes. *Chem. Rev* **2013,** *113*, 5871-5923.
32. Berg, J. M.; Tymoczko, J. L.; Stryer, L., Enzymes Accelerate Reactions by Facilitating the Formation of the Transition State. *Biochemistry, 5th Edition* **2002**.
33. Engelman, D. M.; Steitz, T. A.; Goldman, A., Identifying nonpolar transbilayer helices in amino acid sequences of membrane proteins. *Annu. Rev. Biophys. Biophys. Chem* **1986,** *15*, 321-353.

34. Monera, O. D.; Sereda, T. J.; Zhou, N. E.; Kay, C. M.; Hodges, R. S., Relationship of sidechain hydrophobicity and alpha-helical propensity on the stability of the single-stranded amphipathic alpha-helix. *J. Pept. Sci* **1995,** *1*, 319-329.
35. Tien, M. Z.; Meyer, A. G.; Sydykova, D. K.; Spielman, S. J.; Wilke, C. O., Maximum allowed solvent accessibilites of residues in proteins. *PLoS One* **2013,** *8*, e80635.
36. Chothia, C., Hydrophobic bonding and accessible surface area in proteins. *Nature* **1974,** *248*, 338-339.
37. Kuznetsova, I. M.; Turoverov, K. K.; Uversky, V. N., What Macromolecular Crowding Can Do to a Protein. *Int. J. Mol. Sci* **2014,** *15*, 23090-23140.
38. Timasheff, S. N., The Control of Protein Stability and Association by Weak Interactions with Water: How Do Solvents Affect These Processes? *Annu. Rev. Biophys. Biomol. Struct.* **1993,** *22*, 67-97.
39. Minton, A. P., The influence of macromolecular crowding and macromolecular confinement on biochemical reactions in physiological media. *J. Biol. Chem* **2001,** *276*, 10577-80.
40. Jerome, F. S.; Tseng, J. T.; Fan, L. T., Viscosities of aqueous glycol solutions. *J. Chem. Eng. Data* **1968,** *13*, 496.
41. Han, F.; Zhang, J.; Chen, G.; Wei, X., Density, Viscosity, and Excess Properties for Aqueous Poly(ethylene glycol) Solutions from (298.15 to 323.15) K. *J. Chem. Eng. Data* **2008,** *53*, 2598-2601.
42. Silva, R. M. M.; Minim, L. A.; Coimbra, J. S. R.; Rojas, E. E. G.; da Silva, L. H. M.; Minim, V. P. R., Density, Electrical Conductivity, Kinematic Viscosity, and Refractive Index of Binary Mixtures Containing Poly(ethylene glycol) 4000, Lithium Sulfate, and Water at Different Temperatures. *J. Chem. Eng. Data* **2007,** *52*, 1567-1570.
43. Koshland, D. E., Application of a Theory of Enzyme Specificity to Protein Synthesis. *Proc. Natl. Acad. Sci.* **1958,** *44*, 98-104.
44. Soskine, M.; Tawfik, D. S., Mutational effects and the evolution of new protein functions. *Nat. Rev. Genet* **2010,** *11*, 572-582.
45. Kurahashi, R.; Tanaka, S. I.; Takano, K., Activity-stability trade-off in random mutant proteins. *J. Biosci. Bioeng.* **2019,** *128*, 405-409.
46. Mason, L. S.; Kampmeyer, P. M.; Robinson, A. L., The Viscosities of Aqueous Solutions of Amino Acids at 25 and 35°. *J. Am. Chem. Soc* **1952,** *74*, 1287-1290.
47. Yan, Z.; Wang, J.; Zhang, H.; Xuan, X., Volumetric and Viscosity Properties of α-Amino Acids and Their Groups in Aqueous Sodium Caproate Solutions. *J. Chem. Eng. Data* **2005,** *50*, 1864-1870.
48. Sharp, K. A., Analysis of the size dependence of macromolecular crowding shows that smaller is better. *Proc. Natl. Acad. Sci.* **2015,** *112*, 7990-7995.
49. Md Azmi, N. S.; Anuar, N.; Roberts, K. J.; Abu Bakar, N. F.; Kamalul Aripin, N. F., Molecular aggregation of L-isoleucine in aqueous solution and its impact on the determination of solubility and nucleation kinetics. *J. Cryst. Growth* **2019,** *519*, 91-99.

# Chapter 6

## Contrasting Effect of Hydration Dynamics of $Gdm_2SO_4$ and GdmCl Influences the Stability of Proteins Differently


**Summary**

*Guanidinium chloride (GdmCl) is a well-known denaturant of protein whereas, guanidinium sulphate ($Gdm_2SO_4$) stabilizes the protein slightly. The contrasting behavior of hydration dynamics exerted by $Gdm_2SO_4$ and GdmCl has a great impact on the protein's stability but the correct reason for this contrasting effect is still elusive and controversial. In this study, we have tried to explore the origin of this contrasting effect of $Gdm_2SO_4$ and GdmCl on bulk water network with mid-infrared (MIR) and terahertz time-domain spectroscopic (TTDS) techniques. Using two other inorganic salts, NaCl and $Na_2SO_4$ it has been suggested that neither individual cation nor anion controls the hydration dynamics rather their combined effect alters the water structure network which influences the stability of the human serum albumin (HSA) protein.*

## 6.1 Introduction

Co-solvent and co-solutes often play a crucial role in regulating protein stability and its various functions.[1-3] From the last few decades guanidinium salts have been attracted huge attention to researchers for their contrasting behavior towards protein unfolding/folding depending on the counter-ions of guanidinium cations ($Gdm^+$). Some groups proposed that the weakly hydrated[4-6] $Gdm^+$ has high surface propensity[7] and its planar structure may be the reason for protein unfolding because tetramethyl ammonium cation ($TMA^+$) having same low charge density and low surface affinity stabilizes the folded state of protein.[8] The denaturation behavior of guanidinium chloride (GdmCl) is vastly investigated though the exact mechanism of denaturation is still illusive and controversial. G. Graziano showed that chloride salt of guanidinium cation ($Gdm^+$) denatures protein drastically whereas, sulphate salt of that stabilizes the protein. J. Heyda et al.[9] reported that GdmCl having weakly solvated and low charge density anion acts as strong salting-in agent which increases the solubility of polypeptide and promote unfolding but $Gdm_2SO_4$ containing strongly solvated and high charge density anion behaves as strong salting-out agent which stabilizes the collapsed state of the peptide.[10-12] J. Hunger and coworkers showed that monovalent GdmCl and GdmSCN salts do not show any ionic association whereas, bivalent salts $Gdm_2SO_4$, $Gdm_2CO_3$ show ion aggregation. By investigating the preferential interaction of different guanidinium salts on bovine serum albumin the stability order they found was : guanidinium sulphate > guanidinium acetate > guanidinium chloride.[13] With the aid of both experimental and computational studies it has been found that GdmCl is more effective denaturing agents for human serum albumin in comparison to urea.[14] Hence, it can be understood that $Gdm^+$ exhibits versatile effect on protein stability (or unfolding) which makes it an interesting probe to explore.

Several attempts have been put forward to explain the distinct behavior of GdmCl and $Gdm_2SO_4$ towards denaturation of protein. Graziano proposed a statistical thermodynamic model to vindicate their contradictory behavior.[15] He defined a fundamental term called “reversible work” to create a suitable cavity separately for holding the denatured state and the native state in aqueous medium. In case of GdmCl, this cavity contribution term is not substantial enough to engulf the destabilizing contributions coming from the direct attractive interactions of $Gdm^+$ with the protein surface and the conformational entropy gain during unfolding. But in $Gdm_2SO_4$, the

strongly solvated and very high charge density of $SO_4^{2-}$ increases the number density by interacting strongly with the surrounding water molecules; that's why the comparatively greater work is needed for the cavity formation and this term submerges the two destabilizing contributions reversing the denaturing ability of $Gdm^+$. MD simulation study showed that $Gdm_2SO_4$ stabilizes protein structure by depleting strongly from the protein surface via volume exclusion whereas, GdmCl is indifferent to attract or deplete from the protein surface. Dempsey et al. proposed another explanation[16] both from experimental (neutron diffraction and CD spectroscopic measurement techniques) and MD simulation observation.[6, 17] In highly denaturing salts (GdmCl, GdmSCN), $Gdm^+$ exhibits self-interactions by forming like-charge ($Gdm^+$- $Gdm^+$) ion pair in solution[18-23] above and below the weakly hydrated surfaces of the guanidinium molecular plane. Apart from, due to the presence of multiple sites (three $NH_2$ groups and hydrophobic carbon chain) $Gdm^+$ forms preferential multiple weak interactions involving hydrogen bonding with the peptide backbone and also π-stacking interactions with some planar amino acid residues (Trp, Arg, Gln, Asn) of the protein surface in the molecular plane. But the hetero ion-pairing formation between $SO_4^{2-}$ and $Gdm^+$ in $Gdm_2SO_4$ attenuates these interactions and reverses the denaturing activity of $Gdm^+$ in GdmCl. In another work, the same group argued that in 1.5 m $Gdm_2SO_4$ solution $Gdm^+$ forms aggregated network (clusters) strongly making this peculiar cation unavailable for multiple interactions with the protein backbone; but $Gdm^+$ is randomly distributed in 3m GdmSCN solution making its site free to interact with the protein hydrophobic groups.[17] Apart from that, the tetrahedral structure of $SO_4^{2-}$ can easily assist the development of bonded networks with the surrounding $Gdm^+$ cation and this is how $Gdm_2SO_4$ acts as mild protein stabilizer.

There is huge ambiguities about denaturation mechanism of $Gdm^+$ still persist among researchers. It has been proposed that $Gdm^+$ of GdmCl interacts directly with both the polar and nonpolar groups of protein to denature it.[8, 24] Garde et al. showed that since $Gdm^+$ is planar having three amine groups ($NH_2$), it can form multiple hydrogen bonds with water which destabilizes the folded state of the protein.[8] Scott et al.[25] showed that $Gdm^+$ denatures the protein altering the water network in the medium by forming more preferential strong linear hydrogen bonds with water compared to weak bent hydrongen bonds between water molecules. Few groups[4, 26] claimed that there is no strong hydration around $Gdm^+$ because of its low charge density; however, MD simulation results predicted a significant ordering of hydration layer

depending upon its orientation.[6, 27] Dielectric relaxation study has explored that $Gdm^+$ interacts with the amide group of the protein backbone which is likely the source of disruption of the native state of protein.[28] The infrared photo-dissociation study provides that $Gdm^+$ interacts only with the waters which are at the same plane preferably in a hydrophobic region like protein surface which in turn causes perturbation of the hydration dynamics of protein leads to its denaturation.[29]

Since the efficacy of denaturing agents towards proteins partly depends on the strength of the interaction between protein and its surrounded water molecules, the investigation of hydration dynamics around protein is much needed to understand the mechanism of denaturation. In order to investigate the collective hydration dynamics around biomolecules including different salts, Terahertz spectroscopy is a potential sensitive tool due to its low energy (~ 4 MeV) which does not affect solutes (biomolecules) and also its perfect timescale to probe the ultrafast collective hydrogen bonding dynamics of the solvent waters around the solutes which extends up-to several hydration layers (2-3). Moreover, the absorption coefficient of water at 1.5 THz is increased by a large factor (upto 4-5 times) between 270 K and 370 K which is not possible to observe in other spectral regions.[30] However, using the THz spectroscopy both the phase and amplitude of the transmitted radiation can be measured which enables to calculate various optical parameters like absorption coefficient, complex refractive index and complex dielectric constant of the samples by solving Fresnel's transmittance equations.[31-32] One of the present authors previously investigated the hydration dynamics of HSA during its thermal denaturation using THz techniques.[33] They studied the collective hydration dynamics around HSA during its chemical denaturation with GdmCl as well as compared them with two more salts tetramethylguanidinium chloride (TMGdmCl) and sodium chloride (NaCl) in the 0.3-2.0 THz frequency range using a multiple Debye dielectric relaxation model. From this study, it is suggested that cation and anion of the salt play significant role in the perturbation of the water network which is a contributing factor for the protein denaturation. Hence, in this current contribution we are interested to explore the impact of $Gdm^+$ with its different counter anions $Cl^-$ , $SO_4^{2-}$ on hydration dynamics using both mid-infrared (MIR) and terahertz time-domain spectroscopic (TTDS) techniques to decode their contrasting behavior regarding protein denaturation.

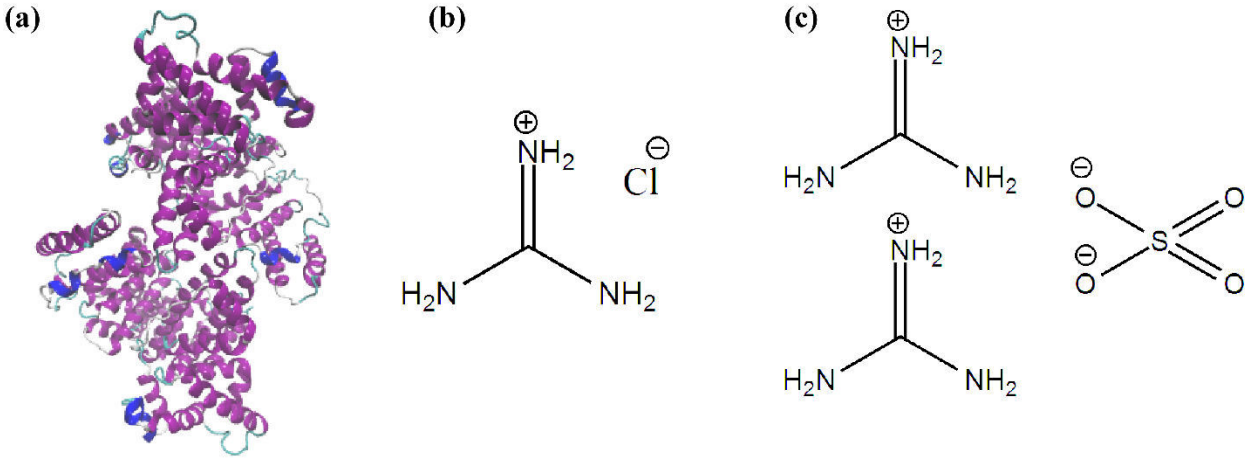


**Figure 6.1:** (a) The tertiary structure of HSA protein; the chemical structure of (b) GdmCl and (c) $Gdm_2SO_4$

## 6.2 Materials and Methods

Human serum albumin (HSA) [molecular weight of 66 kDa and containing 585 amino acid residues], guanidinium chloride (GdmCl), guanidinium sulphate ($Gdm_2SO_4$), sodium chloride (NaCl) and sodium sulphate ($Na_2SO_4$) were purchased from Sigma-Aldrich with ~ 99% purity and used without further purification. All the aqueous solutions were prepared in 10mM sodium phosphate buffer ($NaH_2PO_4$ / $Na_2HPO_4$) of pH ~7.4 using de-ionized Milli-Q water.

Far-UV (190-260 nm) circular dichroism (CD) spectroscopic measurements were performed using JASCO-J-815 spectrophotometer using a 0.1cm path-length quartz cuvette. The CD signal at 222 nm obtained in mili-degree is converted into mean residue ellipticity (MRE) in deg $cm^2$ $dmol^{-1}$, which is given by,

$$\text{MRE} = \frac{\theta_{obs}}{10 \times n \times C \times l} \qquad \ldots\ldots\ldots\ldots\ldots\ldots\ldots \qquad (6.1)$$

Here, $\theta_{obs}$ is the observed ellipticity in mili-degree, $n$ corresponds to the number of amino acid residues in the protein, $C$ is the molar concentration of the protein and $l$ is the path-length of the cuvette in cm. The percentage of α-helix is calculated from the MRE values at 222 nm using the following equation[34-35] :

$$\% \text{ α-helix} = [\frac{(\text{MRE}_{222}-2340)}{30300} \times 100] \qquad \ldots\ldots\ldots\ldots\ldots\ldots \quad (6.2)$$

Fourier transform infrared (FTIR) spectra with 4% $D_2O$ in $H_2O$ were taken by JASCO-FTIR-6300 spectrometer (transmission mode) using $CaF_2$ window in the 2200-2800 frequency windows.

Terahertz time-domain spectroscopy (TTDS) measurements were performed by a commercial terahertz spectrophotometer (TERA K8, Menlo system). A 780 nm Er-doped fiber laser with a pulse width of less than 100 fs and a repetition rate of 100 MHz excited a terahertz emitter antenna to produce terahertz radiation with a bandwidth up to 3.0 THz (>60 dB). This terahertz radiation was then focused on the measuring sample followed by focusing the transmitted part on a terahertz detector antenna which was gated by the probe laser beam. Both the terahertz antennas are gold dipoles with a dipole gap of 5 μm deposited on a low temperature-grown GaAs substrate. All the measurements were carried out under a dry nitrogen atmosphere to avoid water-vapor absorption with a controlled humidity of less than 10% at 293 K using a liquid cell (Bruker, model A 145) with z-cut quartz windows and Teflon spacer of 100 μm thickness. Samples were reloaded five times in the sample cell, and ten full scans were averaged together to minimize the error in the results. By varying the time delay between the probe and the pump beam, the amplitude and phase of the terahertz electric field were measured as a function of time.

Frequency-dependent power and phase of the transmitted pulse were obtained using Fourier analysis of the measured electric-field amplitude $E_{THz}(t)$. Eventually, the frequency-dependent real ($\varepsilon'$) and imaginary ($\varepsilon''$) dielectric constants of the measured samples were extricated as, $\varepsilon' = n^2(\nu) - k^2(\nu)$ and $\varepsilon'' = 2n(\nu)k(\nu)$ in which the complex refractive index is written as, $\tilde{n}(\nu) = n(\nu) - ik(\nu)$.[36] The ultrafast relaxation dynamics of water in different salt solutions were calculated using the frequency-dependent complex dielectric constant $\tilde{\varepsilon}(\nu) = \varepsilon'(\nu) - i\varepsilon''(\nu)$ of those solutions. The errors have been estimated by least-squares method. We applied a Debye-model[36-39] to describe the dynamics of water molecules in different aqueous salt solutions. According to the Debye model, the complex frequency-dependent dielectric response in aqueous salt solutions can be written as[40]:

$$\tilde{\varepsilon}(\nu) = \varepsilon_\infty + \sum_{j=1}^{m} \frac{\varepsilon_j - \varepsilon_{j+1}}{1 + i2\pi\nu\tau_j} + \frac{\sigma}{i\omega\varepsilon_0} \qquad \ldots\ldots\ldots\ldots\ldots\ldots \quad (6.3)$$

Where, $\tau_j$ is the relaxation time for $j$-th relaxation mode, $\varepsilon_\infty$ is the extrapolated dielectric constant at a very high frequency, $\varepsilon_1$ and $\varepsilon_j$ are the static dielectric constant and dielectric constant for different relaxation processes respectively, $m$ describes the number of relaxation modes, $\sigma$ is the dc conductivity of the salt solutions, $\varepsilon_0$ is the dielectric permittivity in vacuum and $\omega = 2\pi\nu$ is the angular frequency. The magnitude of induced polarization is given by the dispersion amplitude, $S_j = (\varepsilon_j - \varepsilon_{j+1})$. The Debye model with $m$=1 is the simplest form associated with the single relaxation mode which indicates the complete relaxation motion. In general, the total dielectric function of a polar liquid in the low-frequency regime is determined by the dielectric relaxation (DR) processes and by intermolecular and intramolecular vibrational modes at higher frequencies.[41] In our previous studies,[33, 42-43] we fitted the relaxation data of pure water in this frequency range by using three different timescales. Here also we fitted the relaxation data in pure water and in presence of different concentrations of four salt solutions using third order Debye relaxation model. According to the third order Debye relaxation model, the frequency-dependent complex permittivity ($\tilde{\varepsilon}(\omega)$) can be written as following form:

$$\tilde{\varepsilon}(\omega) = \varepsilon_\infty + \frac{S_1}{1+i\omega\tau_1} + \frac{S_2}{1+i\omega\tau_2} + \frac{S_3}{1+i\omega\tau_3} + \frac{\sigma}{i\omega\varepsilon_0} \qquad \ldots\ldots\ldots\ldots\ldots\ldots \quad (6.4)$$

in which $S_k$ is the relaxation strength of the $k$-th relaxation mode and $\omega$ is the angular frequency.

## 6.3 Results

***CD study:*** Although it is well-known that GdmCl and $Gdm_2SO_4$ show contrasting behaviour on protein stability, we have verified it using HSA protein in presence of GdmCl and $Gdm_2SO_4$ by far-UV (190-260nm) circular dichroism (CD) spectroscopic measurement to get the idea about the interaction of secondary structure of protein with the two salts. The experimental results have been depicted in figure 6.2a and 6.2b. From the figure 6.2a, it is clearly visible that with the rise of GdmCl concentration CD signal decreases regularly especially beyond 2M concentration. For better understanding, we have also plotted the relative change of CD signal at 222 nm in figure 6.3(a) which gives the notion about the secondary structure of proteins.[44-45] It indicates that the secondary structure of HSA is significantly perturbed beyond 2M concentration of GdmCl and at 5M the structure is completely disrupted, but no perturbation is observed in case of $Gdm_2SO_4$

(figure 6.2b) although both have same guanidinium ($Gdm^+$) cation. This gives a clue that $Gdm^+$ not solely responsible to denature the protein; rather its counter anion has a definite impact on protein unfolding. For this, we have widen our study taking two alkali metal salts (NaCl and $Na_2SO_4$) having the same cation ($Na^+$) to examine the role of anions on the denaturation of protein and the corresponding CD spectra have been shown in figure 6.2c and 6.2d. Both NaCl and $Na_2SO_4$ have no impact on the secondary structure of HSA and they are insensitive towards denaturation or stabilization of protein. To get more quantitative information about the secondary structural content, we further calculate percentage of α-helix of HSA in presence of these four salts using equation 6.2. and plotted it in figure 6.3(b) as a function of salt concentrations. It is observed that α-helical content of protein decreases sharply with GdmCl concentration with a collateral increase in the random coil conformation which indicates the onset of protein unfolding, especially beyond 2M GdmCl concentration. On the contrary, marginal effect is observed in the α-helical content for $Gdm_2SO_4$, NaCl and $Na_2SO_4$ solutions. This study gives a speculative hint that since contrasting behaviour has been shown by GdmCl and $Gdm_2SO_4$ for protein stabilization/destabilization, the contribution of $Gdm^+$ is not the exclusive factor to denature the protein, rather its counter anionic part has a significant contribution. From earlier study, it is found that protein stability depends on various factors like protein-salt interactions, hydrophobic effect, hydration dynamics etc.[46-49] Scott et al.[25] showed that $Gdm^+$ denatures the protein altering the water network in the medium by forming more preferential strong linear hydrogen bonds with water compared to weak bent hydrongen bonds between water molecules. In order to explore the impact of these ionic salts on the dynamics of water network which is an important contributing factors on protein stability, it is necessary to understand first the hydration dynamics of these salts individually which is very elusive till now. For this reason, we further measure terahertz time-domain spectroscopic (TTDS) study of these aqueous salt solutions which extracts information about the collective hydration dynamics in the extended hydration capsule of the salts.

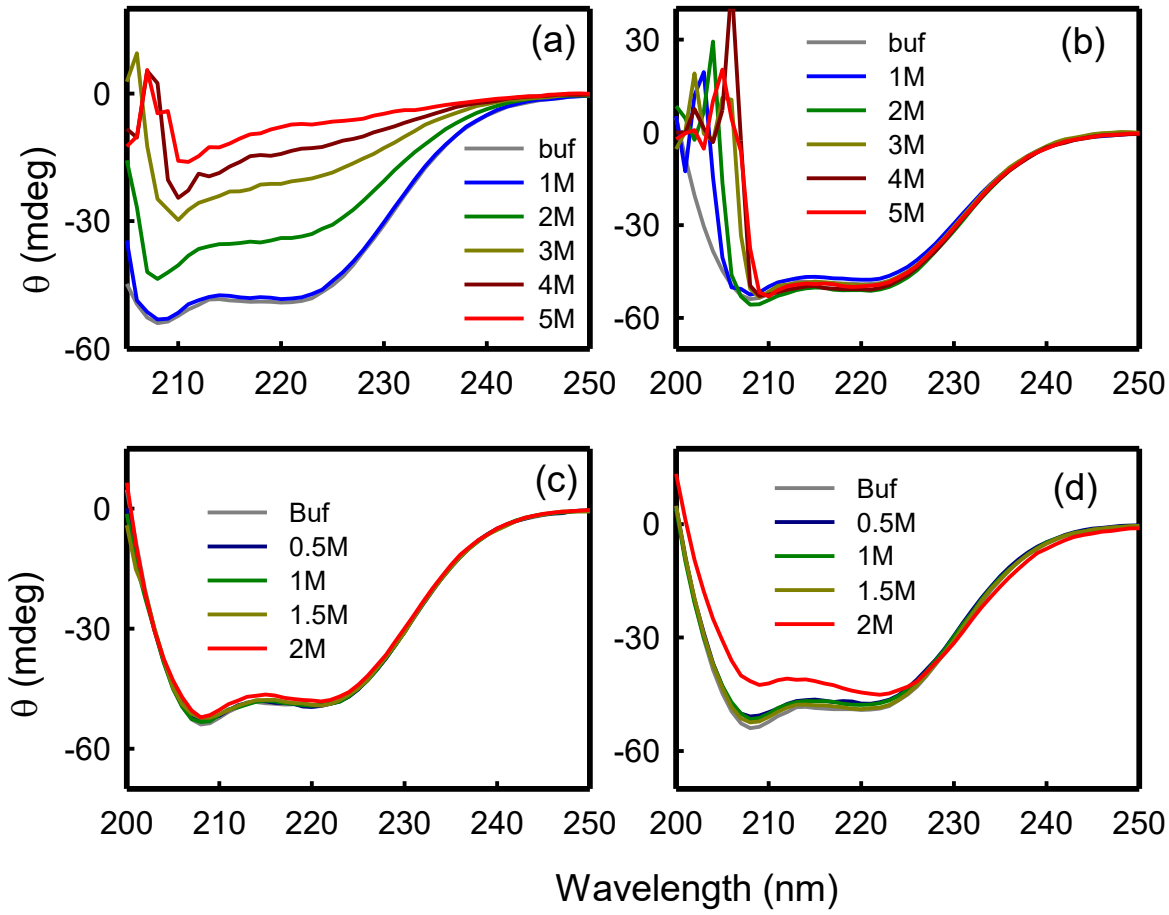


**Figure 6.2:** Room temperature Far-UV CD spectra of HSA in sodium phosphate buffer (pH ~ 7.4) at different concentration of (a) GdmCl (b) $Gdm_2SO_4$ (c) NaCl and (d) $Na_2SO_4$.

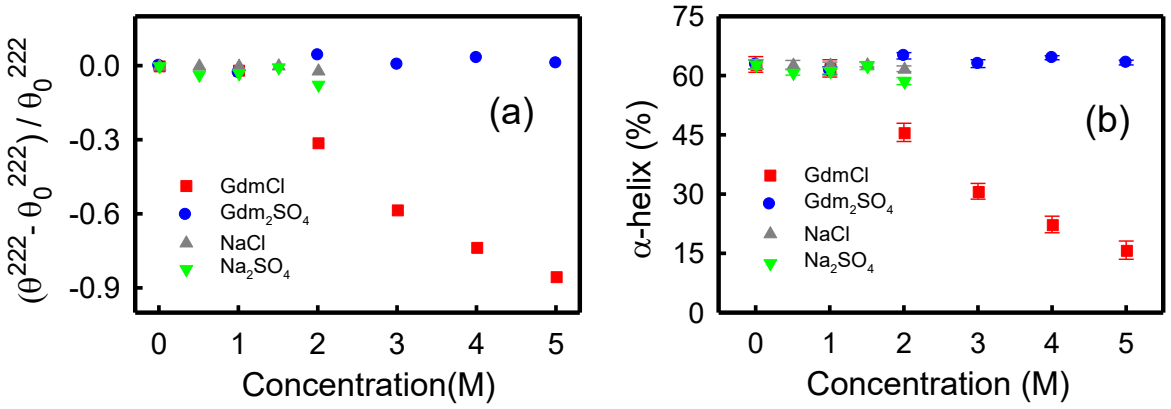


**Figure 6.3.** (a) Relative change of CD signal at 222 nm as a function of different salt concentrations. (b) Percentage of α-helix with respect to salt concentrations.

***TTDS study:*** Earlier our group[33, 43] revealed the effect of GdmCl, NaCl on the collective hydrogen bonding network of water using TTDS technique, hence in this work we are more interested to investigate the impact of $Gdm_2SO_4$ on water network to decode its opposing behavior on protein stability compared to GdmCl salt. We have used terahertz time domain spectroscopy (TTDS) to measure the frequency dependent absorption coefficient (α) of $Gdm_2SO_4$ at varying concentrations and the results are shown in figure 6.4a.

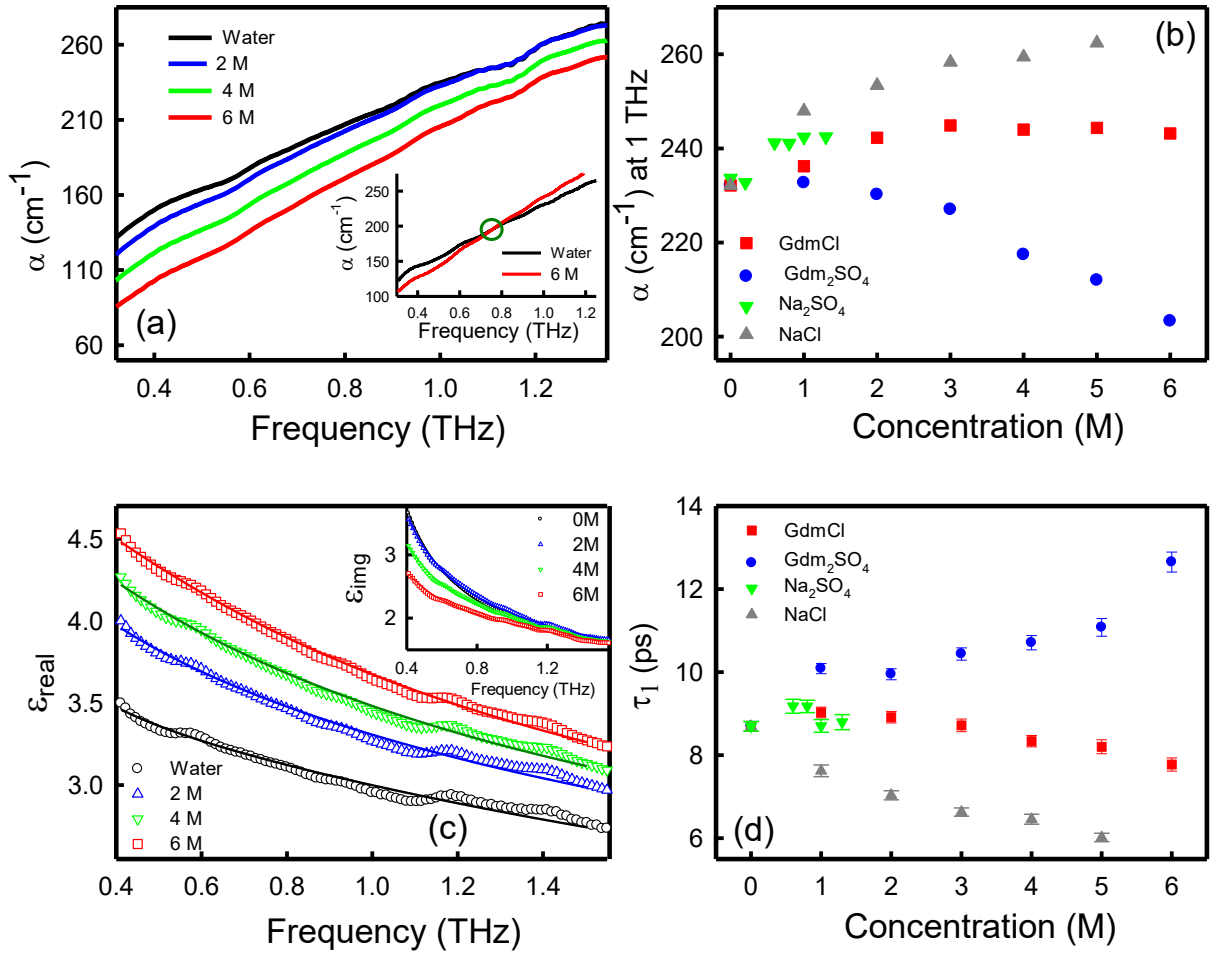


**Figure 6.4:** (a) THz frequency dependent absorption coefficient (α) of aqueous $Gdm_2SO_4$ salt solutions at its different concentrations. Inset shows the representative plot of absorption coefficient (α) of aqueous GdmCl salt solutions at its two different concentrations. The green circle indicates the crossing point. (b) Absorption coefficient (α) at 1 THz as a function of GdmCl, $Gdm_2SO_4$, $Na_2SO_4$ and NaCl salt concentrations. (c) Frequency dependent real dielectric constant ($\varepsilon_{real}$) of aqueous $Gdm_2SO_4$ solutions at different concentrations. Inset shows the imaginary part of dielectric constant of aqueous $Gdm_2SO_4$ solutions of different concentrations as a function of THz frequency. (d) Co-operative relaxation time scales of water ($\tau_1$) as a function of GdmCl, $Gdm_2SO_4$, NaCl and $Na_2SO_4$ salt concentrations.

It is observed that absorption coefficient (α) is linearly increasing with the rise of THz frequency at all measured $Gdm_2SO_4$ concentrations and the $\alpha(\nu)$ sketch for the buffer shows comparable accordance with the previously reported observations.[33, 43] We further notice that THz frequency dependent $\alpha(\nu)$ spectra decreases constantly with the increase in $Gdm_2SO_4$ concentration. We have also shown $\alpha(\nu)$ profiles as a function of THz frequency at different concentrations of GdmCl (representative curves have been depicted in figure 6.4a, inset), $Na_2SO_4$ in figure 6.5 and NaCl solutions in our earlier reports.[33, 43]

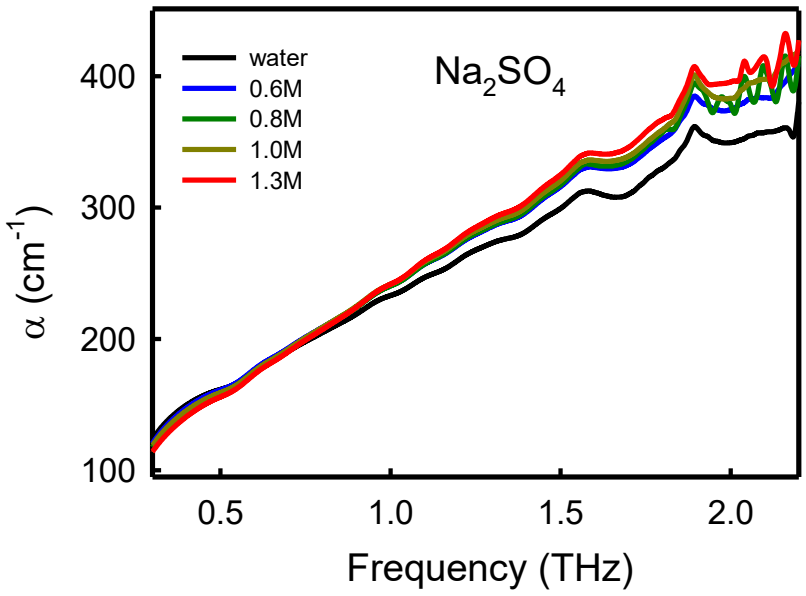


**Figure 6.5:** Absorption coefficient (α) profile as a function of THz frequency for different concentration of $Na_2SO_4$.

If we attentively watch the $\alpha(\nu)$ sketch with those salt concentrations, it divulges an interesting observation; $\alpha(\nu)$ curves of salt solutions bisects the curve of buffer (pure water). At low frequency ($\leq$ 1 THz or 33 $cm^{-1}$) the magnitude of $\alpha_{\text{salt-solution}}$ is comparatively less than $\alpha_{\text{buffer}}$ and beyond this the former suffers high value than the latter. The contrasting behavior of $\alpha_{\text{salt-solution}}$ with THz frequency may be due to fluctuations and oscillations of water dipoles induced by the rattling motions (oscillations of cations and anions) of ions[50] and the polarizability and intermolecular charge fluctuations i.e. oscillating vibrational modes and transition dipole moments of ions which can increase with the pico-second frequency.[51-54] However, the occurrence of such bisections or crossing points (CP) at a particular frequency called the crossing

frequency ($\nu_{CP}$) stipulates that after the $\nu_{CP}$ the aqueous salt solution exhibits larger α value in comparison to that of buffer. The higher α value in salt solution compared to that of buffer is termed as "THz excess".[50, 55] However, a better visualization of such bisections is observed in figure 6.4a, inset where, the green circle demarcates the crossing point in GdmCl solution. We then calculate the $\nu_{CP}$ for all the aqueous salt solutions at its different concentrations and plotted it as a function of salt concentrations in figure 6.6. It indicates that $\nu_{CP}$ endures a blue shift with increasing concentration of all the chosen four salts. Another fascinating observation from the plot is that for 1M concentration of all the salts $\nu_{CP}(Gdm_2SO_4) > \nu_{CP}(Na_2SO_4) > \nu_{CP}(GdmCl) > \nu_{CP}(NaCl)$ and in case of 2M and 3M of $Gdm_2SO_4$, GdmCl and NaCl salts, the order is, $\nu_{CP}(Gdm_2SO_4) > \nu_{CP}(GdmCl) > \nu_{CP}(NaCl)$.

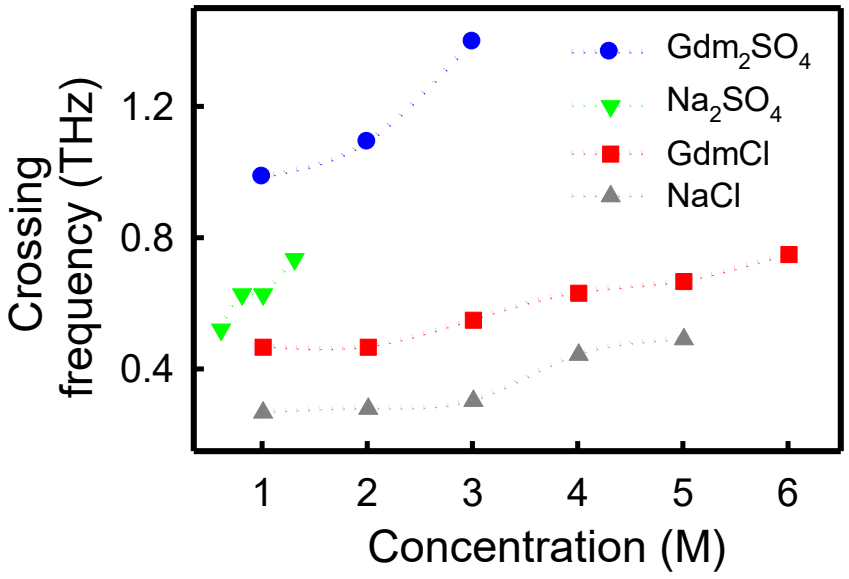


**Figure 6.6:** Plot of crossing frequency (C.F) in THz region as a function of different salt concentration

Several dynamical processes like hydrogen bond rearrangement, rotational and difusional motions of tetrahedrally coordinated water are entailed at picosecond timescales. From MD simulation study, Heyden et al.[54] observed that vibrational density of states of oxygen atoms in hydrogen bond rearrangement dynamics of water, rotational relaxation (calculated from single dipole auto- correlation function) and diffusional motions (calculated from mean square displacemen) of water gets blue-shifted with a concomitant increase in their magnitude for the hydrophobic amino acid residues in comparison to the hydrophilic one and this is explained by

the increased steric effect for water molecules to solvate buried hydrophobic residues of protein which are frequently found within cleft or groove of protein. Laage et al. analytically explained the same observation purely via the excluded volume effect of the solute.[56] So, to cross the absorption coeffcient of buffer ($\alpha_{buffer}$), hydrophobic solute requires less frequency compared to the hydrophilic parts of solute; or, in other words, we can say that $\nu_{CP}$ suffers blue-shifted when water interacts with a hydrophilic surface environment in comparison to the hydrophobic parts.[54, 57] Thus, the trend of $\nu_{CP}$ with solute concentration typically signifies the degree of hydrophilicity (or hydrophobicity) around the solute surface. Here it is important to point out that for 4M-6M concentration of $Gdm_2SO_4$, $\alpha(\nu)$ do not cross at all with the buffer spectra at least upto our measured THz frequency limit (1.3 THz) but such case do not appear for GdmCl, $Na_2SO_4$ and NaCl salts. However, the observed blue shift for all the four salts thus infers that, with the rise of salt concentration, water suffers more hydrophilic surface of those salts along with the change of water network in its extended hydration layer. But as the sulphate dianion ($SO_4^{2-}$) has higher charge density[58-59] compared to the chloride anion ($Cl^-$) for the same concentration, $Gdm_2SO_4$ surface encounters higher $\nu_{CP}$ compared to that of GdmCl surface. The same argument agrees well for $Na_2SO_4$ and NaCl salts since $Na_2SO_4$ provides higher crossing frequency compared to NaCl. In order to understand the variation of $\alpha$ better with the change of salts concentration and to compare the values between them, we plot the absorption coeffient ($\alpha$) at 1THz frequency with respect to salts concentration (figure 6.4b). It is noticed that $\alpha$ decreases steeply with the increase of $Gdm_2SO_4$ concentration, whereas, a complete reverse trend occurs in NaCl; $\alpha$ increases systematically with the NaCl concentration. In case of $Na_2SO_4$, a regular increment is observed upto 0.8 M concentration, beyond which it does not change substantially. Only GdmCl shows some unique bell-shaped profile of $\alpha$ with concentration; the magnitude of $\alpha$ initially is increased upto ~3M, then it becomes saturated for the high concentration (4M-6M) of GdmCl. Heyden *et al.*[54] proclaimed that $\alpha$ specifically signifies the collective information of water dynamics in the THz frequency range which enlarge upto several hydration (2-3) sheath. We can assume an elementary three component model to delineate the observed behavior of $\alpha_{salt\text{-}solution}$. The measured $\alpha_{salt\text{-}solution}$ is the cumulative contribution of absorption coeffcients from bulk-like water (fraction of water which doesn't interact with the cation and anion of salt), cation and anion of salt itself and the solvation shells of cation and anion of the salt (fraction of water which

can interact with the ions of the salt). Several reports[43, 54, 60] also considered the same three component model for different systems in aqueous solvent. Havenith et al.[54, 60] confirmed that the solvation shells of solute (may be protein, salt or sugars) is dynamical in nature and contain distinctly different absorption compared to bulk-like pure water. In case of GdmCl, the regular increased absorption (THz excess) at low concentrations (upto 3M) thus indicates the replacement of highly absorbing buffer with the feebly absorbing salt[60-61], but at the same time simultaneous growth of the amount of stronger absorbing solvation water around the ions of the salt developing an increased total absorption of the salt solution. Similar increased THz absorption (THz excess) at 2.4 THz was reported in presence of $\lambda^*_{6\text{-}85}$–repressor protein at pH 7 and ubiquitin at pH 2.[54] When we further increase the concentration of GdmCl, $Gdm^+$ forms clusters or aggregates[29] and no additional water molecules cannot interact with the cations and anions of GdmCl; so, the hydration shells around the ions of the salt begins to overlap occuring the saturation of $\alpha_{\text{salt-solution}}$ after 3M of GdmCl. Another probable reason is that the aggregates try to lower the $\alpha$ whereas, increased number of free water molecules tend to increase the $\alpha$ value by forming intermolecular hydrogen bond with them which balances and leads to oveall saturation of $\alpha_{\text{salt-solution}}$ after 3M of GdmCl. A similar nonlinear retaliation of this dynamical solvation shells with increasing solute (Trehalose, Lactose, Glucose) concentration was previously observed by Leitner et al.[60, 62] Since in the case of $Gdm_2SO_4$, $Gdm^+$ and $SO_4^{2-}$ creates hetero ion-pair,[12, 63] instead of considering individual ion hydration, the solvation of the ion-pair needs to be considered. Here, instead of two terms (hydration shells of cation and anion separately) only one term (hydration shell of $Gdm_2SO_4$ molecule) contributes to the total absorption of the salt-solution ($\alpha_{\text{salt-solution}}$). This is why $\alpha$ start to decrease from 2M onwards. Increase of concentration of $Gdm_2SO_4$ means the addition of salt; so, another reason is that with increasing concentration, replacement of stronger absorbing bulk-like buffer solution with the weaker absorbing salt results to decrease the total absorption coeffcient of $Gdm_2SO_4$ solution linearly. So, the observed contrasting behavior of GdmCl and $Gdm_2SO_4$ in their absorption coefficient profile (figure 6.4b) indicates that hydration dynamics in presence of these two salts is essentially different. MD simulation study shows that planar $Gdm^+$ interacts strongly with three water molecules present at the same plane with the cation at its first solvation shell, then the water molecules present at the second solvation shell make bonds with the water molecules present in the first solvation shell but not with the $Gdm^+$ any more.[29] It has also been explored

that water interacts significantly with the low concentration of $Gdm^+$ but with the increase in the concentration of GdmCl they form clusters[26] with which water molecules can not interact well, hence water molecules prefer to form intermolecular hydrogen bonds with themselves which is in well agreement with our findings. From figure 6.4b it is found that the absorption coefficient of NaCl is steeply rising with the rise of its concentration which also suggests for different hydration around it. The same linear THz excess in presence of NaCl was reported earlier also by our groups[43] and by Schmidt el al.[50] The combined THz and MD simulation study by the latter group deduced that ion rattling motion on the circumambient water network (oscillations of cation and anion) and the consideration of ions as simple defects in the hydrogen bond network of its extended solvation shell primarily responsible for the increase in THz absorption. S. Heiles and co-workers[29] showed that small sized $Na^+$ is highly solvated by water molecules and the number of water molecules around $Na^+$ and $Cl^-$ in its first solvation shell is greater than that of GdmCl indicating NaCl has higher absorption compared to GdmCl for the same salt concentration which also supported by our data. In the case of $Na_2SO_4$, initiallly $\alpha$ increases upto 0.8M, but beyond that the change is very minimal with the increase of concentration of this salt suggests that the perturbation effect on the surrounding water network by the presence of this salt is not so significant. The representative dielectric responses of $Gdm_2SO_4$ at different concentrations have been depicted in fig. 6.4c and its inset. It is observed that real dielectric permittivity increases with the rise of salt concentration, whereas, imaginary dielectric perimittivity follows opposite trend. We have fitted both real and imaginary dielectric perimittivities with the third order Debye relaxation model (equation 4) and found three timescales ($\tau_1, \tau_2, \tau_3$). For pure water $\tau_1$ is ~8 ps which measures the cooperative hydrogen bond reorientation motion in the system; $\tau_2$ (200 fs ) originates due to rotational motion of individual water molecules and $\tau_3$ (80 fs) accounts for the vibrational band due to the bending of hydrogen bond and its related transverse acoustic phonons[36, 64-66]. Among them only $\tau_1$ shows considerable change with the increase in salt concentrations (figure 6.4d) whereas the change in $\tau_2$ and $\tau_3$ are within error bar (Table 6.1 and 6.2).[33, 43] Hence we have focused our investigation on the $\tau_1$ timescale only which is accounts for the restructuring of the hydrogen bond network around the ions in its extended solvation layer. We have plotted $\tau_1$ with the increase in the concentration of all the four salts. From figure 6.4d, it can be found that the $\tau_1$ values for NaCl and GdmCl decrease with the rise of salt concentration suggesting the fast (or accelerated) and flexible

dynamics of the cooperative hydrogen bond rearrangement of water in presence of these salt. The extent of decrease at fixed salt concentration is highest for NaCl stipulating the water netwok is most significantly perturbed by it whereas, the extent of perturbation is somewhat reduced in case of GdmCl and for $Na_2SO_4$ the change is insignificant. The significant acceleration dynamics beseeches the conviction that both NaCl and GdmCl acts as 'water structure breaker'[33, 43, 67-72] and the structure breaking ability is comparatively larger in the former one; whereas, $Na_2SO_4$ is indifferent to this phenomena. The same conclusion in presence of $Na_2SO_4$ was observed previously by Omta et al.[73] But in case of $Gdm_2SO_4$, we observe the rise of $\tau_1$ values with the increase of salt concentration indicatng the slower dynamics of hydration network around it. Same slower water dynamics in different salt solutions has been observed previously using time-resolved and 2D-IR experiments by several groups.[74-77] Probably $Gdm_2SO_4$ induces water molecules to become more rigid by strenghtening their intermolecular hydrogen bonding in bulk phase and acts as 'water structure maker'.

***MIR-FTIR study:*** In order to investigate about the vibrational strength of hydrogen bonding of the water molecules in presence of these salts we have taken the fourier transform infrared (FTIR) spectra in the Mid-infrared domain (2400-2700 $cm^{-1}$) of the four salts ($Gdm_2SO_4$,GdmCl, $Na_2SO_4$ and NaCl) solution in $D_2O$ and concentration dependent spectra have been shown in figure 6.7a, 6.7b and 6.8 respectively and for NaCl it was shown in our earlier studies.[43] Since water gives too high signal for the FTIR , $D_2O$ is used in place of $H_2O$ as it is known that H and D exchange well. The bonded O-D in pure water shows stretching frequency at ~2510 $cm^{-1}$ in absence of any salts which is excellent agreement with the earlier reports by our groups.[43] The reduction of the strength of hydrogen bond in $D_2O$ indicates the enhancement of free water ($D_2O$) molecules which causes blue shift in the O-D stretching frequency. From figure 6.9a it is observed that for 5M concentration of every salts, $Gdm_2SO_4$ solution shows the highest blue shift in the peak maxima ($\nu_{max}$) of O-D stretching absorption band compared to buffer. In the case of GdmCl the blue shift is minimal whereas NaCl shows red shift in its absorption band for O-D stretching. Figure 6.9b reveals that with the increase of GdmCl concentration $\nu_{max}$ shows blue shift initially at the low concentration range of GdmCl but beyond ~2M it shows continuous red shift upto 6M. Heiles et al. showed that planar $Gdm^+$ interacts strongly with three water molecules present at the same plane with the cation at its first solvation shell, then the water molecules present at the second solvation shell make bonds with the water molecules present in

the first solvation shell but not with the $Gdm^+$ any more.[29] It has also been explored that water interacts significantly with the low concentration of $Gdm^+$ but with the increase in the concentration of GdmCl they form clusters with which water molecules can not interact well, hence water molecules prefer to form intermolecular hydrogen bonds with themselves which is in well agreement with our findings. The bell-shaped profile of $\nu_{max}$ as a function of GdmCl concentration indicates that at low concentration of GdmCl, $Gdm^+$ attracts $D_2O$ molecules to interact with it by breaking its conventional intermolecular hydrogen bond with the bulk deuteriated water, hence the strength of the O-D bond increases causing blue-shift but beyond 2M concentration, probably $D_2O$ molecules cannot interact well with the $Gdm^+$ due to the formation of aggregated cluster structures of $Gdm^+$; hence they try to keep their bulk water hydrogen bond more strongly leads to red shift of its signal. Similar to the absorption coefficient, there is no significant change in the case of $Na_2SO_4$ solution in FTIR measurement again confirms that the influence of this salt in the water molecules is negligible. Although there are few reports[78-79] where it is claimed that $SO_4^{2-}$ interacts strongly with nearby water molecules due to its high charge density, both of our THz spectroscopic and FTIR techniques show that $Na_2SO_4$ salt does not disturb the water network significantly. In the case of $Gdm_2SO_4$, the data shows monotonic red shift with the increment of the salt concentration suggests that probably unlike GdmCl, water molecules are reluctant to interact with $Gdm_2SO_4$ and therefore they try to retain their bulk water hydrogen bonding more strongly due to the presence of $Gdm_2SO_4$ leads to red shift of its FTIR signal. Scott et al.[25] revealed that a significant interaction between $Gdm^+$ of GdmCl and protein along with perturbation of the water network of the system is responsible for the denaturation of protein. In the present study the CD spectra of HSA in the presence of GdmCl shows that in the presence of 1M GdmCl the protein structure is not disturbed at all but from 2M to 5M concentration region of GdmCl the secondary structure is succesively perturbed and at 5M concentration the secondary structure is completely denatured. Since $Gdm^+$ interacts with both protein and water molecules, it is expected that if one interaction becomes prominent it decreases the extent of other interaction. In 1M concentration of GdmCl, $Gdm^+$ is probably busy to interact with water molecules for which protein molecules cannot interact well with $Gdm^+$ and consequently, it cannot denature protein significantly at this concentration. With the increase of the GdmCl concentration, it is explored that the probability of interaction between water and $Gdm^+$ is decreased[29] which may enhance the extent of interaction between protein backbone and

$Gdm^+$ which results to show denaturation of protein structure. Moreover, at higher concentration since $Gdm^+$ forms aggregates that can denature the native state of proteins more effectively. On contrary, Some groups claimed that $SO_4^{2-}$ ions stabilize the protein which overcomes the destabilizing effect of $Gdm^+$ and leads to overall stability of the globular protein.[80] But in our case we can see that both NaCl and $Na_2SO_4$ neither stabilize nor destabilize the protein structure from the CD spectra which contradicts the stabilizing effect of $SO_4^{2-}$. Rather, we can say that $SO_4^{2-}$ ion reduces the destabilizing effect of $Gdm^+$ in $Gdm_2SO_4$. E.R. Williams's group[29] claims that self stacking of $Gdm^+$ in GdmCl causes denaturation of protein whereas, destruction of self stacking of $Gdm^+$ by $SO_4^{2-}$ ion due to hetero-ion pair formation between $Gdm^+$ and $SO_4^{2-}$ makes it able to stabilize the native form of protein. In their study they showed that as $Gdm^+$ can only interact with the water molecules present in the same plane the surface above and below of the $Gdm^+$ becomes less hydrated. So the hydrophobic surface of protein molecule tends to interact with this hydrophobic region around the $Gdm^+$ coordination surface which subsequently leads to protein denaturation of GdmCl. But the strong ion pair formation[5, 12] between $Gdm^+$ and $SO_4^{2-}$ hampers the capacity of $Gdm^+$ to interact strongly with the protein surface; as a result, it diminishes the capability of $Gdm^+$ in $Gdm_2SO_4$ to denature the protein. In our earlier publication[33] it was explored that in presence of HSA, GdmCl showed water structure breaking mechanism; since the alpha value in all concentration range of GdmCl in presence of protein was lower with respect to that of buffer suggesting that the HSA-$Gdm^+$ species is less absorbing compared to water-$Gdm^+$ species.[33] For more quantitative measurement the relative change of absorption coefficient showed that the difference in absorption coefficient of HSA was increasing gradually from buffer to with the rise of GdmCl concentration implying that contribution of HSA-$Gdm^+$ species in the absorption becomes more prominent at higher concentration region of GdmCl which corroborates out study well. Hence, from all these studies it is clearly understood that hydration dynamics has a pivotal role to control the stabilization/destabilization of protein.

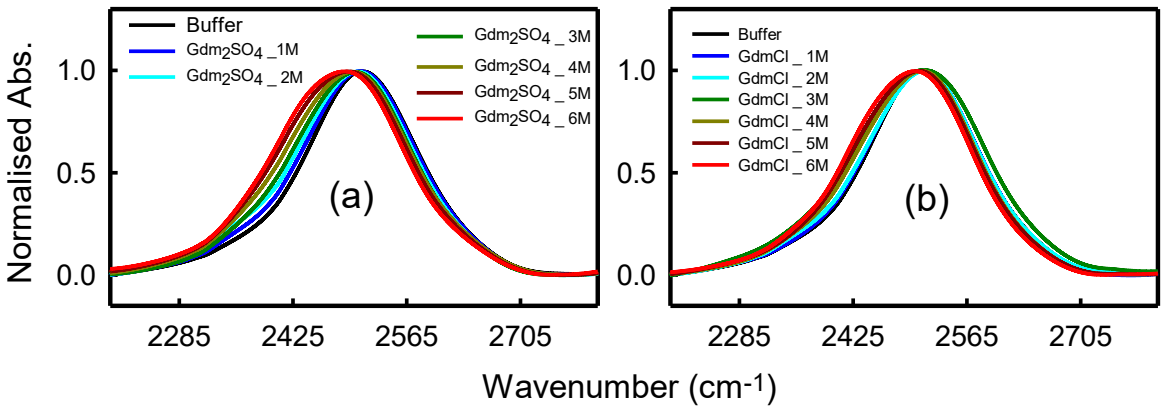


**Figure 6.7:** Normalized spectra of MIR-FTIR measurement of different concentrations of aqueous (a) $Gdm_2SO_4$ and (b) GdmCl salt solutions.

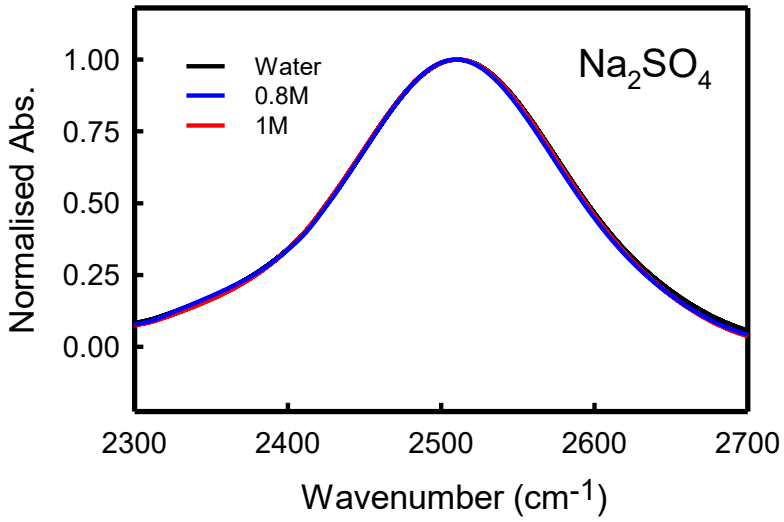


**Figure 6.8:** Normalized spectra of MIR-FTIR measurement of different concentrations of aqueous $Na_2SO_4$ solutions.

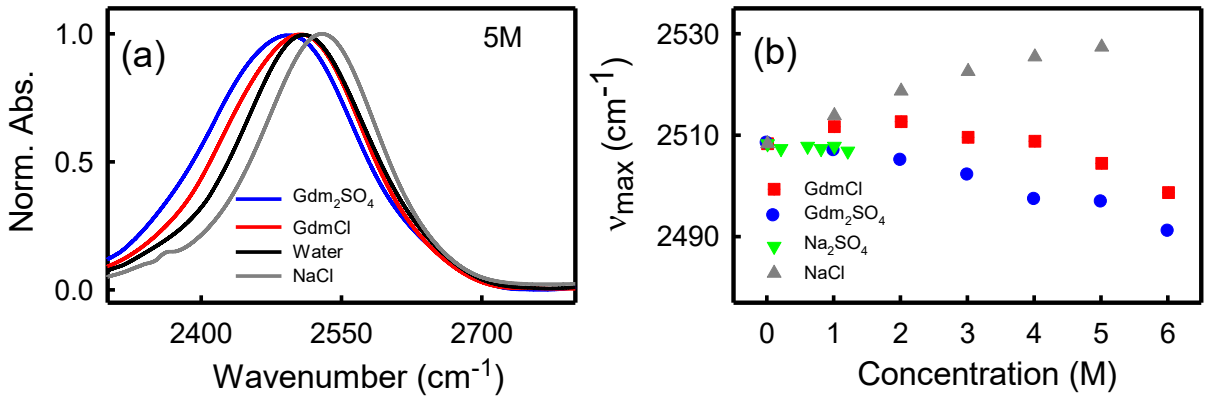


**Figure 6.9:** (a) The normalised absorprtion intensity of FTIR spectra of 5M $Gdm_2SO_4$ (blue), 5M GdmCl (red), 5M NaCl (ash) in $D_2O$ solution. Black line indicates the control experiment of only $D_2O$ (water) solution without presence of any salt. (b) Frequency maxima ( $\nu_{max}$ ) of O-D stretching with respect to the concentration of the salts.

**Table 6.1:** Debye relaxation fitting parameters of aqueous solutions of $Gdm_2SO_4$ at different concentrations.

| [$Gdm_2SO_4$] (M) | $\varepsilon_\infty$ | $S_1$ | $S_2$ | $S_3$ | $\tau_1$ (ps) | $\tau_2$ (fs) | $\tau_3$ (fs) | $\sigma$ (S m$^{-1}$) |
|---|---|---|---|---|---|---|---|---|
| 0 | 1.84 ± 0.02 | 74.3 | 0.35 | 1.46 | 8.70±0.1 | 260±45 | 78 | 0.2 |
| 1 | 2.04 ± 0.02 | 74.0 | 0.68 | 1.30 | 10.08±0.1 | 283±37 | 84 | 4.5 |
| 2 | 2.11 ± 0.02 | 68.4 | 0.84 | 1.22 | 10.0±0.1 | 270±31 | 85 | 5.7 |
| 3 | 2.12 ± 0.02 | 63.2 | 0.97 | 1.28 | 10.5±0.1 | 256±25 | 84 | 7.7 |
| 4 | 2.17 ± 0.02 | 55.5 | 1.10 | 1.25 | 10.7±0.1 | 252±21 | 84 | 8.5 |
| 5 | 2.14 ± 0.02 | 50.2 | 1.13 | 1.34 | 11.1±0.2 | 248±21 | 84 | 9.0 |
| 6 | 2.22± 0.02 | 46.5 | 1.28 | 1.35 | 12.7±0.2 | 241±15 | 84 | 9.6 |

**Table 6.2:** Debye relaxation fitting parameters of aqueous solutions of $Na_2SO_4$ at different concentrations.

| [$Na_2SO_4$] (M) | $\varepsilon_\infty$ | $S_1$ | $S_2$ | $S_3$ | $\tau_1$ (ps) | $\tau_2$ (fs) | $\tau_3$ (fs) | $\sigma$ (S m$^{-1}$) |
|---|---|---|---|---|---|---|---|---|
| 0.8 | 1.85 ± 0.02 | 63.2 | 0.68 | 1.71 | 9.18±0.1 | 346±52 | 78 | 8.5 |
| 1.0 | 1.85± 0.02 | 59.5 | 0.67 | 1.79 | 8.70±0.1 | 356±57 | 79 | 9.4 |
| 1.3 | 1.86 ± 0.01 | 55.0 | 0.87 | 1.92 | 8.79±0.1 | 388±51 | 78 | 10.5 |

## 6.4 Discussion

We have performed extensive spectroscopic measurement to explore the impact of GdmCl and $Gdm_2SO_4$ on water network which paves a path to comment on the orgin of their contrasting behavior on protein stability. Estimation of absorption coefficient shows different behavior between these two salts on hydration dynamics. Due to the planar nature of $Gdm^+$ in GdmCl it perturbs bulk water network upto a certain limit which is a contributing factor for protein denaturation whereas, the tendency of forming hetero-ion pair of $Gdm_2SO_4$ makes it reluctant to perturb the bulk water network which probably keeps the native structure of protein intact. NaCl shows similar impact on water network like GdmCl though the extent is higer in case of NaCl but $Na_2SO_4$ shows completely different trend compared to $Gdm_2SO_4$. The THz relaxation time-scale profile and FTIR data also predict that GdmCl and NaCl behave like a 'water structure breaker' whereas, $Gdm_2SO_4$ acts as 'water structure maker' and $Na_2SO_4$ shows marginal effect. Overall, this study suggests that neither specific cation nor anion alters the hydration dynamics solely rather their combined impact on water is observed which plays the key role to affect the stability of the protein.

## 6.5 Bibliography

1. Canchi, D. R.; García, A. E., Cosolvent effects on protein stability. *Annu. Rev. Phys. Chem.* **2013,** *64*, 273-293.
2. Gorensek-Benitez, A. H.; Smith, A. E.; Stadmiller, S. S.; Perez Goncalves, G. M.; Pielak, G. J., Cosolutes, Crowding, and Protein Folding Kinetics. *J. Phys. Chem. B* **2017,** *121*, 6527-6537.
3. Holthauzen, L. M.; Auton, M.; Sinev, M.; Rösgen, J., Protein stability in the presence of cosolutes. *Methods Enzymol.* **2011,** *492*, 61-125.
4. Mason, P. E.; Neilson, G. W.; Dempsey, C. E.; Barnes, A. C.; Cruickshank, J. M., The hydration structure of guanidinium and thiocyanate ions: Implications for protein stability in aqueous solution. *Proc. Natl. Acad. Sci.* **2003,** *100*, 4557-4561.
5. Ekholm, V.; Vazdar, M.; Mason, P. E.; Bialik, E.; Walz, M. M.; Öhrwall, G.; Werner, J.; Rubensson, J. E.; Jungwirth, P.; Björneholm, O., Anomalous surface behavior of hydrated guanidinium ions due to ion pairing. *J. Chem. Phys.* **2018,** *148*, 144508.
6. Mason, P. E.; Neilson, G. W.; Enderby, J. E.; Saboungi, M. L.; Dempsey, C. E.; MacKerell, A. D.; Brady, J. W., The Structure of Aqueous Guanidinium Chloride Solutions. *J. Am. Chem. Soc.* **2004,** *126*, 11462-11470.
7. Werner, J.; Wernersson, E.; Ekholm, V.; Ottosson, N.; Öhrwall, G.; Heyda, J.; Persson, I.; Söderström, J.; Jungwirth, P.; Björneholm, O., Surface Behavior of Hydrated Guanidinium and Ammonium Ions: A Comparative Study by Photoelectron Spectroscopy and Molecular Dynamics. *J. Phys. Chem. B.* **2014,** *118* (25), 7119-7127.
8. Godawat, R.; Jamadagni, S. N.; Garde, S., Unfolding of hydrophobic polymers in guanidinium chloride solutions. *J. Phys. Chem. B.* **2010,** *114*, 2246-2254.
9. Heyda, J.; Okur, H. I.; Hladílková, J.; Rembert, K. B.; Hunn, W.; Yang, T.; Dzubiella, J.; Jungwirth, P.; Cremer, P. S., Guanidinium can both Cause and Prevent the Hydrophobic Collapse of Biomacromolecules. *J. Am. Chem. Soc.* **2017,** *139*, 863-870.
10. Collins, K. D.; Washabaugh, M. W., The Hofmeister effect and the behaviour of water at interfaces. *Q. Rev. Biophys.* **1985,** *18*, 323-422.
11. Baldwin, R. L., How Hofmeister ion interactions affect protein stability. *Biophys. J.* **1996,** *71*, 2056-2063.
12. Dempsey, C. E.; Mason, P. E.; Jungwirth, P., Complex Ion Effects on Polypeptide Conformational Stability: Chloride and Sulfate Salts of Guanidinium and Tetrapropylammonium. *J. Am. Chem. Soc.* **2011,** *133*, 7300-7303.
13. Arakawa, T.; Timasheff, S. N., Protein stabilization and destabilization by guanidinium salts. *Biochemistry* **1984,** *23*, 5924-5929.
14. Ishtikhar, M.; Khan, A.; Chang, C. K.; Lin, L. T.; Wang, S. S.; Khan, R. H., Effect of guanidine hydrochloride and urea on the interaction of 6-thioguanine with human serum albumin: a spectroscopic and molecular dynamics based study. *J. Biomol. Struct. Dyn.* **2016,** *34*, 1409-1420.

15. Graziano, G., Contrasting the denaturing effect of guanidinium chloride with the stabilizing effect of guanidinium sulfate. *Phys. Chem. Chem. Phys.* **2011,** *13*, 12008-12014.
16. Dempsey, C. E.; Mason, P. E.; Brady, J. W.; Neilson, G. W., The reversal by sulfate of the denaturant activity of guanidinium. *J. Am. Chem. Soc.* **2007,** *129*, 15895-15902.
17. Mason, P. E.; Dempsey, C. E.; Neilson, G. W.; Brady, J. W., Nanometer-Scale Ion Aggregates in Aqueous Electrolyte Solutions: Guanidinium Sulfate and Guanidinium Thiocyanate. *J. Phys. Chem. B* **2005,** *109*, 24185-24196.
18. Vondrášek, J.; Mason, P. E.; Heyda, J.; Collins, K. D.; Jungwirth, P., The Molecular Origin of Like-Charge Arginine−Arginine Pairing in Water. *J. Phys. Chem. B* **2009,** *113*, 9041-9045.
19. Soetens, J.-C.; Millot, C.; Chipot, C.; Jansen, G.; Ángyán, J. G.; Maigret, B., Effect of Polarizability on the Potential of Mean Force of Two Cations. The Guanidinium−Guanidinium Ion Pair in Water. *J. Phys. Chem. B.* **1997,** *101*, 10910-10917.
20. No, K. T.; Nam, K. Y.; Scheraga, H. A., Stability of Like and Oppositely Charged Organic Ion Pairs in Aqueous Solution. *J. Am. Chem. Soc.* **1997,** *119*, 12917-12922.
21. Masunov, A.; Lazaridis, T., Potentials of mean force between ionizable amino acid side chains in water. *J. Am. Chem. Soc.* **2003,** *125*, 1722-1730.
22. Shih, O.; England, A. H.; Dallinger, G. C.; Smith, J. W.; Duffey, K. C.; Cohen, R. C.; Prendergast, D.; Saykally, R. J., Cation-cation contact pairing in water: guanidinium. *J. Chem. Phys.* **2013,** *139*, 035104.
23. Vazdar, M.; Heyda, J.; Mason, P. E.; Tesei, G.; Allolio, C.; Lund, M.; Jungwirth, P., Arginine "Magic": Guanidinium Like-Charge Ion Pairing from Aqueous Salts to Cell Penetrating Peptides. *Acc. Chem. Res.* **2018,** *51*, 1455-1464.
24. O'Brien, E. P.; Dima, R. I.; Brooks, B.; Thirumalai, D., Interactions between Hydrophobic and Ionic Solutes in Aqueous Guanidinium Chloride and Urea Solutions: Lessons for Protein Denaturation Mechanism. *J. Am. Chem. Soc.* **2007,** *129*, 7346-7353.
25. Scott, J. N.; Nucci, N. V.; Vanderkooi, J. M., Changes in Water Structure Induced by the Guanidinium Cation and Implications for Protein Denaturation. *J. Phys. Chem. A* **2008,** *112*, 10939-10948.
26. Hunger, J.; Niedermayer, S.; Buchner, R.; Hefter, G., Are nanoscale ion aggregates present in aqueous solutions of guanidinium salts? *J. Phys. Chem. B.* **2010,** *114*, 13617-13627.
27. Wernersson, E.; Heyda, J.; Vazdar, M.; Lund, M.; Mason, P. E.; Jungwirth, P., Orientational Dependence of the Affinity of Guanidinium Ions to the Water Surface. *J. Phys. Chem. B* **2011,** *115*, 12521-12526.
28. Balos, V.; Bonn, M.; Hunger, J., Quantifying transient interactions between amide groups and the guanidinium cation. *Phys. Chem. Chem. Phys.* **2015,** *17*, 28539-28543.
29. Heiles, S.; Cooper, R. J.; DiTucci, M. J.; Williams, E. R., Hydration of guanidinium depends on its local environment. *Chem. Sci* **2015,** *6*, 3420-3429.
30. Ro/nne, C.; Thrane, L.; Åstrand, P. O.; Wallqvist, A.; Mikkelsen, K. V.; Keiding, S. R., Investigation of the temperature dependence of dielectric relaxation in liquid water by THz

reflection spectroscopy and molecular dynamics simulation. *J. Chem. Phys.* **1997,** *107*, 5319-5331.
31. Beard, M. C.; Turner, G. M.; Schmuttenmaer, C. A., Terahertz Spectroscopy. *J. Phys. Chem. B* **2002,** *106*, 7146-7159.
32. Elton, D. C., The origin of the Debye relaxation in liquid water and fitting the high frequency excess response. *Phys. Chem. Chem. Phys.* **2017,** *19*, 18739-18749.
33. Samanta, N.; Mahanta, D. D.; Mitra, R. K., Collective hydration dynamics of guanidinium chloride solutions and its possible role in protein denaturation: a terahertz spectroscopic study. *Phys. Chem. Chem. Phys* **2014,** *16*, 23308-23315.
34. Chen, Y. H.; Yang, J. T.; Martinez, H. M., Determination of the secondary structures of proteins by circular dichroism and optical rotatory dispersion. *Biochemistry* **1972,** *11*, 4120-4131.
35. Yasmeen, S.; Riyazuddeen; Rabbani, G., Calorimetric and spectroscopic binding studies of amoxicillin with human serum albumin. *J. Therm. Anal. Calorim.* **2017,** *127*, 1445-1455.
36. Kindt, J. T.; Schmuttenmaer, C. A., Far-Infrared Dielectric Properties of Polar Liquids Probed by Femtosecond Terahertz Pulse Spectroscopy. *J. Phys. Chem* **1996,** *100*, 10373-10379.
37. Gestblom, B., Dielectric relaxation time of bound water in biological materials. *J. Phys. Chem* **1991,** *95*, 6064-6066.
38. Sato, T.; Buchner, R., Dielectric Relaxation Processes in Ethanol/Water Mixtures. *J. Phys. Chem. A* **2004,** *108* (23), 5007-5015.
39. Nandi, N.; Bhattacharyya, K.; Bagchi, B., Dielectric relaxation and solvation dynamics of water in complex chemical and biological systems. *Chem. Rev.* **2000,** *100*, 2013-2046.
40. van der Post, S. T.; Tielrooij, K. J.; Hunger, J.; Backus, E. H. G.; Bakker, H. J., Femtosecond study of the effects of ions and hydrophobes on the dynamics of water. *Faraday Discuss.* **2013,** *160*, 171-189.
41. Møller, U.; Cooke, D. G.; Tanaka, K.; Jepsen, P. U., Terahertz reflection spectroscopy of Debye relaxation in polar liquids *J. Opt. Soc. Am. B* **2009,** *26*, 113-125.
42. Polley, D.; Patra, A.; Mitra, R. K., Dielectric relaxation of the extended hydration sheathe of DNA in the THz frequency region. *Chem. Phys. Lett* **2013,** *586*, 143-147.
43. Das Mahanta, D.; Samanta, N.; Mitra, R. K., The effect of monovalent cations on the collective dynamics of water and on a model protein. *J. Mol. Liq.* **2016,** *215*, 197-203.
44. Sreerama, N.; Woody, R. W., Computation and analysis of protein circular dichroism spectra. *Methods Enzymol.* **2004,** *383*, 318-351.
45. Kelly, S. M.; Price, N. C., The use of circular dichroism in the investigation of protein structure and function. *Curr. Protein Pept. Sci.* **2000,** *1*, 349-384.
46. Pace, C. N.; Fu, H.; Fryar, K. L.; Landua, J.; Trevino, S. R.; Shirley, B. A.; Hendricks, M. M.; Iimura, S.; Gajiwala, K.; Scholtz, J. M.; Grimsley, G. R., Contribution of hydrophobic interactions to protein stability. *J Mol Biol* **2011,** *408*, 514-28.
47. Pace, C. N.; Scholtz, J. M.; Grimsley, G. R., Forces stabilizing proteins. *FEBS Lett* **2014,** *588*, 2177-84.

48. Pace, C. N.; Fu, H.; Lee Fryar, K.; Landua, J.; Trevino, S. R.; Schell, D.; Thurlkill, R. L.; Imura, S.; Scholtz, J. M.; Gajiwala, K.; Sevcik, J.; Urbanikova, L.; Myers, J. K.; Takano, K.; Hebert, E. J.; Shirley, B. A.; Grimsley, G. R., Contribution of hydrogen bonds to protein stability. *Protein Sci* **2014,** *23*, 652-61.
49. Stickle, D. F.; Presta, L. G.; Dill, K. A.; Rose, G. D., Hydrogen bonding in globular proteins. *J. Mol. Biol* **1992,** *226*, 1143-59.
50. Schmidt, D. A.; Birer, Ö.; Funkner, S.; Born, B. P.; Gnanasekaran, R.; Schwaab, G. W.; Leitner, D. M.; Havenith, M., Rattling in the Cage: Ions as Probes of Sub-picosecond Water Network Dynamics. *J. Am. Chem. Soc.* **2009,** *131*, 18512-18517.
51. Harder, E.; Eaves, J. D.; Tokmakoff, A.; Berne, B. J., Polarizable molecules in the vibrational spectroscopy of water. *Proc. Natl. Acad. Sci.* **2005,** *102*, 11611-11616.
52. Sharma, M.; Resta, R.; Car, R., Intermolecular Dynamical Charge Fluctuations in Water: A Signature of the H-Bond Network. *Phys. Rev. Lett.* **2005,** *95*, 187401.
53. Ebbinghaus, S.; Kim, S. J.; Heyden, M.; Yu, X.; Heugen, U.; Gruebele, M.; Leitner, D. M.; Havenith, M., An extended dynamical hydration shell around proteins. *Proc. Natl. Acad. Sci.* **2007,** *104*, 20749-20752.
54. Heyden, M.; Havenith, M., Combining THz spectroscopy and MD simulations to study protein-hydration coupling. *Methods (San Diego, Calif.)* **2010,** *52*, 74-83.
55. Matvejev, V.; Zizi, M.; Stiens, J., Hydration Shell Parameters of Aqueous Alcohols: THz Excess Absorption and Packing Density. *J. Phys. Chem. B* **2012,** *116*, 14071-14077.
56. Laage, D.; Stirnemann, G.; Hynes, J. T., Why Water Reorientation Slows without Iceberg Formation around Hydrophobic Solutes. *J. Phys. Chem. B* **2009,** *113*, 2428-2435.
57. Heyden, M.; Sun, J.; Funkner, S.; Mathias, G.; Forbert, H.; Havenith, M.; Marx, D., Dissecting the THz spectrum of liquid water from first principles via correlations in time and space. *Proc. Natl. Acad. Sci.* **2010,** *107*, 12068-12073.
58. Collins, K. D., Charge density-dependent strength of hydration and biological structure. *Biophysical J.* **1997,** *72*, 65-76.
59. Hribar, B.; Southall, N. T.; Vlachy, V.; Dill, K. A., How ions affect the structure of water. *J. Am. Chem. Soc.* **2002,** *124*, 12302-12311.
60. Heyden, M.; Bründermann, E.; Heugen, U.; Niehues, G.; Leitner, D. M.; Havenith, M., Long-range influence of carbohydrates on the solvation dynamics of water--answers from terahertz absorption measurements and molecular modeling simulations. *J. Am. Chem. Soc.* **2008,** *130* (17), 5773-5779.
61. Jockusch, R. A.; Kroemer, R. T.; Talbot, F. O.; Snoek, L. C.; Çarçabal, P.; Simons, J. P.; Havenith, M.; Bakker, J. M.; Compagnon, I.; Meijer, G.; von Helden, G., Probing the Glycosidic Linkage: UV and IR Ion-Dip Spectroscopy of a Lactoside. *J. Am. Chem. Soc.* **2004,** *126*, 5709-5714.
62. Leitner, D. M.; Gruebele, M.; Havenith, M., Solvation dynamics of biomolecules: modeling and terahertz experiments. *HFSP J.* **2008,** *2*, 314-323.

63. Mason, P. E.; Dempsey, C. E.; Vrbka, L.; Heyda, J.; Brady, J. W.; Jungwirth, P., Specificity of Ion−Protein Interactions: Complementary and Competitive Effects of Tetrapropylammonium, Guanidinium, Sulfate, and Chloride Ions. *J. Phys. Chem. B* **2009,** *113*, 3227-3234.
64. Mahanta, D. D.; Patra, A.; Samanta, N.; Luong, T. Q.; Mukherjee, B.; Mitra, R. K., Non-monotonic dynamics of water in its binary mixture with 1,2-dimethoxy ethane: A combined THz spectroscopic and MD simulation study. *J. Chem. Phys* **2016,** *145*, 164501.
65. Vij, J. K.; Simpson, D. R. J.; Panarina, O. E., Far infrared spectroscopy of water at different temperatures: GHz to THz dielectric spectroscopy of water. *J. Mol. Liq* **2004,** *112*, 125-135.
66. Walrafen, G. E.; Chu, Y. C.; Piermarini, G. J., Low-Frequency Raman Scattering from Water at High Pressures and High Temperatures. *J. Phys. Chem* **1996,** *100*, 10363-10372.
67. Kondoh, M.; Ohshima, Y.; Tsubouchi, M., Ion Effects on the Structure of Water Studied by Terahertz Time-Domain Spectroscopy. *Chem. Phys. Lett.* **2014,** *591*, 317-322.
68. Alonso, D. O. V.; Dill, K. A., Solvent denaturation and stabilization of globular proteins. *Biochemistry* **1991,** *30*, 5974-5985.
69. Breslow, R.; Guo, T., Surface tension measurements show that chaotropic salting-in denaturants are not just water-structure breakers. *Proc. Natl. Acad. Sci.* **1990,** *87*, 167-169.
70. Kim, J. S.; Wu, Z.; Morrow, A. R.; Yethiraj, A.; Yethiraj, A., Self-Diffusion and Viscosity in Electrolyte Solutions. *J. Phys. Chem. B* **2012,** *116*, 12007-12013.
71. Marcus, Y., Effect of Ions on the Structure of Water: Structure Making and Breaking. *Chem. Rev.* **2009,** *109*, 1346-1370.
72. Wachter, W.; Kunz, W.; Buchner, R.; Hefter, G., Is There an Anionic Hofmeister Effect on Water Dynamics? Dielectric Spectroscopy of Aqueous Solutions of NaBr, NaI, NaNO3, NaClO4, and NaSCN. *J. Phys. Chem. A* **2005,** *109*, 8675-8683.
73. Omta, A. W.; Kropman, M. F.; Woutersen, S.; Bakker, H. J., Negligible effect of ions on the hydrogen-bond structure in liquid water. *Science (New York, N.Y.)* **2003,** *301*, 347-349.
74. Tielrooij, K. J.; Garcia-Araez, N.; Bonn, M.; Bakker, H. J., Cooperativity in ion hydration. *Science (New York, N.Y.)* **2010,** *328*, 1006-1009.
75. Park, S.; Odelius, M.; Gaffney, K. J., Ultrafast Dynamics of Hydrogen Bond Exchange in Aqueous Ionic Solutions. *J. Phys. Chem. B* **2009,** *113*, 7825-7835.
76. Moilanen, D. E.; Wong, D.; Rosenfeld, D. E.; Fenn, E. E.; Fayer, M. D., Ion-water hydrogen-bond switching observed with 2D IR vibrational echo chemical exchange spectroscopy. *Proc. Natl. Acad. Sci.* **2009,** *106*, 375-380.
77. Park, S.; Fayer, M. D., Hydrogen bond dynamics in aqueous NaBr solutions. *Proc. Natl. Acad. Sci.* **2007,** *104*, 16731-16738.
78. DiTucci, M. J.; Stachl, C. N.; Williams, E. R., Long distance ion–water interactions in aqueous sulfate nanodrops persist to ambient temperatures in the upper atmosphere. *Chem. Sci.* **2018,** *9*, 3970-3977.

79. Kulichenko, M.; Fedik, N.; Bozhenko, K. V.; Boldyrev, A. I., Hydrated Sulfate Clusters SO(4)(2-)(H(2)O) (n) ( n = 1-40): Charge Distribution Through Solvation Shells and Stabilization. *J. Phys. Chem. B* **2019,** *123*, 4065-4069.

80. Dempsey, C. E.; Mason, P. E.; Brady, J. W.; Neilson, G. W., The reversal by sulfate of the denaturant activity of guanidinium. *J. Am. Chem. Soc* **2007,** *129*, 15895-15902.

# *Chapter 7*

## *Summary and Future Viewpoint*

## 7.1 Abridgement of the dissertation

In the present dissertation, we have looked into the effects of some crowding agents on protein structure, functionality, thermal stability and activity. The secondary structural change has been monitored by CD spectroscopy. Thermal stability of the protein has been detected by temperature dependent CD and DSC measurement technique. The change in local environment of the intrinsic Trp moiety has been measured by fluorescence technique. In the first part, we have used different externally added amino acids to observe their osmolytic effect on a model globular protein bovine serum albumin (BSA). We have found that amino acids stabilize the native form of BSA although the extent of stabilization doesn't follow any distinct trend with either the solvent accessible surface area (SASA) or the hydrophobicity of the amino acids. We have found that amino acids also stabilize the urea induced partially unfolded form of BSA. The contrasting results observed in different thermodynamic parameters indicates that associated hydration dynamics of the protein and amino acids play pivotal role on the stabilizing effect of amino acids on protein structure.

In the next part, we have used different non-polar hydrophobic amino acids to understand systematically the role of hydrophobicity on the conformational and thermal stability of globular proteins containing different α-helical protein. Our findings reveals that structural and conformational stability of those proteins and the associated energetic parameters do not depend on the hydrophobicity of amino acids; rather they are protein specific and the α-helicity of protein has a remarkable impact on it.

Next, I have studied the enzymatic activity of a model protein lysozyme on a dead cell bacteria (M. Lys.) in presence of different non-polar amino acids. We have observed that for most of the amino acids, catalytic activity shows bell-shaped profile where activity increases at low concentration and decreases gradually with the concentration of the added amino acids. We have also found that activity follows a regular trend with the size and hydrophobicity of the amino

acids at its low concentration regime, whereas, the pattern is random at the high concentration zone.

Apart from that, I have tried to understand the debatable question behind the contrasting denaturation (or stabilization) nature of guanidinium chloride (GdmCl) and guanidinium sulphate ($Gdm_2SO_4$) on a model protein human serum albumin (HSA) using CD, THz and FTIR spectroscopic studies. Our study dictates that ionic contribution of the salts is not the sole factor, rather the alteration of water dynamics or the collective hydrogen bond network of the salt-water system plays important role to denature (or stabilize) protein structure.

Briefly, this thesis explores the detailed and systematic in-vitro understanding of the conformational structure, thermal stability of the native as well as partially unfolded form, functionality, activity and water dynamics of water soluble globular protein in presence of different macromolecular crowding agents (amino acids, chemical denaturants) at the physiological environment.

## 7.2 Future Viewpoint

During my Ph.D tenure, I have studied different canonical amino acids as osmolytes/macromolecular crowders to observe their effect on protein stability and enzymatic activity. This canonical or natural amino acids are formed directly by DNA in the genetic code. But there are some amino acids which are not found in normal polypeptide chains and these are called Non-canonical (ncAAs) amino acids. In recent days, people are much more interested to synthesize and to incorporate these modified form of amino acids in place of its natural canonical counterpart in the large peptide chains and proteins because these may enrich protein stability, function, structural change, catalytic activity, protein-protein interactions and so on. In this regard, fluorine incorporation into the canonical amino acids have gained extensive interest to the researchers because of its special electronic properties like small size, high electronegativity and the potential to increase the stability and activity of natural proteins.[1-2] C-F bond is longer as well as stronger than a C-H bond; apart from that the high electronegativity of fluorine atom makes the C-F bond less polarizable and also the polarization is opposite in direction than a C-H

bond.[3] This all properties make the fluorocarbon molecules chemically inert and also their unusual self "phase-segregating" behavior is quite important to stabilize protein in crowded environments through enhanced hydrophobic interactions between them. Fluorine molecules prefer to exist with nearby fluorine molecules in solution and this unique effect is called as '*fluorous effect*'[4] and due to that reason, they can form clusters in native state as well as in non-native state. Various groups[5-10] are working to synthesize different fluorinated amino acid derivatives and substitution of these derivatives replacing its hydrocarbon amino acid moiety in proteins increase the thermal stability by decreasing its denaturation rate. It has been observed that incorporation of fluorinated amino acid into proteins enhances its melting temperature ($T_m$) although the structure of proteins remains intact after fluorination. Although several attempts[11-15] have been put forward on small coiled-coil peptide and proteins, a more detailed investigation is needed taking α-helical and β-sheet rich proteins to generalize its effect on protein structure. Apart from this, study on externally added fluorinated amino acid on protein rather than substitution of amino acids in peptide chains is crucial to understand their stabilizing/ destabilizing role in protein folding-unfolding equilibrium and the location of its binding and research on this area is very much limited. Keeping this point in mind, I have plan to study different fluorinated amino derivatives on various types of secondary structural content proteins by externally adding them into the protein and to calculate the associated thermodynamic fingerprints by measuring the change of free energy(ΔG), enthalpy(ΔH), entropy(ΔS), heat capacity($\Delta C_p$). I have plan to study their effect in presence of strong denaturants like urea, guanidinium chloride, guanidinium thiocyanate etc. I want to study enzymatic activity of a stable, native presence in presence of these modified amino acids to understand their role in modulation of catalytic activity. I will use circular dichroism (CD), fluorescence spectroscopy, dynamic light scattering (DLS) technique to understand the change of structural content of protein. Thermodynamic analysis can be performed by differential scanning calorimetry (DSC), isothermal titration calorimetry (ITC) and temperature dependent CD and fluorescence measurement. Protein activity (kinetics) can be measured by UV-visible spectrophotometer and stopped flow measurement technique. I have plan to observe the change of hydration dynamics (monitoring of water structure network) in presence of the fluorinated derivatives in protein environment as well as in only amino acids-solvent medium by using THz spectroscopy,

dielectric relaxation measurement in the GHz range, FTIR and far-IR measurement technique. I want to study molecular dynamics (MD) simulation to understand the interactions of these amino acids with protein and also the location of the interactions using Gromacs and docking mechanism. I expect hydrophobic nature of fluorocarbon molecules will play a major role to modulate different biophysical properties of protein in the crowded environment.

The structure of some fluorinated amino acid derivatives are shown below:

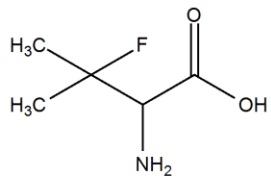


3-Fluorovaline

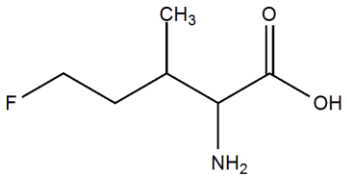


5-Fluoroisoleucine

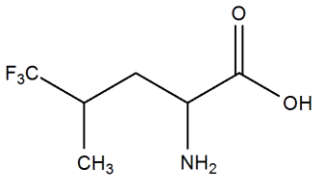


5,5,5-Trifluoroleucine

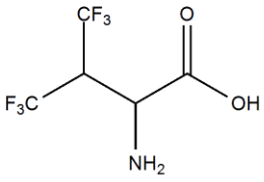


4,4,4,4',4',4'-Hexafluorovaline

Apart from that, I want to work with Adenosine-5′-triphosphate (ATP) which is commonly known as universal energy source for most of the biochemical reactions in the living cells. ATP is a nucleotide and comprises of an adenine base, a pentose ribose sugar and three phosphate groups having high energy containing phosphate bonds. Recent studies reported that ATP hampers the fibrillation or aggregation of proteins at its milli-molar concentrations and the formation of liquid-liquid phase separation (LLPS).[16-20] It can behave as a potent and efficient co-solvent which stabilizes secondary and tertiary structures of protein and also increase the solubility of protein.[21-22] Due to those potential of ATP, I plan to use ATP as co-solute or osmolyte to observe the effect of thermal stability of different globular proteins viz. HSA, BSA, lysozyme, RNase-A etc. using CD, fluorescence and DSC method. I want to measure hydration dynamics around protein in absence and in presence of varying concentrations of ATP using THz spectroscopic techniques and Far-IR methods.

## 7.3 Bibliography

1. Salwiczek, M.; Nyakatura, E. K.; Gerling, U. I. M.; Ye, S.; Koksch, B., Fluorinated amino acids: compatibility with native protein structures and effects on protein–protein interactions. *Chem. Soc. Rev.* **2012,** *41*, 2135-2171.
2. Buer, B. C.; Marsh, E. N., Fluorine: a new element in protein design. *Protein Sci.* **2012,** *21*, 453-462.
3. Harsanyi, A.; Sandford, G., Organofluorine chemistry: applications, sources and sustainability. *Green Chem.* **2015,** *17*, 2081-2086.
4. Horváth, I. T., Fluorous Biphase Chemistry. *Acc. Chem. Res.* **1998,** *31*, 641-650.
5. Marsh, E. N. G., Fluorinated Proteins: From Design and Synthesis to Structure and Stability. *Acc. Chem. Res.* **2014,** *47*, 2878-2886.
6. Anderson, J. T.; Toogood, P. L.; Marsh, E. N., A short and efficient synthesis of L-5,5,5,5',5',5'-hexafluoroleucine from N-Cbz-L-serine. *Org. Lett* **2002,** *4*, 4281-4283.
7. Chiu, H. P.; Cheng, R. P., Chemoenzymatic synthesis of (S)-hexafluoroleucine and (S)-tetrafluoroleucine. *Org. Lett* **2007,** *9*, 5517-5520.
8. Tang, Y.; Ghirlanda, G.; Petka, W. A.; Nakajima, T.; DeGrado, W. F.; Tirrell, D. A., Fluorinated Coiled-Coil Proteins Prepared In Vivo Display Enhanced Thermal and Chemical Stability. *Angew. Chem. Int. Ed.* **2001,** *40*, 1494-1496.

9. Wang, P.; Fichera, A.; Kumar, K.; Tirrell, D. A., Alternative Translations of a Single RNA Message: An Identity Switch of (2S,3R)-4,4,4-Trifluorovaline between Valine and Isoleucine Codons. *Angew. Chem. Int. Ed.* **2004,** *43*, 3664-3666.

10. Smits, R.; Cadicamo, C. D.; Burger, K.; Koksch, B., Synthetic strategies to α-trifluoromethyl and α-difluoromethyl substituted α-amino acids. *Chem. Soc. Rev* **2008,** *37*, 1727-1739.
11. Tang, Y.; Ghirlanda, G.; Vaidehi, N.; Kua, J.; Mainz, D. T.; Goddard, W. A.; DeGrado, W. F.; Tirrell, D. A., Stabilization of Coiled-Coil Peptide Domains by Introduction of Trifluoroleucine. *Biochemistry* **2001,** *40*, 2790-2796.
12. Bilgiçer, B.; Fichera, A.; Kumar, K., A Coiled Coil with a Fluorous Core. *J. Am. Chem. Soc.* **2001,** *123*, 4393-4399.
13. Panchenko, T.; Zhu, W. W.; Montclare, J. K., Influence of global fluorination on chloramphenicol acetyltransferase activity and stability. *Biotechnol. Bioeng* **2006,** *94*, 921-930.
14. Jäckel, C.; Salwiczek, M.; Koksch, B., Fluorine in a native protein environment--How the spatial demand and polarity of fluoroalkyl groups affect protein folding. *Angew. Chem. Int. Ed.* **2006,** *45*, 4198-4203.
15. Hodges, J. A.; Raines, R. T., Stereoelectronic effects on collagen stability: the dichotomy of 4-fluoroproline diastereomers. *J. Am. Chem. Soc* **2003,** *125*, 9262-9263.

16. Kang, J.; Lim, L.; Song, J., ATP binds and inhibits the neurodegeneration-associated fibrillization of the FUS RRM domain. *Commun. Biol.* **2019,** *2*, 223.
17. Dang, M.; Kang, J.; Lim, L.; Li, Y.; Wang, L.; Song, J., ATP is a cryptic binder of TDP-43 RRM domains to enhance stability and inhibit ALS/AD-associated fibrillation. *Biochem. Biophys. Res. Commun.* **2020,** *522*, 247-253.
18. Kang, J.; Lim, L.; Lu, Y.; Song, J., A unified mechanism for LLPS of ALS/FTLD-causing FUS as well as its modulation by ATP and oligonucleic acids. *PLoS Biol.* **2019,** *17*, 1-33.
19. Rice, A. M.; Rosen, M. K., ATP controls the crowd. *Science* **2017,** *356*, 701-702.
20. Bukau, B.; Weissman, J.; Horwich, A., Molecular chaperones and protein quality control. *Cell* **2006,** *125*, 443-451.
21. Patel, A.; Malinovska, L.; Saha, S.; Wang, J.; Alberti, S.; Krishnan, Y.; Hyman, A. A., ATP as a biological hydrotrope. *Science* **2017,** *356*, 753-756.
22. Sridharan, S.; Kurzawa, N.; Werner, T.; Günthner, I.; Helm, D.; Huber, W.; Bantscheff, M.; Savitski, M. M., Proteome-wide solubility and thermal stability profiling reveals distinct regulatory roles for ATP. *Nat. Commun.* **2019,** *10*, 1155.